The role of the carboxyl-terminus of tropomyosin in actin binding

(トロポミオシンのアクチン結合におけるカルボキシル端の役割)

Ken-Ichi Sano

佐野　健一

2000

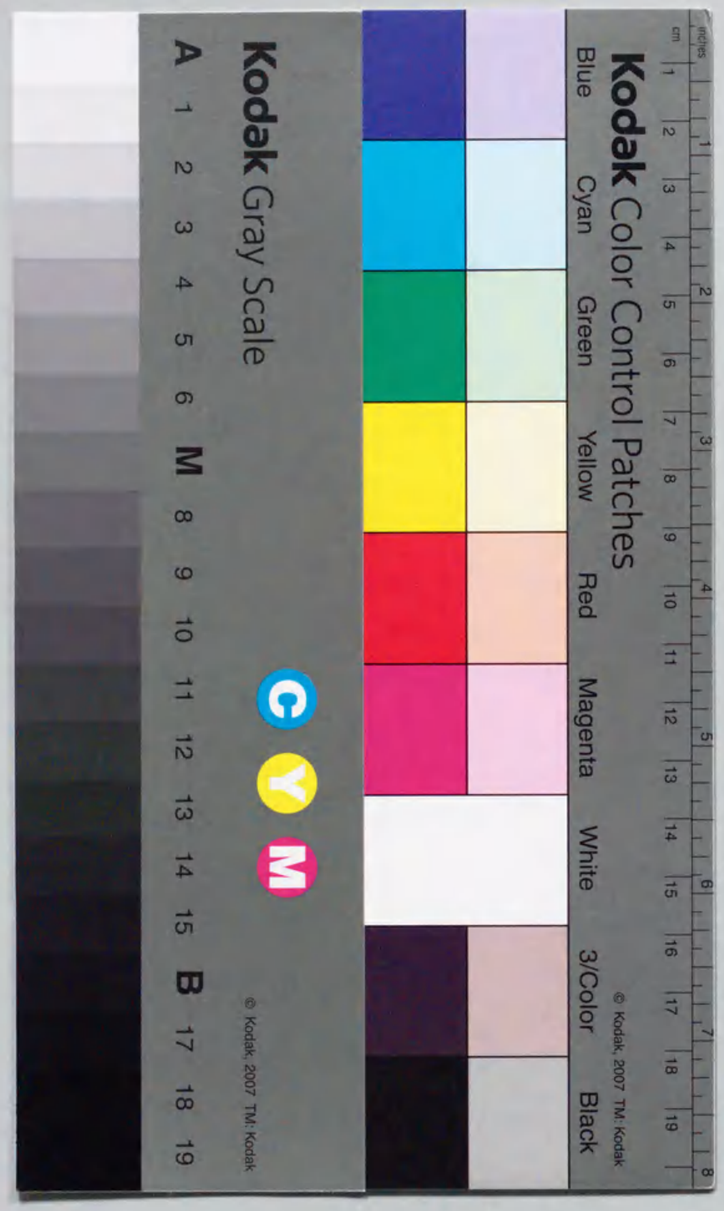

(1)

The role of the carboxyl-terminus of tropomyosin in actin binding

(トロポミオシンのアクチン結合におけるカルボキシル端の役割)

Ken-Ichi Sano

佐野　健一

2000

要旨

トロポミオシンはトロポニンと共に筋肉の細いフィラメント(アクチンフィラメント)上にあって、筋収縮のカルシウム調節に重要な役割を果たす蛋白質である。トロポミオシンは長さ400Åの棒状蛋白質で、一分子のC端と次の分子のN端のhead-to-tail相互作用により重合する。

この相互作用には、分子の両端から7-9残基が関係していると考えられている。この相互作用領域の欠失・化学修飾などにより、トロポミオシンはアクチンへの結合能を著しく損なうことから、この領域がトロポミオシンの機能において非常に重要な役割を果たすと考えられている。また、トロポミオシンはアクチンフィラメントに協同的に結合したり、トロポミオシン・アクチン複合体の協同的な状態変化が、あたかも隣接したトロポミオシンを介して変化が伝搬するように振る舞う。これらのことは、head-to-tail相互作用によるとの説明がなされてきた。本研究では、このhead-to-tail相互作用とトロポミオシンの機能との関係をより多面的に調べるために、以下の3系列の実験を行った。いずれも、トロポミオシンのC端側の構造を人為的に変化させ、アクチン・トロポミオシン複合体の機能の変化を調べた。

(I) トロポミオシンには、選択的スプライシングによって産生される組織特異的なアイソフォームが存在する。本研究では、ロブスター速筋型・遅筋型のアイソフォームに着目した。これらのアイソフォームの差違はエキソン2(a.a. 39-80)の領域、つまり分子の中間部に限られるにもかかわらず、低イオン強度下での重合度、すなわちhead-to-tail相互作用の強さに大きく影響を与える。この蛋白質では中間部の差違の影響が分子全体に及んでいるようであり、種々の理由により、影響は特に分子のC端側の形態を変えていると考えられる。両アイソフォームの機能と構造の比較実験を行ったところ、遅筋型アイソフォームは速筋型アイソフォームに比べて、より柔軟で、より強くアクチンへ結合した。また、低濃度のミオシンS1存在下ではトロポミオシンがアクトS1のATPase活性を低下させるこの阻害作用の点では、遅筋型アイソフォームがより強い作用を示した。

(II) 次に、トロポミオシンのC端領域の機能を詳細に調べるために、遅筋型アイソフォームのC端側を段階的に欠失させた変異蛋白質を作成し検討を加えた。溶液中でのhead-to-tail相互作用は欠失残基が多くなるにつれ段階的に弱まった。一方、アクチンへの結合の強さは、C端側から3残基欠失では野生型とほとんど変わらず、さらに一残基の欠失により大きく減少した。また、7残基欠失ではアクチン結合能はもはや失

われていた。また、アクチンとの複合体によるアクトS1のATPaseの活性阻害作用は、3残基欠失までは野生型とあまり変わらないが、4残基欠失では半減する。これらの結果を総合してC端側の機能領域のマップを作った。

(III) 溶液中でのhead-to-tail相互作用の強さが異なる点変異トロポミオシンを作成し、アクチンフィラメントへの結合を調べた。この結果、溶液中でのhead-to-tail相互作用の強さは、アクチンへの結合の強さとも、またアクチンへの結合の協同性とも相関関係がないことを明らかにした。この結果から、トロポミオシンの溶液中での head-to-tail相互作用は、アクチンフィラメント上でのトロポミオシン間の相互作用を直接反映しているものではなく、アクチン・トロポミオシン複合体におけるトロポミオシン分子間の相互作用は、アクチンとトロポミオシンとの相互作用を考慮する必要がある。さらに、N端側とC端側の相互作用領域をそれぞれ欠失した変異トロポミオシンを2種作成し、head-to-tail 相互作用の強さを分析型超遠心機による直接測定により求め、$Ka = 2.6\times10^{4}$ M^{-1}という非常に弱い相互作用であるとの結論を得た。

以上のことから、(I)～(III) の結果を総合すると、C端領域の状態は、アクチンフィラメント上でのアクチン・トロポミオシンの相互作用に大きな影響を与えることが明らかになった。トロポミオシンがアクチンフィラメントにどのように結合するか、またどのようにトロポミオシンが複合体で機能するかはまだ解明されていない。今後の研究課題として、アクチン・トロポミオシン複合体の構造情報が複合体の機能を解明していく上で非常に重要になってくると思われる。

トロポミオシンはN末端がアセチル化されて初めて機能するが、この翻訳後修飾は大腸菌を用いた発現系では起こらず、真核細胞を用いた発現系では可能である。そのため、本研究を通してトロポミオシン試料調製にはバキュロウイルス発現系を用いた。その際、ロブスター・トロポミオシン遺伝子の非翻訳配列の一部が偶然バキュロウイルス発現系に持ち込まれ、それが蛋白質発現を強力に増加させることを見つけた。この配列は、ウサギ由来のトロポミオシンの発現量を約20倍にも増加させ、他の一般的な蛋白質発現にも有効であるとの予備的結果が得られている。

Abstract

Tropomyosin is located on the muscle thin filament (actin filament) in association with troponin, plays important roles in calcium regulation of muscle contraction. Tropomyosin is a rod like protein about 400 Å long. The C-terminus of one tropomyosin molecule interacts with the N-terminus of the next molecule in a head-to-tail manner. This head-to-tail interaction is due to the overlap of 7-9 residues between N- and C-termini of tropomyosin. It has been believed since long time that the head-to-tail interaction is important for its function, since tropomyosin loses its actin binding ability upon deletion or chemical modification of the terminal regions. Moreover, the head-to-tail interaction has accounted for not only the cooperative binding of tropomyosin to actin filament but also the cooperative transition of states of actin-tropomyosin. In the present study, in order to know more about the relationship between the head-to-tail interaction and the functions of tropomyosin, three series of experiments have been carried out, by using tropomyosin variants in which the structure of C-terminus was artificially changed.

(I) In spite that two isoforms of lobster muscle tropomyosin, *fTm* (fast muscle specific isoform) and *sTm1* (slow muscle specific isoform), differ from each other in the amino acid sequence of the internal region, the putative exon 2 coding region (a.a. 39-80), *sTm1* shows remakably higher low salt viscosity than *fTm*, that is indicative of stronger head-to-tail interaction. The present analyses of lobster tropomyosin isoforms *in vitro* have shown that the local differences in the internal region influence the conformation of the whole molecule, and there are some evidences that the C-terminal region is mainly affected. It has been revealed that *sTm1* is more flexible and binds to actin more strongly as compared with *fTm*. And *sTm1* inhibits more the acto-S1 ATPase in the presence of low concentration of S1 than *fTm* dose.

(II) A serious of C-terminal deletion mutants of sTm1 have been prepared and studied. The strength of head-to-tail interaction in solution gradually decreases as more residues are removed from the C-terminus. The

actin affinity has been hardly reduced by the deletion of 3 residues, substantially reduced by deletion of 4 residues and almost abolished by the deletion of 7 residues or more. The inhibitory activity of tropomyosin on the acto-S1 ATPase also almost maintains by the deletion of 3 residues, but is reduced by almost half by the deletion of 4 residues. From these results, functional domains in the C-terminal region of tropomyosin has been mapped.

(III) A series of tropomyosin variants have been prepared in which serine-283 is replaced by another amino acid to alter the strength of head-to-tail interaction in solution. By using these variants, no correlation has been observed between the strength of head-to-tail interaction in solution on one hand and the strength or the cooperativity in the binding of tropomyosin to actin on the other. This indicates that there is no simple parallel between the head-to-tail interaction of tropomyosin in solution and that on the actin filament. When tropomyosin is on the actin filament, the interaction between actin and tropomyosin could have significant influences on the head-to-tail interaction between tropomyosin molecules. In addition, using two kinds of tropomyosin deletion mutants, one with an intact N- and a defective C-terminus and the other with a defective N- and an intact C-terminus, the association constant for the head-to-tail interaction in solution has been first directly measured as $Ka = 2.6 \times 10^4\ M^{-1}$, being indicative of a fairly week interaction.

In conclusion, the conformation of the C-terminal region makes great influences on the interaction between actin and tropomyosin. Therefore, for further understanding of the functions of actin-tropomyosin complex, we should collect more structural information on the interaction between actin and tropomyosin.

Throughout this study, I have used the baculovirus-based expression system to prepare tropomyosin variants. This is because N-terminal acetylation is essential for the function of tropomyosin and because N-terminal acetylation occurs when tropomyosin is expressed in the baculovirus-based expression system but not in the bacterial system. I have

found a *cis* element that increases expression levels of exogenous genes. This element is untranslated sequence of cDNA for lobster tropomyosin that was accidentally carried over into the expression system. Using this sequence, the expression level of rabbit α-tropomyosin has increased by a factor of 20. Preliminary results have also indicated that this sequence does work not only for tropomyosin but also for other proteins.

Contents

Abbreviations

ADP, adenosine 5'-diphosphate
Ap5A, P^1, P^5-di(adenosine-5')-pentaphosphate
ATP, adenosine 5'-triphosphate
cDNA, complimentary DNA
Da, dalton
DTT, (±)-dithiothreitol
EDTA, ethylenediaminetetraacetic acid
fTm, lobster fast muscle specific tropomyosin isoform;
HEPES, 2-[4-(2-hydroxyethyl)-1-piperazinyl]ethanesulfonic acid
IPTG, isopropyl β-D(-)-thiogalactopyranoside
L21, 21 bp leader sequence originated from lobster tropomyosin cDNA
MOPS, 3-(*N*-morpholino)propanesulfonic acid
NEM-S1, *N*-ethyl maleimide modified S1;
PAGE, polyacrylamide gel electrophoresis
PCR, polymerase chain reaction
PMSF, phenylmethylsulfonyl fluoride
rpm, revolutions per minute
S1, myosin subfragment 1
SDS, sodium dodecylsulfate
sTm1, lobster slow muscle specific tropomyosin type 1 isoform
Tris, tris(hydroxymethyl)aminomethane

Chapter 1

General introduction

Muscle cell

Muscle cell or muscle fibers, especially striated muscle, are one of highly differentiated cells, and accommodate the well aligned contractile apparatus. Muscle fiber is a bundle of myofibrils, and the myofibril has striation when it is observed under phase contrast light microscope. The striation is formed as the unit, the sarcomere, repeats one after the other. As schematically indicated in Figure 1-1, the sarcomere has A-, I- and H band between the boundaries, Z lines. The band pattern originates from the arrangement of the thick and thin filaments within sarcomere. As muscle shortens, the sarcomere shortens. Within the sarcomere, only the I-band shortens, while the A-band remains at the fixed length (Figure 1-2). Based on this observation, the sliding filament theory of muscle contraction was proposed [1, 2]. The sliding force is generated by the interaction between myosin molecules in the thick filament and actin which forms the thin filament.

Thin filament structure

Figure 1-3 shows the schematic drawing of the striated muscle thin filament, which consists of mainly three components, actin, tropomyosin, and troponin. The backbone of the thin filament is the actin filament that is polymerized actin monomers forming a two-stranded helix. Tropomyosin lies on the groove of actin filament and spans seven actin monomers [3, 4]. Troponin is located at regular intervals on the actin-tropomyosin complex, and consists of three subunits [5, 6]. Troponin C is a calcium binding subunit, troponin I has an inhibitory activity of actin activated myosin ATPase (the actomyosin ATPase) and troponin T binds tropomyosin [7]. The contraction of striated muscle is regulated by the thin filament [8]. When the signal for contraction reaches through the neurons to the muscle cell, Ca^{2+} are released from the sarcoplasmic reticulum. The released Ca^{2+} binds to troponin C on the thin

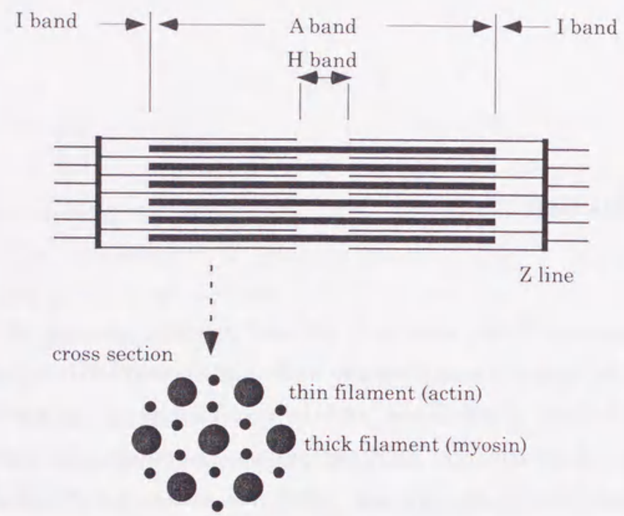

Figure 1-1 Schematic drawing of a sarcomere.

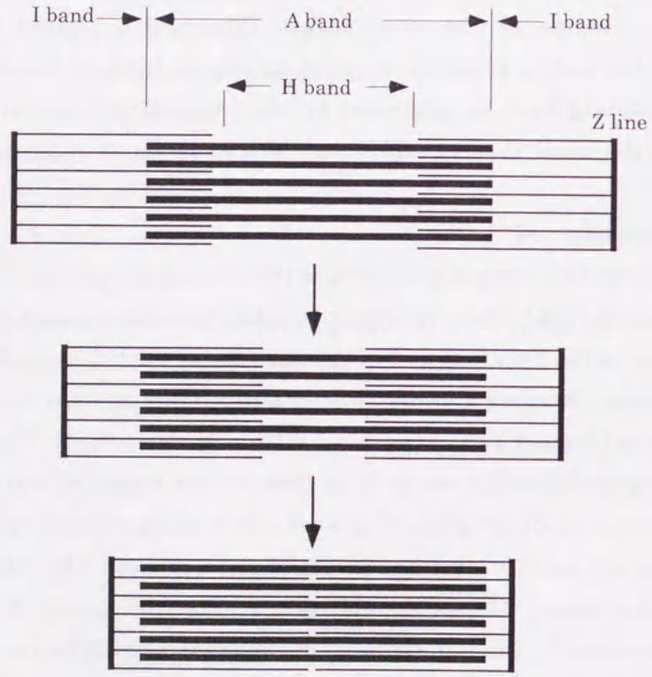

Figure 1-2 Schematic drawing of the sliding filament model.

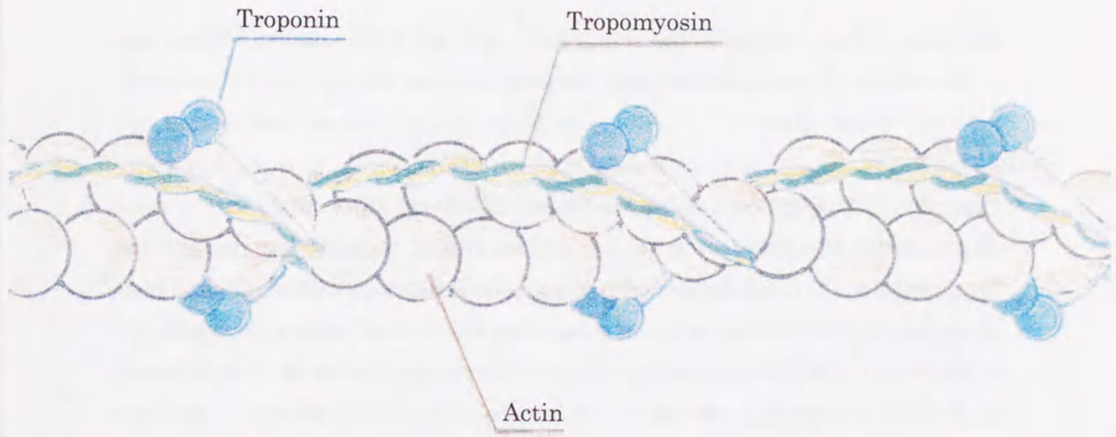

Figure 1-3 Schematic representation of striated muscle thin filament.

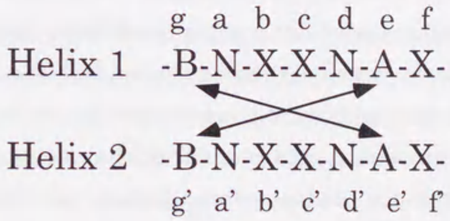

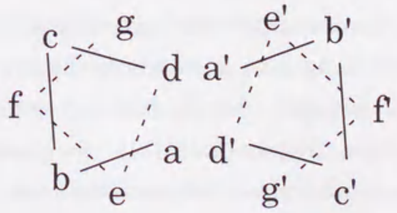

Figure 1-4 The unit of hepta-peptide repeat in the amino acid sequence of tropomyosin. Seven positions are designated as *a* to *g*. N stands for non-polar residues, B indicates frequent occupation by basic residues, whereas A by acidic residues. The bottom is the end-on view of the heptad repeat of pairing two α-helices, indicating the spatial relationship between the residues. (From McLachlan and Stewart 1975, and Smillie 1979 with modification)

filament, which releases the inhibitory action of troponin I. Then the conformation of actin-tropomyosin complex must be changed and the switch for contraction turns on.

Discovery of tropomyosin and its α-helical coiled-coil formation

Tropomyosin was discovered in 1940s from rabbit skeletal muscle, and its function was unknown for many years [9]. In spite of this, tropomyosin was intensively studied mainly out of structural interests. Tropomyosin belongs to the group of α-fibrous proteins. X-ray diffraction patterns show reflections at 5.1-5.2 Å, which is accounted for by the α-helical coiled-coil of two- or three-stranded ropes. The straight α-helix gives rise to the reflections at 5.4 Å [10].

Tropomyosin was characterized as a two-stranded α-helical coiled-coil protein, since the molecular weight under high salt conditions is about 66,000, whereas 33,000 under denaturing conditions. Crick [10] pointed out that, in the case of two-stranded α-helical coiled-coil, the structure would be stabilized by non-polar residues in the interface region between two chains, and outside of the interface region by polar or charged residues that interact with the partner chain and/or other protein molecules. Therefore a characteristic repeat of non-polar and polar or charged residues is required, and each period corresponds almost two turns of an α-helix with 3.5 residues per turn, therefore the repeat unit becomes seven. In a hepta-peptide repeat, each position is designated as *a* to *g*, in which the positions *a* and *d* are occupied by hydrophobic residues whereas *b, c, e, f,* and *g* are occupying by polar or charged residues (Figure 1-4) [11]. As shown in Figure 1-4, hydrophobic interactions take place between residues at a, a', d and d', whereas charge-charge interactions between *e* and *g'* as well as between *e'* and *g*. Both types of interactions stabilize tropomyosin molecule [11]. Amino acid sequence analysis of rabbit skeletal tropomyosin revealed that tropomyosin had the sequence characteristic to the α-helical coiled-coil protein [11, 12]. This analysis have shown that there is indeed a regular pattern of hydrophobic residue which extends the entire molecule 284 amino

acid residues (Figure 1-5) [11, 12].

The head-to-tail interaction of tropomyosin

In low salt solution, tropomyosin interacts in a head-to-tail manner to form a train of molecules [13]. This head-to-tail interaction is due to 7-9 residues overlap between N- and C-termini of tropomyosin [11]. It has been believed since long time that the head-to-tail interaction is essential for the affinity of tropomyosin to actin. Early studies showed that the deletion of either end of the molecule, first 9 residues at N-terminus or 9-11 residues at the C-terminus, abolished the affinity to actin [14-16]. The idea of the close link between the head-to-tail interaction and the actin binding was further supported by the study of recombinant tropomyosin. With the *Escherichia coli* expressed recombinant tropomyosin, the actin binding and the head-to-tail interaction are abolished concomitantly. This is due to the lack of acetylation of the N-terminal at Met-1 in the *E. coli* expressed tropomyosin. In the authentic tropomyosin or the recombinant tropomyosin expressed by use of the baculovirus based expression system, the N-terminal acetylation occurs [17-19]. Moreover, it was thought that the cooperative binding of tropomyosin to actin was caused by the head-to-tail interaction between tropomyosin molecules (to be discussed further in Chapter 4).

The sequence of the N-terminal head-to-tail interaction region is well conserved as MDAIKKKMQ, and the importance of this region was also indicated by the results that chemical modification of Lys-7 resulted in loss of both polymerizability and actin binding [15]. This sequence is also found in other actin binding proteins, like those in the gelsolin family [20] and cofilin [21]. In these actin binding proteins, however, this sequence appears not to contribute to actin binding [20, 22]. In contrast, in the case of tropomyosin, the conserved N-terminal sequence contributes to actin binding more than any other internal segment does. Therefore the question still remains how this conserved N-terminal region contributes to the actin binding. The C-terminal sequence, on the other hand, is fairly variable between tropomyosin species [23-25], although the C-terminal region is

MDAIKKKMQMLKLDKENALDRAEQAEADKKAAEDR
SKQLEDELVSLQKKLKGTEDELDKYSEALKDAQEK
LELAEKKATDAEADVASLNRRIQLVEEELDRAQER
LATALQKLEEAEKAADESERGMKVIESRAQKDEEK
MEIQEIQLKEAKHIAEDADRKYEEVARKLVIIESD
LERAEERAELSEGKCAELEEELKTVTNNLKSLEAQ
AEKYSQKEDKYEEEIKVLSDKLKEAETRAEFAERS
VTKLEKSIDDLEDELYAQKLKYKAISEELDHALND
MTSI

Figure 1-5 Amino acid sequence of rabbit skeletal muscle α-tropomyosin. The positions *a* and *d* of the hepta-peptide repeat are boxed in red. The first residue M is at the position *a*.

functionally important as our own results indicate (Chapter 3&4).

Tropomyosin isoform diversity and alternative splicing

Tropomyosins are a diverse group of proteins found in eukaryotes from yeast to human [26]. Tropomyosins are associated with the thin filaments in muscle cells and the micro-filaments of non-muscle cells. In many animals, there are multiple tropomyosin isoforms. These isoforms originate from multiple genes in association with alternative splicing of a transcript from a single gene (Figure1-6&7) [27]. In mammalian cells, it is known that there are four tropomyosin genes; α-gene, β-gene, and hTMnm gene have nine exons and are known to have at least nine (α-gene) or two (β-gene and hTMnm) isoforms, whereas TM-4 gene has eight exons and encodes only one isoform [27].

In α-, β- and hTMnm genes, there are three or four alternatively spliced exons, exon 1, 2 (only in α-gene), 6, and 9. One of the most interesting questions about the diversity of tropomyosin isoforms is the functional significance of the isoforms, and each alternative spliced exon is thought to correspond to specific functions of each isoform. In other words, each alternatively spliced exon may correspond to a functional domain of tropomyosin. The most important function of tropomyosin is to bind to actin filament. Each isoform differs from each other in the affinity and the number of interacting actin monomers. As Figure 1-7 shows, there are two groups of tropomyosin molecules of different lengths. On one hand, there are tropomyosin species of high molecular weight consisting of mostly 284 residues. On the other, low molecular weight tropomyosin species are of either 245, 248 or 251 residues. The high molecular weight species binds to seven, whereas the low molecular weight species spans six actin monomers. In early reports, the high molecular weight tropomyosin could bind more strongly to actin filament compared with the low molecular isoforms, and this difference was explained in terms of the number of binding sites [28]. The recent studies, however, have suggested that the affinity to actin filament is not much dependent on the number of binding sites but more

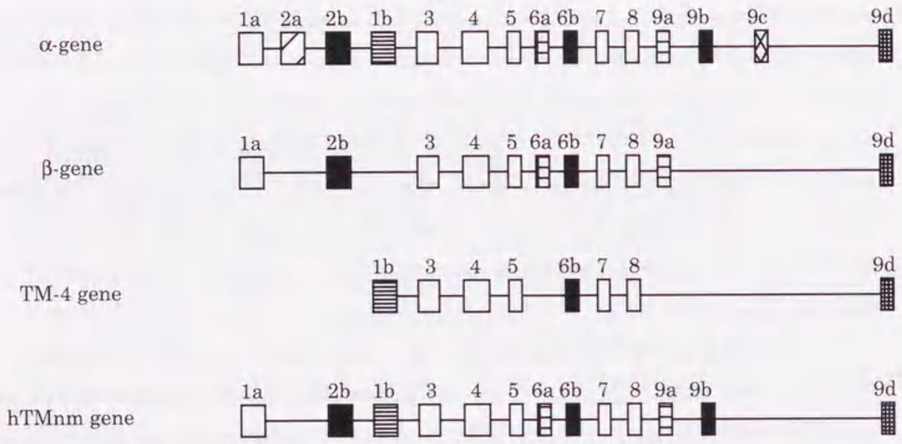

Figure 1-6 The intron-exon organization of the mammalian tropomyosin genes. Exons are represented by boxes, whereas introns by horizontal lines. The numbering systems 1a to 9d is used to facilitate comparison between genes. The open boxes depict exons common to all genes. (From Pittinger, et al. 1994)

dependent on the exon which is expressed [29, 30]. It is worth noting that the binding of tropomyosin to actin filament is also influenced by tropomyosin binding proteins (like troponin) whose binding is also dependent on tropomyosin isoforms, that is, choice of exons.

Two of alternatively spliced exons, the exons 1 and 9, encode N- and C-terminal regions which are essential for actin binding, whereas other two exons, exon 2 and 6, encode internal regions which little contribute to the overall actin binding affinity [31].

Choice of exon 1 is straightforward; exon 1a is chosen for the high molecular weight tropomyosins whereas exon 1b is chosen for the low molecular weight isoforms. Functional significance of the choice of exon 9 of vertebrate α-tropomyosin is well studied. Various versions of exon 9 are alternatively spliced in a tissue specific manner, giving rise to isoforms for different functions [29, 32]. The isoforms are different in the strength of head-to-tail interaction [29], in the thermal stability of α-helix [33], in the affinity for actin and in the troponin binding [29]. Troponin binds to tropomyosin only in the striated muscle, and exon 9a which is expressed exclusively in the striated muscle is indispensable for interaction with troponin [29].

Exon 6 is one of the two internal exons which are alternatively spliced. The exon 6 encoding region includes the caldesmon binding region of tropomyosin [34, 35], as well as the region for Ca^{2+} sensitive interaction with troponin [36]. Recent study of exon 6 of rat α-tropomyosin showed that alternative splicing of exon 6 does not affect the troponin binding but the actin affinity [37]. They discussed the possibility that the sequence in exon 6 could have an effect on the conformation of the functional end regions.

Some previous reports focussed on the role of alternatively spliced exon 2 using chimera mutants or deletion mutants. A study of rat α-tropomyosin also indicated that the alternatively spliced exon 2a and 2b have an effect on the overall stability of molecule, but have little effect on the actin binding affinity [29, 33]. The study of deletion mutants of tropomyosin also indicated that most part of exon 2 encoding region has little association

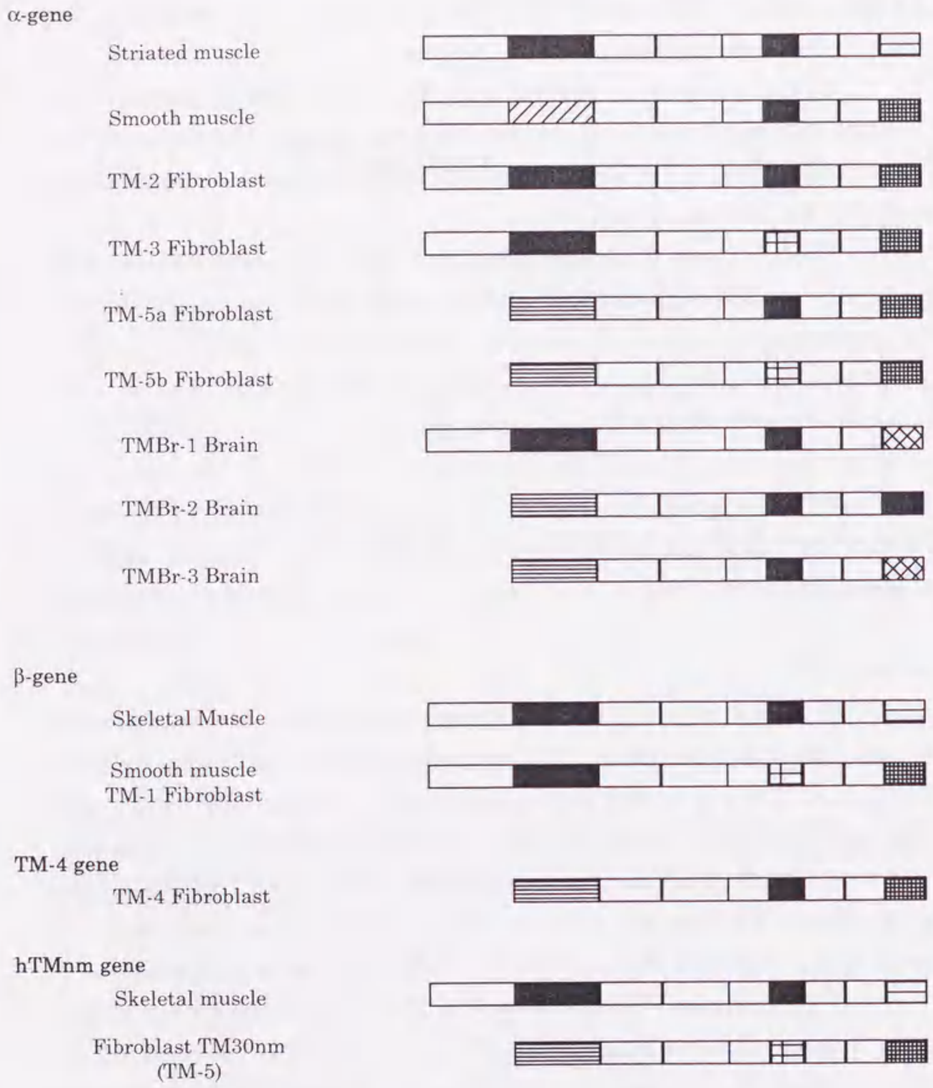

Figure 1-7 Schematic representation of arrangements of exons in various tropomyosin isoforms. (From Pittinger, et al. 1994)

with the affinity for actin [30]. The question still remains unanswered whether the alternatively spliced exon 2 encoding region has any effect on tropomyosin function or not. Using the lobster tropomyosin isoforms, I studied the role of exon 2 and revealed that the choice of exon 2 changes the flexibility of the molecule and thereby gives rise to isoform specific functions (in Chapter 2).

Cooperative interaction between myosin head and actin-tropomyosin complex

Cooperative and allosteric interactions between thin filament and myosin has been studied since 1970s [38, 39]. In 1982, Lehrer and Morris demonstrated that tropomyosin alone (without troponin) can inhibit interaction between actin and myosin at low concentrations of myosin and can activate at high concentrations of myosin [40]. They demonstrated that the actin-tropomyosin complex works as a cooperative/allosteric unit even without troponin, troponin being an allosteric activator (troponin with Ca^{2+}) or an inhibitor (troponin without Ca^{2+} or troponin I alone) [40, 41].

In 1987, Geeves and Halsall proposed the two-step ligand cooperative binding model [42]. The denoted myosin head (S1) as a ligand. S1 binds to actin-tropomyosin complex by two-steps; at first S1 binds weekly (A-state binding) and then after the isomerization occurs, S1 binding becomes strong and S1 works as an activator of cooperative ligand binding (Figure 1-8). In their two-state model, actin-tropomyosin complex is in the equilibrium between open- (ON) and closed- (OFF) states, and S1 isomerization requires filament state to be open. The isomerization affects the equilibrium of the filament, and then ligand binding becomes cooperative. This model is based on the cooperative/allosteric model by Monod, Wyman, and Changeux [43], and there are only four parameters to specify this model; K_1 as the initial S1 binding constant (A-state binding), K_2 as the isomerization constant, K_T as the equilibrium constant [open]/[closed] of the actin-tropomyosin complex and n for the cooperative unit size (in the Figure 1-8 described as seven).

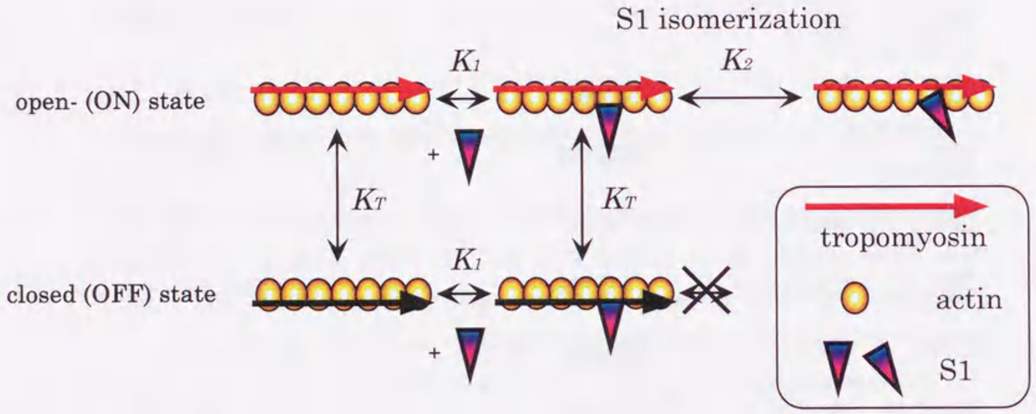

Figure 1-8 The two-state model for actin-tropomyosin complex. K_1, the equilibrium constant for initial binding of S1 to actin-tropomyosin, being independent on the state of actin-tropomyosin. K_2, the equilibrium constant for isomerization, which requires actin-tropomyosin to be in open-state. K_T, the equilibrium constant [open]/[close]. Here the cooperative unit size (n) is assumed to be 7 (from Lehrer & Geeves 1998, with modifications).

Chapter 2

Amino acid replacements in an internal region of tropomyosin alter the properties of the entire molecule

Introduction

In American lobster (*Homarus americanus*), the abdominal flexor muscle which occupies almost all the space in the tail is a fast muscle, whereas the muscles within the crusher claw are slow muscles. Mass spectrometry analysis shows that tropomyosin prepared from the tail muscle consists mainly of one isoform, designated as *fTm* (*f* for fast), whereas tropomyosin from the crusher claw muscle contains at least two isoforms, one of which is designated as *sTm1* (with a chain weight of 32,950 Da) (Figure 2-1). Complimentary DNA sequence analysis of *fTm* and *sTm1* strongly suggested that both isoforms may originate from the common transcript by means of alternative splicing, because the differences are restricted to one stretch of the sequence corresponding to the amino acid residues 39-80 (Figure 2-2). This region corresponds to exon 2 of tropomyosin genes of many other animals (Figure 2-3) [26, 44].

Functions of the exon 2 encoding region are still unknown. In order to know the functions of this region, the two isoforms *fTm* and *sTm1* of lobster muscle tropomyosin were studied. These isoforms are naturally occurring proteins, not chimera. Therefore the isoforms should be suitable specimen for this study. As will be described in this chapter, the results demonstrate that the amino acid replacements in this internal region alter the conformation of the ends of the molecule as well as the flexibility of the entire molecule. It is possible that in this way exon 2 expresses the isoform specific functions.

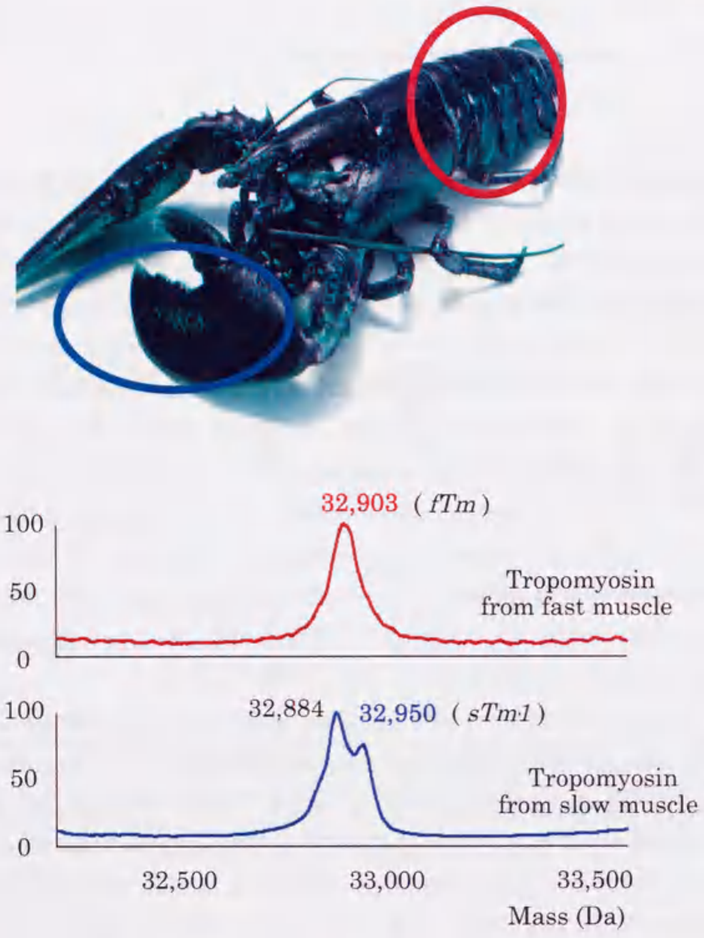

Figure 2-1 The MS profiles of two preparations of lobster muscle tropomyosin.


```
CCAAGGCAGGCCCACGGTCCTAGCGTTCTCAGTTCTTTTTTGTTGGTTGGGAAACTCCTA   60
AAAAACCGCCACCATGGACGCAATCAAGAAGAAGATGCAGGCGATGAAGCTGGAGAAGGA  120
          M  D  A  I  K  K  K  M  Q  A  M  K  L  E  K  D

TAACGCCATGGACCGGGCGGATACCTTGGAACAGCAAAATAAGGAGGCCAACATCAGGGC  180
 N  A  M  D  R  A  D  T  L  E  Q  Q  N  K  E  A  N  I  R  A

       T        G  A  A CTT  G    G      A  AC T    C
TGAGAAGACCGAGGAGGAGATTCGCATCACGCATAAGAAGATGCAGCAGGTGGAGAATGA  240
 E  K  T  E  E  E  I  R  I  T  H  K  K  M  Q  Q  V  E  N  E

C  T       G     ATC   GCTGAA   A  C  CC A  G  A  G  G  C
ACTGGACCAGGTTCAGGAGCAGCTCTCTCTGGCTAATACTAAGCTTGAGGAAAAAGAAAA  300
 L  D  Q  V  Q  E  Q  L  S  L  A  N  T  K  L  E  E  K  E  K

    C CTCT  C
GGCTTTGCAGAATGCTGAGGGTGAGGTGGCCGCTCTTAACCGTCGCATCCAGCTGCTGGA  360
 A  L  Q  N  A  E  G  E  V  A  A  L  N  R  R  I  Q  L  L  E

AGAGGACCTGGAACGCTCTGAGGAGCGCCTCAACACCGCCACCACCAAGCTGGCCGAGGC  420
 E  D  L  E  R  S  E  E  R  L  N  T  A  T  T  K  L  A  E  A

TTCTCAGGCCGCCGACGAGTCCGAGCGCATGCGCAAGGTGCTCGAGAACCGCTCCCTGTC  480
 S  Q  A  A  D  E  S  E  R  M  R  K  V  L  E  N  R  S  L  S

CGACGAGGAGCGCATGGATGCCCTCGAGAACCAGCTTAAGGAGGCCCGTTTCCTGGCTGA  540
 D  E  E  R  M  D  A  L  E  N  Q  L  K  E  A  R  F  L  A  E

GGAGGCCGACAGGAAATACGACGAGGTTGCCCGTAAGCTGGCCATGGTTGAAGCCGACCT  600
 E  A  D  R  K  Y  D  E  V  A  R  K  L  A  M  V  E  A  D  L

TGAGCGTGCTGAGGAGCGTGCCGAGACTGGTGAATCAAAGATCGTCGAGCTTGAGGAGGA  660
 E  R  A  E  E  R  A  E  T  G  E  S  K  I  V  E  L  E  E  E

GCTGCGTGTCGTTGGCAACAACTTGAAGTCTCTTGAAGTGTCTGAGGAGAAGGCCAACCA  720
 L  R  V  V  G  N  N  L  K  S  L  E  V  S  E  E  K  A  N  Q

GCGTGAGGAGGCTTACAAGGAGCAGATCAAGACCCTTGCCAACAAGCTGAAGGCGGCTGA  780
 R  E  E  A  Y  K  E  Q  I  K  T  L  A  N  K  L  K  A  A  E

GGCTCGAGCTGAGTTCGCCGAGAGGTCTGTGCAGAAGCTCCAGAAGGAGGTCGACAGGCT  840
 A  R  A  E  F  A  E  R  S  V  Q  K  L  Q  K  E  V  D  R  L

CGAAGACGAACTGGTTAACGAAAAGGAGAAGTACAAGTCCATTACCGACGAGCTGGACCA  900
 E  D  E  L  V  N  E  K  E  K  Y  K  S  I  T  D  E  L  D  Q

GACTTTCAGCGAACTGTCTGGCTACTAAACACTCTCTGCTCCAAACTGTTCTGCCATCTC  960
 T  F  S  E  L  S  G  Y  *

TCTTCCTATGCCCTCAGCTGGCCTGTAACCTATTTTTTCATAAGCTTATGTAATTCAGTT 1020
TATAAGAATTCTTTTTACTTTTCCTTCTTTTTATGTGTTGCATTTGACCTCCAATTGAGT 1080
CAGTATCATCACTAAATCATTCGATATCGTGGTTAAGTCTGCCATTGAGGTAATTTTAAT 1140
GTTATTAAACTTAAATTTATTCAGGAAACTTAATTTTGAATTTTTTTTCAAAATTTTAGG 1200
TTTCATGTACTCTATGGCTTAATAACATAAAGAAATAAATATTTATTATCAAAAAAAAAA 1260
AAAAAAAAAGCCATGTTGCTCTCAAGGAAAAAAGAAGAAAACATGAAAAAAGATGAAAA 1320
AAGGGGAAAAAACCTTCCCTGAATACCTCTTGTCTTTCACGTTCAAGACAAAGTTATGCG 1380
TCACCCTCAGGGGCTTCGTCGCCATAATGGGATACCAAGAGCGCCATGATTTATTTACTT 1440
TCATATTAAGGAAGGACAACGTCATCATCATAAGTTAACAAGAAACATCTGTTATCTTCA 1500
GTTCTGTGGCTTATTTCCACTGTTAATTTTTAATTAGTATTAACATCACTTATTCTTTAT 1560
CTCTCTGTCTCTCTCTGATCTTTTCTTCTGTGCTCATTGTTGCTCTGTGTCTGTACCCTC 1620
TGAAACTGTGTACTCCTGCTGTGTACGTACTCCTGCTGTGTGCGTACTTGTGCGTGTGCG 1680
TAACTGTGTTGTATGCGTACTGTTGTGAGGGTGTGTGTTAGTGCAGGCTCGCCCCCAACT 1740
CAGGCTGACCCCACACCGTCCTGGCGGGGCCAACAAGTATGTGTCTCGGGAACCCAGCCA 1800
CCGTCACGTAGTTTGCTGCGGCAGGCGTGTGTGGGGCGGCCGGAAGCTGTCCTAACCAAG 1860
TGGCGGGGGACATCCTACGGCCAGGGCGCCTCAAACCTGCCTCCTGAAGGACCTGGGCGT 1920
AGGTCCGTAGGGCGTGCGTGCCGAGTCCTCAGGTGAAGGGGGCATCATCGCCAGTGGTCA 1980
CATAGGATTCCCGCGTCGCAACAATTATTTTATTCTTTTCATATCACAGTCTTATCATTG 2040
TACGACTCGATCATTGATACTGTTGATGTGTTTCAGATATAAGTAATAATAATGATAACT 2100
```

Figure 2-2 Nucleotide and deduced amino acid sequences of cDNA encoding lobster slow muscle tropomyosin (*sTm1*). The middle row is cDNA sequence for *sTm1* and the bottom row is deduced amino acid sequence. In the top row, bases replaced in cDNA for fast muscle tropomyosin (*fTm*) are indicated. The putative exon 2 encoding region were boxed in red.

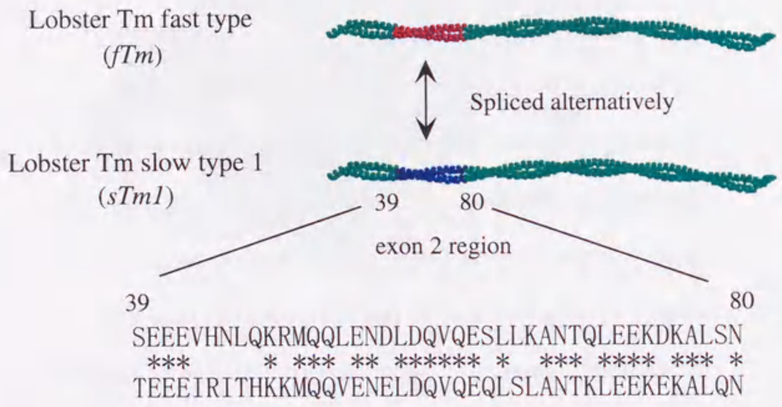

Figure 2-3 Amino acid sequence differences between two isoforms of lobster tropomyosin, *fTm* and *sTm1*. In the upper half, the position of the exon 2 region, either in red or in blue, is indicated within the entire tropomyosin molecule. In the rest, in green, two isoforms share the common sequence. In the lower half, the amino acid sequence 39-80 is compared between *fTm* (the top row) and *sTm1* (the bottom row). The asterisks indicate the residues common to both.

Experimental Procedures

Complimentary DNA cloning and constructions of the transfer vectors for tropomyosin expression

The *fTm* and *sTm1* cDNAs were amplified from a lobster fast and slow muscle cDNA bank by PCR and were subcloned into the pVL1392 transfer vector at the *Xba*I and *Bam*HI sites. The PCR primer sequences were designed so that the amplified fragments contained the entire tropomyosin coding sequences as well as *Xba*I or *Bam*HI sites for subcloning within each primer. The primers used were 5'-GGTCT AGAAA CTCCT AAAAA ACCGCC ACC-3' and 5'-TTGGA TCCGA GAGTG TTTAGT AGCCA GAC-3', respectively. The DNA manipulations were performed basically as described in Sambrook et al. [45].

Expression of various tropomyosins in insect cell

Recombinant baculovirus for each construct was obtained using Baculogold transfection kit (Pharmingen). Plaque purification and amplification of recombinant viruses were performed according to Summers and Smith [46]. Sf9 cells were cultured in modified SF900II medium, which contained 90 % of SF900II (Gibco BRL), 9 % of Grace's insect medium supplemented (Gibco BRL) and 1 % of fetal calf serum (Sigma) at 27 ℃. In suspension culture, Pluronic F68 (Gibco BRL) was added to a final concentration of 0.2 %. For expression of tropomyosin isoforms, a Cell Master Controller (Wakenyaku) was used which enables us to control the level of oxygen in the media to 60-70 % saturation. A three liter culture of Sf9 cells (about 2×10^6 cells/ml) in a spinner flask was infected with recombinant virus at multiplicity of 0.5-2. After 48-52 hours post-infection, infected cells were collected by centrifugation at 4,000 rpm for 10 min using Beckman J6 rotor, and the cells were kept frozen at -80 ℃ for storage and cell lysis.

Preparation of tropomyosin isoforms

Frozen cells were thawed at room temperature. Sf9 cells were lysed by

suspending them in the hypotonic lysis buffer; 20 mM Tris-HCl pH 8.0, 0.5 mM EDTA, 5 mM DTT and 1 tablet of protease inhibitor cocktail Complete™ (Boehringer Mannheim) per 50 ml solution. After the cells were lysed, the cell debris was removed by centrifugation. To the cell lysate, sodium chloride was added to a final concentration of 150 mM and the lysate was subjected to an ammonium sulfate fractionation. The fraction 35-70 % was collected, being dissolved in 20 mM Tris-HCl pH 8.0, 1 mM EDTA and 5 mM DTT, and dialyzed against the same buffer. After the dialysis, the solution was heated up at 80-85 ℃ for 10 min, and then the solution was cooled down to room temperature. After denatured proteins were removed by centrifugation, the pH of the supernatant was adjusted to pH 4.5 for an isoelectric precipitation. The resulting pellet, which contains tropomyosin, was dissolved in 10 mM Tris-HCl pH 8.0 and 0.5 mM DTT, and dialyzed against the same buffer. The tropomyosin solution was applied to a Mono-Q HR 16/10 column (Pharmacia) which was pre-equilibrated with the same buffer as used for the dialysis. All the tropomyosin preparations in this study were eluted from the Mono-Q column with a 90 ml gradient of 250-500 mM NaCl. The tropomyosin containing fractions from the Mono-Q column were dialyzed against 100 mM potassium-phosphate buffer pH 6.8, 300 mM KCl and 0.5 mM DTT and applied to a Gigapito (Hydroxyapatite) column (Seikagaku corporation). From the column, tropomyosin was eluted with 400 ml gradient of 100-500 mM potassium phosphate buffer.

Before being used for each measurement, the tropomyosin preparations were denatured by 4 M guanidine hydrochloride and renatured by dialysis at 4 ℃ against each solution used for a particular experiment.

Preparation of other proteins

Actin and myosin subfragment 1 (S1) were prepared from rabbit white muscle, as described by Suzuki and Mihashi [47] and by Weeds and Taylor [Weeds, 1975 #42], respectively.

Viscosity measurements

Measurements were carried out at 25 ℃ with an Ostowald type capillary viscometer, using 1 ml of sample solution, and the flow rate of the buffer alone was 42 sec. Before measurements, each sample was dialyzed against 10 mM Tris-HCl pH 8.0, 10 mM KCl, and 0.5 mM DTT, and the concentrations of tropomyosin and KCl were adjusted by dilution and/or the addition of a small volume of a concentrated KCl solution.

Circular dichroism measurements

Circular dichroism spectra were obtained using a JASCO model J-720 or J-725 spectropolarimeter using a cell of 1 mm path length. The temperature dependence of circular dichroism was monitored at 222 nm at 1 ℃ intervals with an equilibration time of 3 min. The samples contained 2 μM of protein in 10 mM Tris-HCl pH 8.0 with or without 250 mM NaCl.

OmpT digestion

The reaction was carried out at 37 ℃ by mixing tropomyosin with bacterial cells. Overnight culture of *E. coli*, XLI-blue for OmpT plus and AD202 for OmpT minus, were collected and washed twice by a solution containing 10 mM Tris-HCl pH 8.0 and 0.5 mM DTT. Then 0.16 A (OD: 600nm) of *E. coli* cells were mixed with 0.2 mg/ml tropomyosins in 10 mM Tris-HCl pH 8.0 and 0.5 mM DTT. The reaction was stopped by centrifugation, and the supernatant was analyzed by a 15% SDS-PAGE gel which was stained by Coomassie Brilliant Blue.

Proteolytic analysis using trypsin and chymotrypsin

Proteolysis was performed as described by Pato et al. [48] and Ueno [49]. 0.5 mg/ml tropomyosin in 10 mM Tris-HCl pH 8.0 and 0.5 mM DTT, was digested at 25 ℃. Each reaction was started by adding trypsin or chymotrypsin to a final concentration of 260 ng/ml or 1 μg/ml, respectively, and was terminated by adding soybean trypsin inhibitor to a final concentration of 40 μg/ml or PMSF to a final concentration of 4 mM. SDS-PAGE was carried out using a 15 % acrylamide gel, which was stained with

Coomassie Brilliant Blue.

Mass spectrometry

Samples for mass spectrometry were first digested by trypsin or chymotrypsin for 30 min or 2 hours, respectively, as described above. The digested sample was concentrated, and the buffer was replaced by 10 mM Tris-HCl pH 8.0 and 5 M guanidine hydrochloride by using a Centricon 10 (Amicon) concentrator. The samples were then applied to a Superdex 70 10/30 gel filtration column (Pharmacia) equilibrated with 10 mM Tris-HCl pH 8.0 and 5 M guanidine hydrochloride, at the flow rate of 0.2 ml/min. The fraction containing peptides with a chain mass in the range of 20-30 kDa was collected, desalted, and subjected to mass spectrometry measurements, as described by Taniguchi et al. [50].

Actin binding assay

Co-sedimentation combined with densitometry of the stained gels was employed. A mixture of 21 μM actin and 0.2-8 μM tropomyosin was incubated at room temperature for 1.5 hour in 70 μl of 13 mM HEPES-NaOH, pH 7.0, 60 mM NaCl, 3 mM $MgCl_2$, 0.5 mM DTT, and 1 mM NaN_3. After centrifugation at 70,000 rpm for 30 min at 20 ℃ in a Beckman TL-100 centrifuge using a TLA 100 rotor, the supernatant and the pellet were separately subjected to SDS-PAGE on 12% acrylamide gels. The gels were stained with 0.1% Fast Green, and the resulting gel patterns were digitized by an image scanner (GT-8000, Epson), and transferred to a Macintosh computer for further analysis using NIH-Image version 1.59. The amounts of tropomyosin and actin in the gels were determined by comparing the integrated optical densities against standards obtained from known amounts of tropomyosin and actin. The apparent binding constant and the Hill coefficient of actin binding of tropomyosin isoforms were determined by fitting the data points obtained by co-sedimentation with a curve based on the Hill equation using a routine in the MicroCal Origin 5.0 software.

ATPase assay

The acto-S1 ATPase rate was measured by the time course of phosphate liberation in 20 mM Tris-HCl pH 7.5, 40 mM KCl, 3 mM $MgCl_2$, and 0.5 mM DTT at 25 ℃. Each reaction was started by adding the appropriate concentration of Mg-ATP. From the reaction mixture, an aliquot was removed every minute and the reaction was stopped by diluting the aliquot ten-fold with 0.2 M perchloric acid. The concentration of free phosphate was determined by colorimetry of malachite green at 650 nm; to the aliquot an equal volume of MG solution (0.2 % sodium molybdate, 0.03% malachite green oxalate (gift from Dr. T. Kodama), and 0.05 % Triton X-100 in 0.7 M HCl was added and the mixture was incubated for 25 min at 25℃.

Preparation of NEM-S1

NEM-S1 was prepared as follows; 1 mM *N*-ethyl maleimide (NEM) was mixed with 100 μM S1 in 20 mM imidazole-HCl pH 7.0 and incubated at 25 ℃ for 30 min. Reaction was stopped by adding DTT at a final concentration of 20 mM, and then applied to Econopack 10DG column (BioRad). The collected fractions were mixed again with 10-fold excess of NEM and incubated at 25 ℃ for 30 min. After the reaction was stopped by adding 20-fold excess of DTT relative to NEM, the mixture was applied to an Econopack 10DG column. The collected fractions containing NEM-S1 were dialyzed against 0.5 mM sodium bicarbonate. The extent of NEM modification and the concentration of NEM-S1 were determined as described in Nagashima and Asakura [51].

Measurement of NEM-S1 ATPase

The time course of phosphate liberation was measured as described above using the solutions of the same composition. The concentrations of proteins used were, 10 μM actin, 4 μM tropomyosin, 0.5 μM S1, and 0-9 μM NEM-S1.

S1-ADP binding to actin-tropomyosin filament

Binding of S1-ADP to the reconstituted actin-tropomyosin filament was

measured by monitoring the fluorescent intensity of pyrene-labeled actin [52]. Actin was labeled by pyrene iodoacetamide, as described by Kouyama and Mihashi [53]. The extent of labeling was more than 95 % in this study. For the S1 titration study, the solution conditions of McKillop and Geeves [54] were slightly modified: 0.5 μM pyrene actin, 1 μM phalloidine, and 0.2 μM tropomyosin in 20 mM MOPS-NaOH pH 7.0, 140 mM KCl, 5 mM $MgCl_2$, 0.5 mM DTT, 2 mM ADP, 1 μM hexokinase, 2 mM glucose, and 50 μM Ap5A. Fluorescence emission was measured at 407 nm after excitation at 365 nm with a Hitachi F-3010 fluorescence spectrophotometer.

Results

Expression and purification of tropomyosin isoforms

The lobster tropomyosin isoforms used in this chapter were expressed in Sf9 insect cells. When tropomyosin variants are expressed in Sf9 cells, but not expressed in *E. coli*, tropomyosin molecule has an acetylated N-terminus like authentic tropomyosin, and N-terminal acetylation is essential for its function [17-19]. The expressed lobster tropomyosin isoforms, *fTm* and *sTm1* were purified as described in "Experimental Procedures", and the final products are shown in Figure 2-4.

Strength of head-to-tail interaction

It is widely believed that seven to nine amino acid residues at each end of tropomyosin are involved in the head-to-tail interaction [11]. The strength of the head-to-tail interaction between tropomyosin molecules *in vitro* was estimated by viscometry at low ionic strengths (see also Chapter 4 for related discussions). The isoform *sTm1* showed substantially higher viscosity, by a factor of two to three, as compared with *fTm* (Figure 2-5A&B). This indicates that the *in vitro* head-to-tail interaction of *sTm1* is stronger than that of *fTm*, although the region of the replaced amino acid sequence does not directly contribute to the head-to-tail interaction. The results suggest that the conformation of the N- and/or C-terminus should be affected by the structure of the internal region of the molecule, the putative exon 2 encoding region of amino acids 39-80.

Thermal stability

The effect of the sequence of residues 39-80 on the overall stability of lobster tropomyosin isoforms was evaluated by measuring the ellipticity at 222 nm. Figure 2-6A shows the melting transition profiles of *fTm* and *sTm1*. The overall profiles were similar to each other, with the half-melting temperature at 37-38 ℃ (Figure 2-6B), indicating that the thermal stabilities, and therefore, the α-helix conformations, of *fTm* and *sTm1* are almost identical.

Figure 2-4 Purified lobster tropomyosin isoforms used in this study.

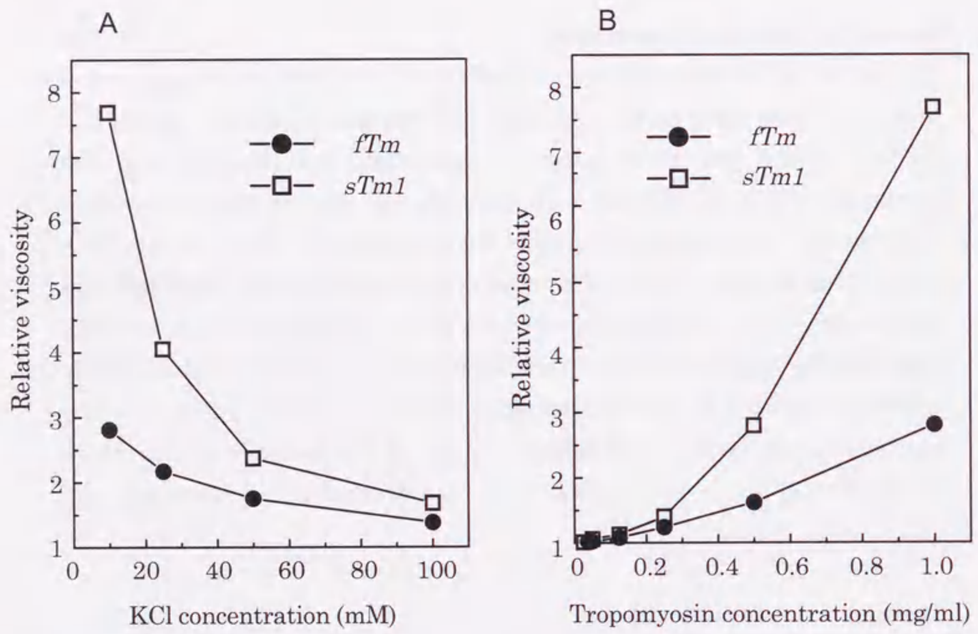

Figure 2-5 Relative viscosity of lobster tropomyosin isoforms. The solution contained appropriate concentrations of KCl and tropomyosin of either species, 10 mM TrisHCl pH 8.0, and 0.5 mM DTT. (A) The effect of ionic strength on viscosity, with a fixed concentration of tropomyosin at 1 mg/ml. (B) The effect of protein concentration on viscosity with the KCl concentration fixed at 10 mM. Symbols: filled circles for *fTm* and open squares for *sTm1*. Viscosity measurements were carried out using an Ostowald type capillary viscometer at 25 ℃.

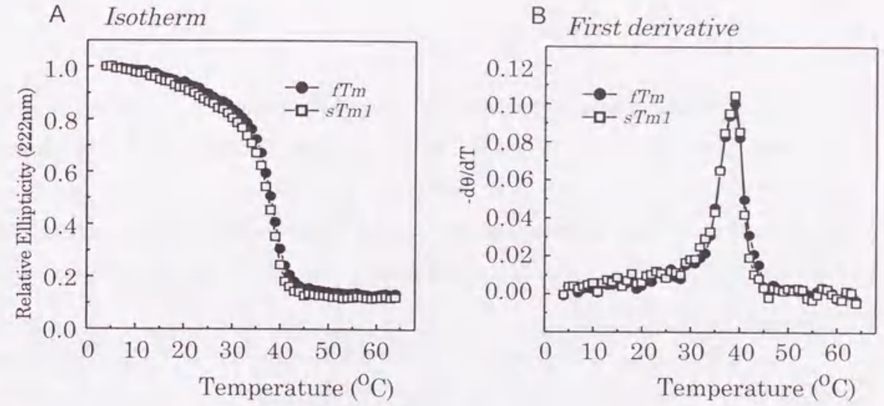

Figure 2-6 The thermal unfolding profiles of lobster tropomyosin isoforms in a low salt solution, similar to the condition employed for the viscometry and proteolysis. (A) The temperature dependence of α-helix content measured as the ellipticity at 222 nm. Solution conditions: 2 μM tropomyosin in 10mM TrisHCl pH8.0. Data points represent the average of three independent measurements. Relative ellipticity at temperature T is given by $[\theta]^T$-$[\theta]^{64}$ / $[\theta]^4$-$[\theta]^{64}$, where $[\theta]^4$ and $[\theta]^{64}$ are the ellipticity at 4 ℃ and at 64 ℃, respectively. (B) First derivative of the data in (A). Symbols: filled circles for *fTm* and open squares for *sTm1*.

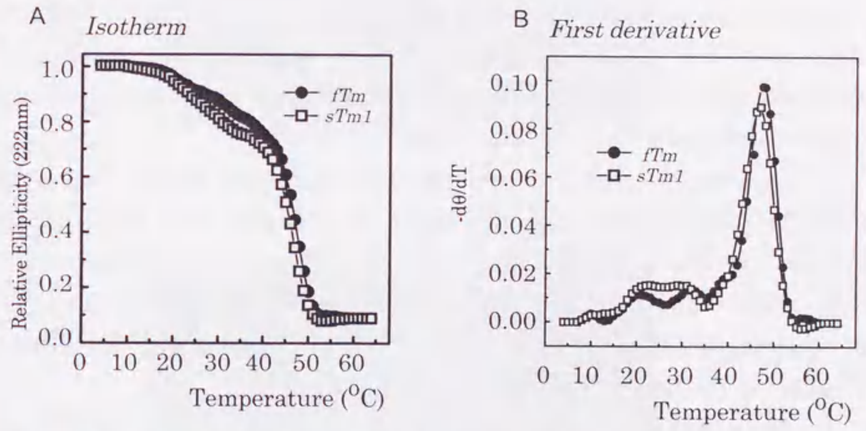

Figure 2-7 The thermal unfolding profiles of lobster tropomyosin isoforms in a high salt solution. (A) The temperature dependence of α-helix content measured as the ellipticity at 222 nm. Solution conditions: 2 μM tropomyosin in 10mM TrisHCl pH8.0 and 250mM NaCl. Data points represent the average of three independent measurements. Relative ellipticity at temperature T is given by $[\theta]^T$-$[\theta]^{64}$ / $[\theta]^4$-$[\theta]^{64}$, where $[\theta]^4$ and $[\theta]^{64}$ are the ellipticity at 4 ℃ and at 64 ℃, respectively. (B) First derivative of the data in (A). Symbols: filled circles for *fTm* and open squares for *sTm1*.

Moreover, under the solution conditions employed for the viscometry and proteolysis, neither *fTm* nor *sTm1* was significantly unfolded. On closer inspection of the profiles, however, it turned out that at 25 ℃ the loss of α-helical content of *sTm1* is by about 10 % more than that of *fTm*, which might partly account for the greater susceptibility of *sTm1* to proteolysis (see below).

It is known that difference in thermal stability of tropomyosin is easier to detect under high salt conditions (Figure 2-7), rather than under low salt as for Figure 2-6. The profiles were different from each other at relatively lower temperature region, from 15 ℃ to 35 ℃. Figure 2-7B shows the first derivatives of the plots in Figure 2-7A, indicating substantial differences in the melting transition profiles between two isoforms.

Proteolysis analysis

The results of the viscometry (Figure 2-5) suggested that the conformations of the two isoforms would differ from each other not only within the region of amino acids 39-80 but also outside of the region. In order to test this, limited proteolytic digestions with OmpT, trypsin, and chymotrypsin were performed to detect local conformational differences [19, 48, 49].

In order to detect any conformational difference in the N-terminal region between the isoforms, the *ompT* gene product was used. OmpT protease is a periplasmic protein of *E. coli* and is known to cleave specifically between Lys-6 and Lys-7 of tropomyosin in a manner highly dependent on the conformation of the N-terminus. The results (Figure 2-8A) indicated no difference in the time course of cleavage patterns.

Next, trypsin (Figure 2-8B) and chymotrypsin (Figure 2-8C) were used. In either case, *fTm* was mainly cleaved into halves, whereas *sTm1* gave rise to not only halves but also larger fragments.

To determine chain weights of the larger fragments, the electron spray mass spectrometry was employed. For tryptic digestion, the reaction was terminated after 30 min and the sample was fractionated by a gel filtration on a Superdex-75 column (Figure 2-9A). The fractions 1-4

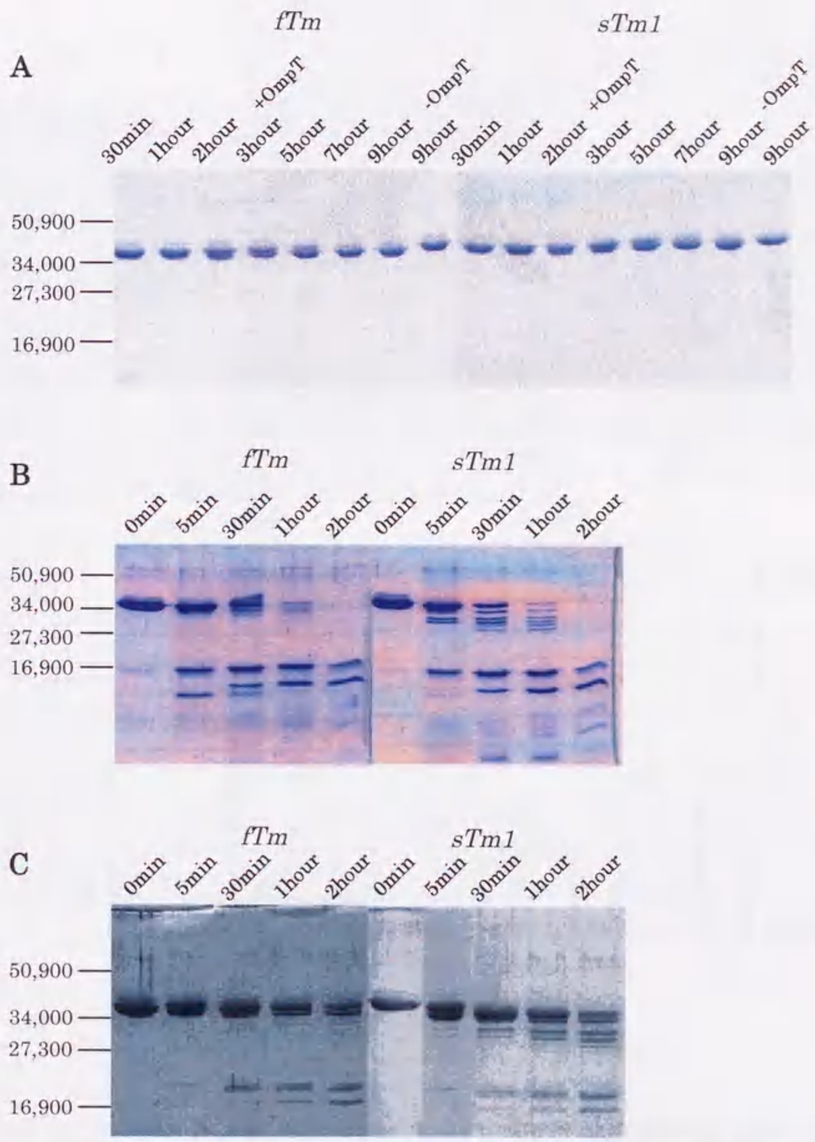

Figure 2-8 Time courses of proteolytic digestion patterns on SDS-PAGE. The enzyme employed are OmpT in A, trypsin in B and chymotrypsin in C. The numerals on the left-hand side of each gel indicate molecular weights of markers.

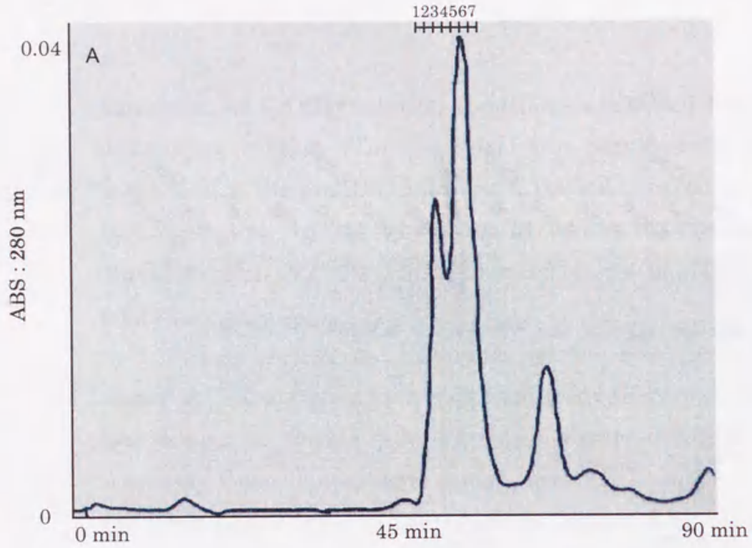

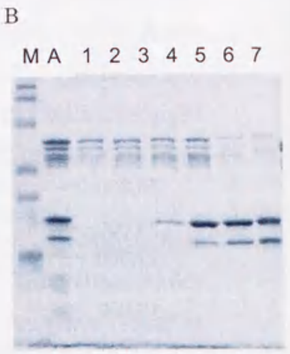

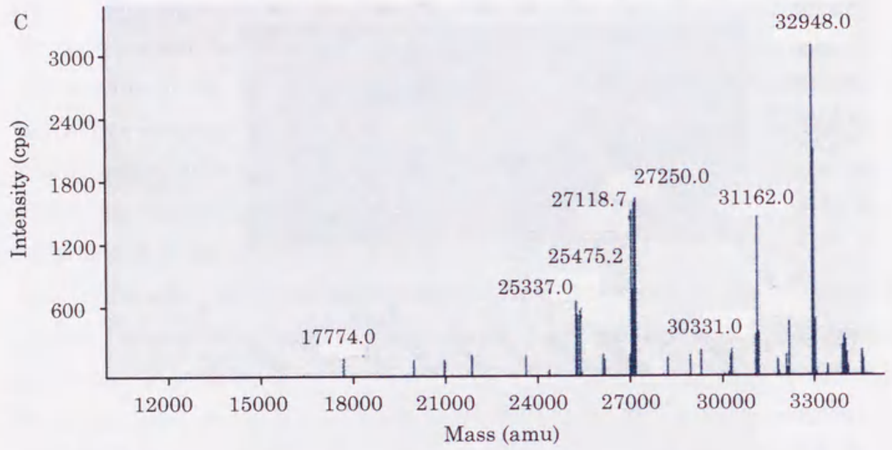

Figure 2-9 Identifying *sTm1* specific tryptic fragments. *sTm1* was digested as described in Experimental Procedures. (A) The separation of tryptic fragments of *sTm1* using a Superdex 75 10/30 column. (B) Lane M is the molecular weight marker, while lane A is the sample before fractionation. Lanes 1-7 correspond to the fractions 1-7 in (A). (C) The mass spectrum of the tryptic fragments (the combined fractions 1-4) of *sTm1*.

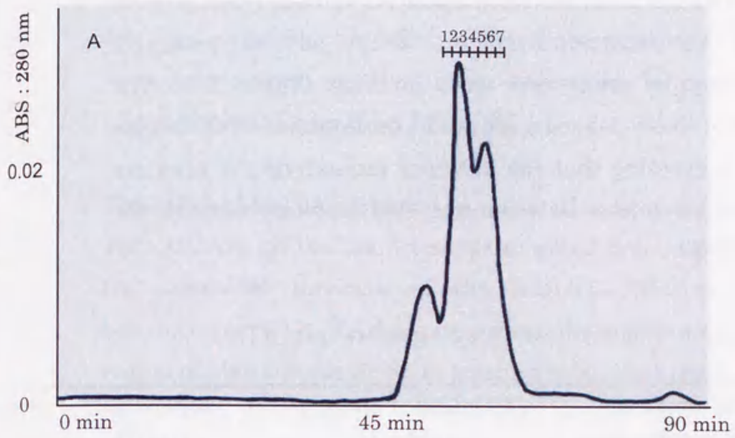

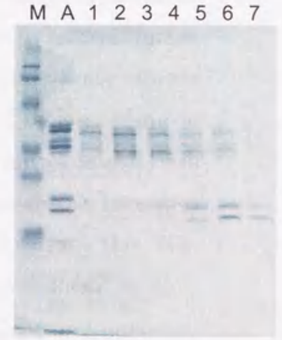

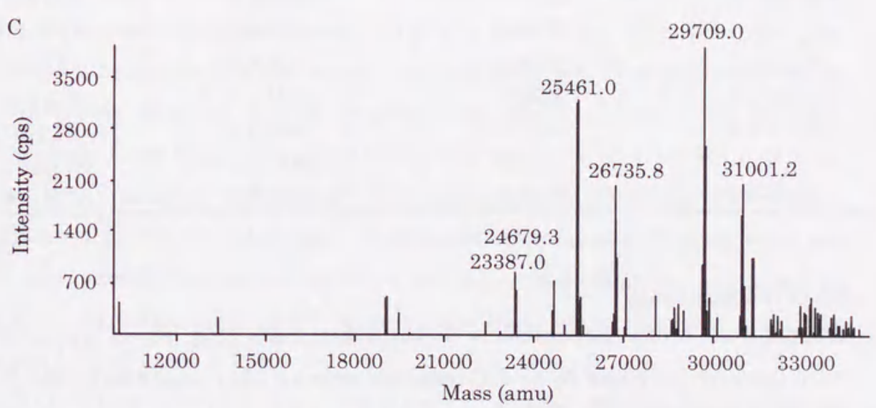

Figure 2-10 Identifying *sTm1* specific chymotryptic fragments. *sTm1* was digested as described in Experimental Procedures. (A) The separation of chymotryptic fragments of *sTm1* using a Superdex 75 10/30 column. (B) Lane M is the molecular weight marker, while lane A is the sample before fractionation. Lanes 1-7 correspond to the fractions 1-7 in (A). (C) The mass spectrum of the chymotryptic fragments (the combined fractions 1-3) of *sTm1*.

containing larger fragments (Figure 2-9B) were combined and analyzed by mass spectrometry (Figure 2-9C). For chymotryptic digestion, the digestion time was 2 hours and the fractions 1-3 were collected and analyzed (Figure 2-10A,B,C). Although the tryptic fragments could not be assigned, assignments of chymotryptic fragments were possible (Table 2-1). The results show that most of these cleaved sites are located outside of the region of amino acids 39-80, suggesting that the different proteolytic patterns are due to conformational differences between the two isoforms outside the region of amino acids 39-80.

Table 2-1 Assignment of chymotryptic fragments from *sTm1*.

Measured chain weights (I)	Assignment a.a. residue no.	Calculated chain weights (II)	Differences (I)-(II)
31001.2	4-270	31003.7	-2.5 (-0.008%)
29709.0	12-267	29716.0	-7.0 (-0.024%)
	19-274	29704.0	+5 (+0.017%)
26735.8	26-256	26736.8	-1 (-0.004%)
25461.0	2-221	25461.3	-0.3 (-0.001%)
24679.3	26-239	24679.4	-0.1 (-0.0004%)
	57-270	24678.5	+0.8 (+0.003%)
23387.0	20-221	23385.8	+1.2 (+0.005%)

Actin binding assay

Tropomyosin binds cooperatively to actin filaments [55]. For a cooperative actin binding, both the N- and C-terminal regions play important roles [31]. Since a conformational difference in the terminal regions between the two isoforms was implied from our viscometry, the actin binding of the both tropomyosin isoforms was measured by cosedimentation experiments followed by colorimetric analysis of the proteins on SDS-PAGE gels. The colorimetry had to be employed, because unlike rabbit skeletal muscle α- and β-tropomyosin, neither isoform of lobster tropomyosin has a cystein at residue 190 that can be readily isotopically labeled without substantially impairing the functions. The results (Figure 2-11) indicate that *sTm1* has

actin affinity that is about three times higher than that of *fTm*; the apparent dissociation constants were 1.3 $\pm 0.2\times10^{-7}$ M for *sTm1* and $4.4\pm0.6\times10^{-7}$ for *fTm*. The Hill coefficient was obtained as 1.2 ± 0.3 for *sTm1* and 1.9 ± 0.4 for *fTm*, although the difference was not significant, due to the scattered data points that resulted from difficulties in determining tropomyosin concentrations lower than 7×10^{-8} M.

The effect of tropomyosin on the interaction between actin and myosin S1

Tropomyosin makes the actomyosin interaction cooperative, as indicated by the sigmoidal increase in the acto-S1 ATPase rate versus the S1 concentration [40]. To determine how the amino acid replacements in the region of amino acids 39-80 of tropomyosin affect the cooperative actomyosin interaction, the acto-S1 ATPase rate versus the S1 concentration in the presence of either of the two isoforms were measured (Figure 2-12A). Throughout the S1 concentration range examined, up to the S1 to actin ratio of 5.5, *sTm1* inhibited the acto-S1 ATPase rate more than *fTm* did. No activation was observed with either of the two isoforms. This is in contrast to the vertebrate striated muscle tropomyosin, which activates the acto-S1 ATPase rate more than that of acto-S1 alone at an S1 to actin ratio of 2 or higher [40]. This was not because the amount of tropomyosin added was insufficient, leaving a substantial number of tropomyosin binding sites on actin unoccupied. The inhibitory effect was saturated when the tropomyosin to actin molar ratio reached 1/7, whether the S1 to actin ratio was low (1/3) or high (10/3) (Figure 2-12B).

To know whether the activation of acto-S1 ATPase occurs when lobster tropomyosin isoforms are on actin-filaments, the acto-S1 ATPase in the presence of NEM-S1 was measured (Figure 2-13). Low concentrations of NEM-S1 induced the activation of acto-S1 ATPase in the presence of lobster tropomyosin. This result indicates that actin-lobster tropomyosin filaments have ability to activate the acto-S1 ATPase [51].

In order to rule out the possibility that the observed regulatory action of lobster tropomyosin on the actin filament, being independent of the

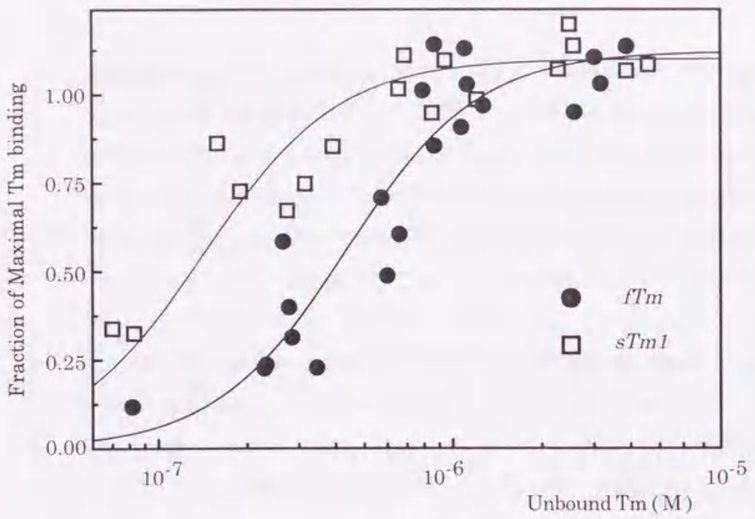

Figure 2-11 Actin binding of lobster tropomyosin isoforms. Tropomyosin (0.2-8 μM) was cosedimented with 21 μM actin at 20 ℃ in 13 mM HEPES-NaOH pH 7.0, 60 mM NaCl, 3 mM $MgCl_2$, 0.5 mM DTT, and 1 mM NaN_3. Solid curves were drawn using the Hill equation, with the apparent binding constant of $4.4 \pm 0.6 \times 10^7$ M^{-1} and the Hill coefficient of 1.9 ± 0.4 for *fTm*, whereas $1.3 \pm 0.2 \times 10^7$ M^{-1} and 1.2 ± 0.3 were used for *sTm1*. Symbols: filled circles for *fTm* and open squares for *sTm1*.

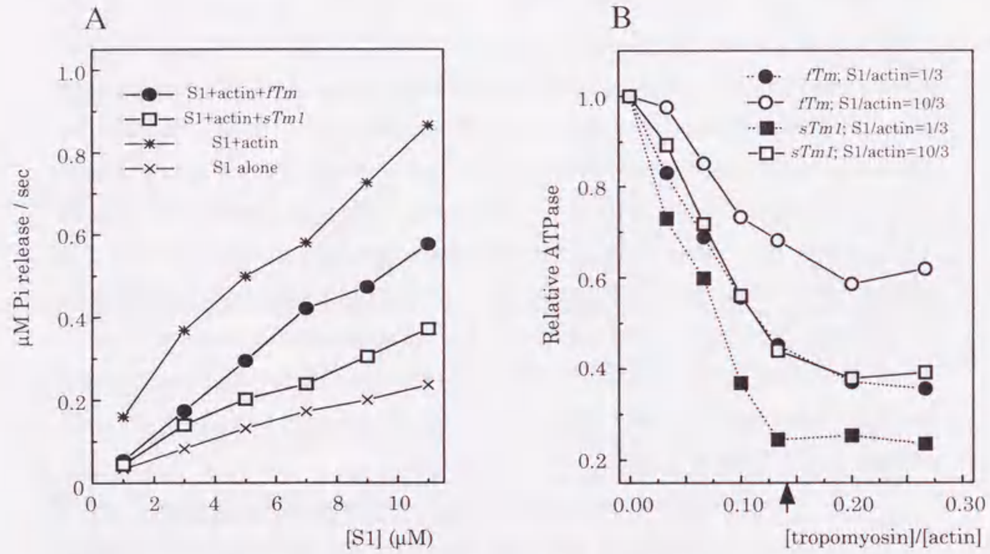

Figure 2-12 The effect of *fTm* and *sTm1* on the acto-S1 ATPase rate. The solution conditions: 20 mM TrisHCl pH 7.5, 40 mM KCl, 3 mM $MgCl_2$, and 0.5 mM DTT at 25 ℃. (A) The relationship between the acto-S1 ATPase rate and the concentration of S1. Protein concentrations added were 2 μM actin and 0.5 μM tropomyosin. Symbols: filled circles for actin with *fTm*, open squares for actin with *sTm1*, asterisks for actin alone without tropomyosin, and crosses for S1 alone. (B) The relationship between the acto-S1 ATPase rate and the molar ratio of tropomyosin to actin. Experiments were repeated at two different ratios of S1 to actin, 1 / 3 and 10 / 3, at the fixed actin concentration of 3 μM. The arrowhead on the horizontal axis indicates the molar ratio of tropomyosin to actin of 1 / 7. Symbols: circles for *fTm* and squares for *sTm1*, filled symbols with dotted lines for the molar ratio of S1 to actin of 1 / 3, and open symbols with solid lines at the molar ratio of S1 to actin of 10 / 3.

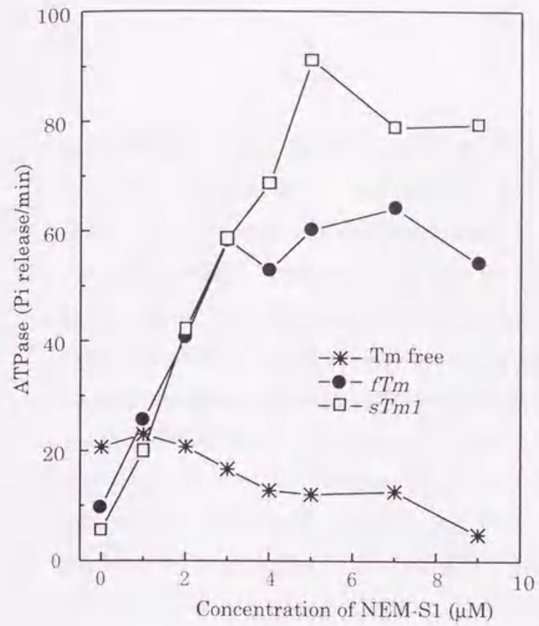

Figure 2-13 The effect of the NEM-S1 on the lobster tropomyosin-actin complex. The solution conditions: 20 mM TrisHCl pH 7.5, 40 mM KCl, 3 mM $MgCl_2$, and 0.5 mM DTT at 25 ℃. Protein concentrations were; 10 μM actin, 0.5 μM S1, with (4 μM) or without tropomyosins, and 0-9 μM NEM-S1. Symbols: circles for *fTm*, squares for *sTm1*, and asterisks for actin alone.

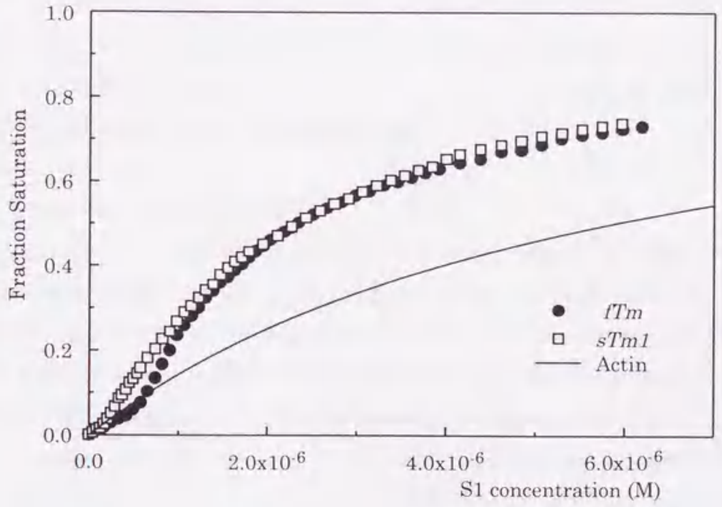

Figure 2-14 Binding of S1-ADP to actin-tropomyosin, measured as fluorescence intensity from pyrene-actin. S1 was added to the solution containing 0.5 μM pyrene actin, 1 μM phalloidine, and 0.2 μM tropomyosin in 20 mM MOPS-NaOH pH 7.0, 140 mM KCl, 5 mM $MgCl_2$, 0.5 mM DTT, 2 mM ADP, 1 μM hexokinase, 2 mM glucose, and 50 μM Ap5A. The solid line indicates the binding to actin alone, as expected from the dissociation constant of 5.6×10^{-6} M of the best fitted data points from 5 independent experiments. Symbols: filled circles for *fTm* and open squares for *sTm1*.

S1 to actin ratio, is due to reduced S1 affinity for actin-tropomyosin, the binding of S1-ADP to actin-tropomyosin was measured. The results indicated that S1-ADP bound cooperatively to reconstituted actin filaments for both *fTm* and *sTm1* (Figure 2-14). Between the two isoforms, *fTm* made the binding more cooperative as compared with *sTm1*; S1-ADP bound to actin-*sTm1* more strongly than actin-*fTm* at low concentrations of S1, and the binding curve of *fTm* increased more steep than that of *sTm1* after the initial lag.

Discussion

The present study was initiated, when Ms. Andrea Miegel and I observed remarkably higher viscosity at low salt with the slow muscle type (*sTm1*) lobster tropomyosin, as compared with the fast muscle type (*fTm*) isoform, in spite of the fact that the amino acids replaced between the two isoforms are limited to the internal region of amino acids 39-80. The present study indicated that the replacements in the region of amino acids 39-80 alter not only the properties of tropomyosin in solution but also the manner of its interactions with actin and myosin. Firstly, the properties of tropomyosin in solution were identified; isoform *sTm1* shows much higher low salt viscosity and higher susceptibility to proteolysis as compared with *fTm*. Secondly, the interaction of tropomyosin with actin was measured; isoform *sTm1* binds more strongly to actin than *fTm*. Thirdly, differences were also identified in the properties of the actin-tropomyosin complex; as compared with *fTm*, *sTm1* inhibits acto-S1 ATPase to a larger extent and makes the binding of S1-ADP to actin-tropomyosin less sigmoidal.

Solution properties of tropomyosin

Judging from the extraordinarily large difference of viscosity in the low salt, the two isoforms must have distinct conformations, at least in the terminal regions. It is interesting to ask which part of the terminal regions, either the N- or C-terminal region, is more affected by the internal sequence of amino acids 39-80. There are some evidences that the C-terminal region is mainly affected by the replaced sequence, although all the evidences for this proposal are indirect. Thus, conformational difference was not observed in the N-terminal region between the two isoforms by proteolysis with the *ompT* gene product (Figure 2-8). The *OmpT* protease is a periplasmic protein of *E. coli* [56] and is known to cleave between Lys-6 and Lys-7 of tropomyosin in a manner highly dependent on the conformation of the N-terminus [19]. Secondly, deletion of three residues at the C-terminus of *sTm1* gave rise to a drastic decrease of the low salt viscosity, down to the level of *fTm* (see

Chapter 3). This is in contrast to skeletal tropomyosin, which is hardly influenced by the same extent of deletion from the C-terminus [14, 15].

Therefore, it is plausible that the conformation of these terminal residues, especially those of *sTm1*, can be strongly influenced by the physical properties of the entire molecule, like the flexibility, which is dependent on the amino acid sequence in the internal region. Indeed, tropomyosin is a semi-flexible rod in solution [57, 58] and in the crystal [59], as well as on the actin filament [60, 61]. If tropomyosin lacked sufficient flexibility, then it could not bind to actin filament or follow the helical tracks around the filament axis. Moreover, without flexibility, tropomyosin could not change its manner of interaction with actin on the thin filament, which must be crucial for physiological functions like calcium regulation. It may be possible that each isoform gains an isoform-specific flexibility by choosing the correct exon at the right place, using alternative splicing. The distinct susceptibility to proteolysis shown in Figure 2-9&10 suggests that *sTm1* may be more flexible than *fTm*.

In order to understand how the amino acid replacements in the internal region influence the flexibility of the molecule, we closely looked at the amino acid replacements. No correlation, however, was found between the amino acid replacements and the distinct properties of the isoforms. Between the two isoforms studied here, 15 residues are replaced out of the 42 residues (through 6 heptad repeats) from 39 to 80. Among the hydrophobic residues at positions *a* and *d* of the heptad repeat, four residues (one at position *a* and three at position *d*) are replaced. It is not possible, however, to conclude that these replacements affect the stability of the coiled-coil [62, 63]. It is also known that an ionic pair between position *g* of one heptad repeat and position *e* of the next repeat could contribute to the coiled-coil stability [64, 65]. In the region of amino-acids 39-80, *fTm* has two potential ion pairs (Arg-35(*g*) to Glu-40(*e*), and Arg-49(*g*) to Glu-54(*e*)), whereas *sTm1* has one extra pair (Lys-70(*g*) to Glu-75(*e*)). The extra ion pair could make *sTm1* more stable or less flexible as compared with *fTm*. This appears to be inconsistent, however, with the present result that *sTm1* is more susceptible to

proteolysis.

Functions of alternative spliced exon 2

Two isoforms of lobster tropomyosin, *fTm* and *sTm1*, may be generated from the common gene by alternative splicing of exon 2. The analyses of lobster tropomyosin isoforms *in vitro* have shown that the local differences in amino acid sequence encoding putative exon 2 influence the conformation of the whole molecule including the functional terminal region, and modify the functions of the molecule. Tropomyosins are expressed as tissue specific isoforms in each tissue [27]. It may be possible that each isoform gains the isoform-specific flexibility on its functional domain by choosing a right exon at a right place using the alternative splicing. Tropomyosin has a long α-helical structure, and due to the nature of tropomyosin structure it may be easy to change the flexibility of whole molecule by changing the flexibility of a shorter part of α-helix [33]. Therefore tropomyosin can express tissue specific functions by alternatively splicing not only the exons encoding the functional region directly but also the exons, like exon 2, encoding the regions far from the functional region (Figure 2-15).

Properties of actin-tropomyosin complex

In the acto-S1 ATPase measurements in the presence of lobster tropomyosin, it was not observed any activation, even at the high S1 to actin ratio of 5.5 (Figure 2-12A), which is sufficient for the activation of acto-S1 ATPase with vertebrate tropomyosin on the actin filament [40]. It appears that the actin-lobster tropomyosin complex does not work as a cooperative/allosteric unit and loses the ability to activate the acto-S1 ATPase. However the S1-ADP binding to actin-tropomyosin indicated a cooperative interaction (Figure 2-14). Moreover, the cooperative activation of acto-S1 ATPase was observed when NEM-S1 was added (Figure 2-13) [51]. These results indicated that, in the framework of the two-state model [42], the equilibrium between the open- (ON-) and closed- (OFF-) states of the actin-lobster tropomyosin complex should be shifted further towards the closed-state as compared with

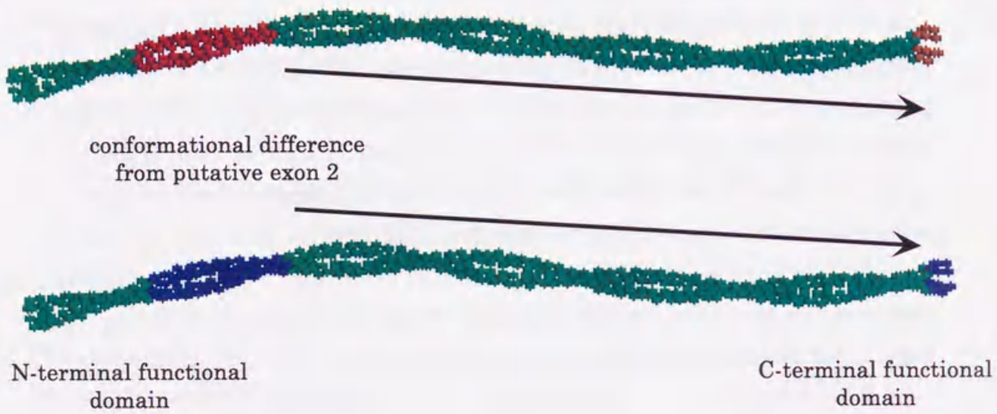

Figure 2-15 Differentiated functions could originate from the conformational difference at the C-terminal region, that in turn could be caused by the different conformation of the putative exon 2 encoding region.

the vertebrate tropomyosin.

In the same way, the present result that *sTm1* inhibits the acto-S1 ATPase more than *fTm* can be interpreted such that *sTm1* shifts the equilibrium towards more closed-state than *fTm* does. This interpretation, however, appears to be inconsistent with the results of the S1-ADP binding to actin-tropomyosin (Figure 2-14); at low S1-ADP concentrations, S1-ADP has higher affinity to actin-*sTm1* than to actin-*fTm*, which may be interpreted in terms of a greater equilibrium shift toward the open-state for *sTm1* than for *fTm*.

In order to interpret the data in Figure 2-14, a set of parameters was optimized by curve-fitting based on the two-state model (see Chapter 1, Figure 1-8) [42]; for *fTm*, K_T (the equilibrium constant for the open- and closed-states of the filament) = 0.22 ± 0.03, K_1 (the equilibrium constant for the weakly binding state) = 2.78 ± 0.16×10^4 M^{-1}, and a cooperative unit size of 7 were deduced. On the other hand, for *sTm1*, if K_T is to be smaller than the value for *fTm*, then a cooperative unit size of 21 should be assumed (K_T = 0.16 ± 0.05, K_1 = 2.43 ± 0.10×10^4 M^{-1}). For these curve-fittings, K_2 (the equilibrium constant for S1 isomerization) was fixed to 18 in both cases [66]. Essentially, within the actin-tropomyosin complex, *sTm1*, the isoform with higher flexibility and a stronger head-to-tail interaction, exerts a transition from the closed- to the open-state with a larger cooperative unit size, and *fTm*, with lower flexibility and a weaker head-to-tail interaction, is associated with a smaller cooperative unit size. This is compatible with the previous results of a comparative study on three species of tropomyosin, which have different C-terminal sequences, resulting in different strengths of the head-to-tail interaction. Gizzard muscle tropomyosin and *5a* tropomyosin, which both have stronger head-to-tail interactions, are associated with larger cooperative unit sizes, as compared with rabbit skeletal tropomyosin [67]. This comparative study postulated that the sequence, and therefore the structure, of the C-terminus should determine the strength of the head-to-tail interaction between two tropomyosin molecules on the actin filament, through which the cooperative unit size is

also affected [67]. The two isoforms, *sTm1* and *fTm*, analyzed in the present study, have an identical C-terminus sequence but give rise to different cooperative unit sizes. This could be accounted for by the distinct C-terminal conformations of the two isoforms. The question remains as to how the internal sequence of amino acids 39-80 alters the conformation of the C-terminal region of the molecule on the actin filament.

Chapter 3

Mapping of C-terminal functional domains of tropomyosin.

Introduction

The importance of the C-terminus for the function of striated muscle tropomyosin is well established. The deletion study using carboxypeptidase A demonstrated that, when C-terminal 9-11 residues are removed, the head-to-tail interaction of tropomyosin is abolished and the affinity of tropomyosin for actin is greatly reduced [14, 15]. However when proteolytic deletions are employed to remove the residues, the results are ambiguous because of heterogeneity of the preparations.

In the present study, to circumvent this problem, recombinant proteins were used. A series of C-terminal deletion mutants were expressed in Sf9 cells and the functional domains in the C-terminal region were mapped.

Experimental Procedures

Construction of *sTm*1 deletion mutants

The cDNA cloning, DNA sequencing and subcloning of *sTm*1 were already described in "Experimental Procedures" of Chapter 2. Constructions of transfer vectors for a series of *sTm1* deletion mutants, which were deleted from the C-terminal 3, 4, 5, 6, 7 and 11 amino acid residues, were carried out by PCR. Oligonucleotides which were used for PCR shown in Table 3-1 were designed on the basis of sequence in Figure 2-2, and were also designed so that the PCR product had a *Xba*I site upstream of the initiation codon and a *Bam*HI site downstream of the termination codon. Each PCR product was inserted into pVL1392 at the sites of *Xba*I and *Bam*HI. The DNA manipulation was conducted basically as described in [Sambrook, 1989 #26].

Table 3-1 Oligonucleotide sequences used in the study of this chapter

	sequence
conventional primer for sense strand	5'-GGTCTAGAAACTCCTAAAAAACCGCCACC-3'
antisense primer for *sTm1*-dC3	5'-GTTTAGGATCCTTACAGTTCGCTGAAAGTCTGG-3'
antisense primer for *sTm1*-dC4	5'-GTTTAGGATCCAGATTATTCGCTGAAAGTC-3'
antisense primer for *sTm1*-dC5	5'-GTTTAGGATCCAGACAGTTAGCTGAAAGTCTGG-3'
antisense primer for *sTm1*-dC6	5'-AAAAGGATCCTTAGAAAGTCTGGTCCAGCTCG-3'
antisense primer for *sTm1*-dC7	5'-GCCAGACGGATCCCTTTAAGTCTGGTCC-3'
antisense primer for *sTm1*-dC11	5'-GTTCGCTGGGATCCGGTCTTACTCGTCGG-3'

Protein preparations

The tropomyosin mutants were expressed as described in "Experimental Procedures" of Chapter 2. Purification of *sTm1* was already described in "Experimental Procedures" of Chapter 2, and *sTm1*-dC3 was prepared in the same way as *sTm1*. Other *sTm1* deletion mutants were prepared with minor modifications; no sodium chloride was added at an ammonium sulfate fractionation.

Preparation of rabbit white muscle actin and S1 was also described in "Experimental Procedures" of Chapter 2.

Assays

All the measurements of the properties of tropomyosin mutants were undertaken as described in "Experimental Procedures" of Chapter 2, except for the measurement of the binding of tropomyosin to actin, which was conducted in the same solution condition as ATPase assay. For this measurement, 3 μM actin and 1-5 μM tropomyosin were mixed for 1.5 hour at room temperature in 20 mM Tris-HCl, 40 mM KCl, 3 mM $MgCl_2$ and 0.5 mM DTT. And then the mixture was centrifuged at 70,000 rpm for 30 min at 20 ℃ by a Hitachi himac CS150GX centrifuge using a S100AT3 rotor. After the centrifugation, the pellet was applied on a 12 % SDS-PAGE gel and the gel was stained with Coomassie Brilliant Blue, and then analyzed by GelDoc 2000 image analyzer (BioRad).

Calculations and curve fitting

Mathematica (Wolfman Research) was used to compare the data points of the binding of S1-ADP to actin-tropomyosin with the calculated values by use of the equation with a set of parameters, and the parameters were optimized manually. The curve fittings were performed both with the raw data points (θ versus x) and with the points re-plotted as the Hill plot, ln (θ/(1-θ)) versus ln x.

$$\frac{\sum_{l=0}^{n}\frac{l!}{l!(n-l)!}(K_1x)^l\{\sum_{m=0}^{W-1}m\frac{l!}{m!(l-m)!}K_2^{\,m}+\sum_{m=W}^{l}m\frac{l!}{m!(l-m)!}K_2^{\,W-1}K_3^{\,m-W+1}\}}{n\sum_{l=0}^{n}\frac{l!}{l!(n-l)!}(K_1x)^l\{K_T^{\,-1}+\sum_{m=0}^{W-1}\frac{l!}{m!(l-m)!}K_2^{\,m}+\sum_{m=W}^{l}\frac{l!}{m!(l-m)!}K_2^{\,W-1}K_3^{\,m-W+1}\}}$$

Results

Throughout the present study, the preparations used were lobster slow muscle type 1 tropomyosin (*sTm1*) variants expressed in Sf9 cells. These *sTm1* variants were lacking 3, 4, 5, 6, 7, and 11 residues from the C-terminus, each variant being designated as *sTm1*-dCX, where X is the number of deleted residues.

Viscosity measurements

It is known that the head-to-tail interaction of tropomyosin is contributed by 7-9 residues at either terminal region [11, 68]. In order to know more precisely the contribution of each residue in the C-terminal region, the effect of the C-terminal deletion on the strength of the head-to-tail interaction were measured. The low salt viscosity was measured as a function of ionic strength (Figure 3-1A) and as a function of protein concentrations (Figure 3-1B). The results indicated that the deletion of 3 residues from the C-terminus (*sTm1*-dC3) dramatically reduced the viscosity. Deletion of one more residue (*sTm1*-dC4) gave rise to another large drop of the viscosity. Further deletion resulted in further decrease. Although as shown in Figure 3-2, the viscosity of *sTm1*-dC7 and *sTm1*-dC11 appears to be almost the same, the viscosity of the two variants were practically distinct. When *sTm1*-dC11 was concentrated by *Centricon* (Amicon), *sTm1*-dC11 was much more quickly concentrated than *sTm1*-dC7 (Yamamoto, K. personal communication). This observation indicated that the head-to-tail interaction is not negligible even after the removal of 7 residues from the C-terminus.

It is interesting to note that *sTm1* shows a much higher viscosity than *fTm* as described in Chapter 2, and the viscosity of *sTm1*-dC3 is almost the same as that of *fTm*.

Actin binding assay

The binding of the C-terminal deletion mutants of *sTm1* to actin was measured by co-sedimentation in combination with gel-electrophoresis and

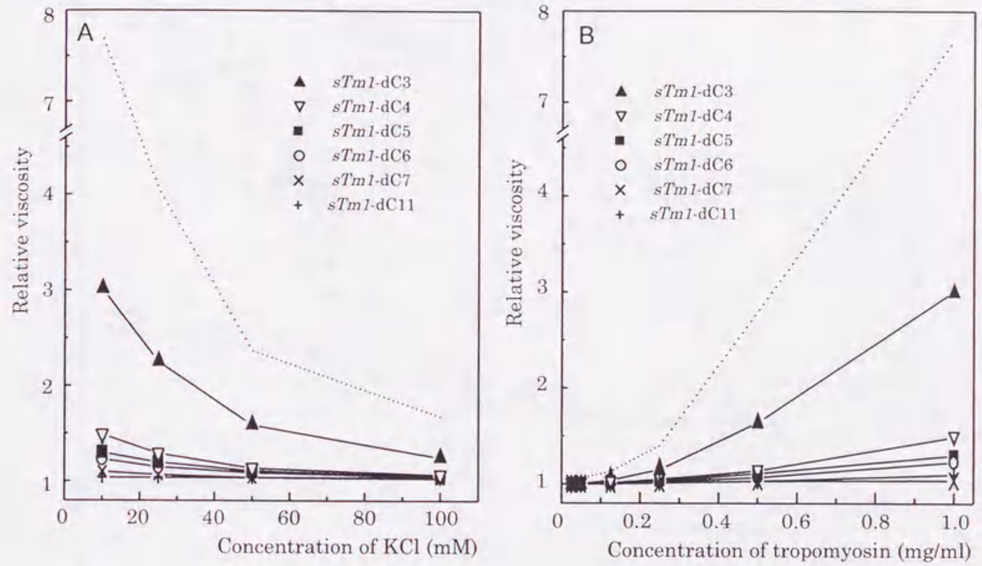

Figure 3-1 The low salt viscosity of the C-terminal deletion mutants of *sTm1*. The relative viscosity was measured using an Ostwald type capillary viscometer at 25 ℃. Symbols: dotted line, *sTm1* (see Figure 2-5), filled closed triangles, *sTm1*-dC3; reversed open triangles, *sTm1*-dC4; closed squares, *sTm1*-dC5; open circles, *sTm1*-dC6; X marks, *sTm1*-dC7; and crosses, *sTm1*-dC11.

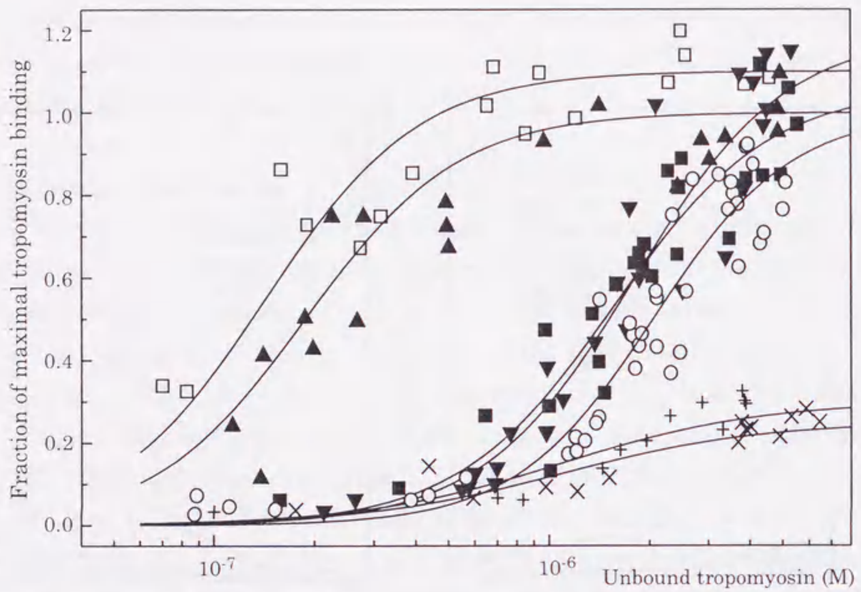

Figure 3-2 The actin binding of the C-terminal deletion variants of *sTm1*. 0.2 to 8.5 μM tropomyosin was cosedimented with 21 μM actin at 20 ℃ in 13 mM HEPES-NaOH pH7.0, 60 mM NaCl, 3 mM MgCl2 , 0.5 mM DTT and 1 mM NaN_3. The continuous curves were drawn using the Hill equation with the fitted parameters, the apparent binding constant (Kapp) and the Hill coefficient, as shown in Table 4-2. Symbols: open squairs, *sTm1* (see Figure 2-11), filled closed triangles, *sTm1*-dC3; reversed open triangles, *sTm1*-dC4; closed squares, *sTm1*-dC5; open circles, *sTm1*-dC6; X marks, *sTm1*-dC7; and crosses, *sTm1*-dC11.

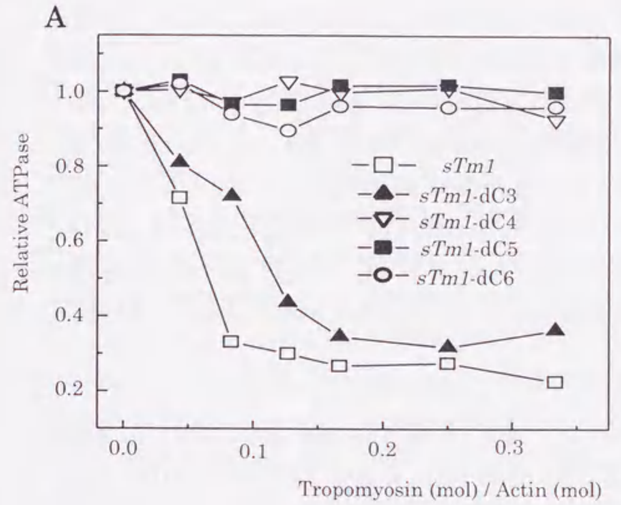

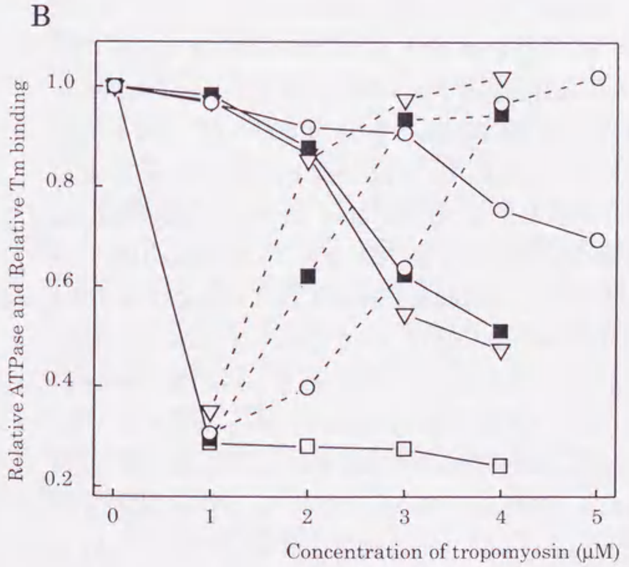

Figure 3-3 The effect of the C-terminal deletion variants of *sTm1* on the acto-S1 ATPase. (A) The rate of the acto-S1 ATPase is plotted versus the amount of tropomyosin added as the ratio [tropomyosin] / [actin]. The protein concentrations were; actin, 3 μM; S1, 0.5 μM; and tropomyosin, 0-0.1 μM. The solution condition was 20 mM Tris-HCl pH7.5, 40 mM KCl, 3 mM $MgCl_2$, and 0.5 mM DTT. Each data points represents the averaged value over four independent measurements. The symbols are; open squares, *sTm1* (wild type); closed triangles, *sTm1*-dC3; reversed open triangles, *sTm1*-dC4; closed squares, *sTm1*-dC5; and open circles, *sTm1*-dC6. (B) The rate of the acto-S1 ATPase and the rateof tropomyosin binding on the actin filament existance of the high concentration of tropomyosin. 0-5 μM tropomyosin were added and the other solution condition was same as (A). The symbols are identical to (A), symbols with solid lines for relative ATPase and symbols with dotted lines for Relative tropomyosin binding to actin filament.

colorimetry (Figure 3-2). The gel-electrophoresis and colorimetry had to be employed because *sTm1* has no cystein residue which serves for isotope labeling. This method is prone to large errors in determining small amount of tropomyosin bound to actin. In spite of the scattered data points, Figure 3-2 shows clearly that actin affinity was slightly reduced by the deletion of 3 residues (*sTm1*-dC3), substantially reduced, by an order of magnitude, by the deletions 4 to 6 residues, and almost abolished by the deletion of 7 residues or more. The data points were fitted by the Hill equation and the parameters were summarized in Table 3-2. Because of extremely weak affinity, *sTm1*-dC7 and -dC11 were not used in other assays described below.

Inhibition of acto-S1 ATPase

Tropomyosin inhibits the acto-S1 ATPase at the low ratio of S1 to actin without troponin [40]. At the ratio S1 to actin of 1/6, the acto-S1 ATPase was measured by adding *sTm1* C-terminal deletion mutants (Figure 3-3A, Table 3-2). At tropomyosin concentration of 1 μM, the inhibitory activity of *sTm1*-dC1 was almost maintained as compared with *sTm1* (0.36 ± 0.04 versus 0.23 ± 0.05). Further deletion was completely lost inhibitory activity of the acto-S1 ATPase, *sTm1*-dC4, -dC5, and -dC6 (0.93 ± 0.08, 1.00 ± 0.08, and 0.96 ± 0.09). The loss of inhibitory activity can be explained by the dissociation of *sTm1* C-terminal mutants from the actin filament at this concentration range of free tropomyosin as indicated in Figure 3-2. To confirm this, the concentration of *sTm1* mutants was increased from 1 to 4 or 5 μM and the acto-S1 ATPase together with the binding to actin filament was measured (Figure 3-3B). Actin binding of these mutants was saturated in this range of tropomyosin concentration and the inhibitory activity was observed with reduced extents. Thus the inhibitory activity was less prominent as more residues were deleted; relative ATPase rates were 0.47 for *sTm1*-dC4, 0.51 for -dC5 at 4 μM of added tropomyosin, and 0.69 for *sTm1*-dC6 at 5 μM of added tropomyosin.

Measurement of cooperative binding of S1-ADP to actin-tropomyosin complex

Tropomyosin makes the binding of S1 to actin filament cooperative. To test whether the C-terminal deletion mutants have this property of tropomyosin or not, fluorescence intensities from pyrene-actin-*sTm1* mutants were measured by titrating S1-ADP (Figure 3-5). The intensity of fluorescence from pyrene-actin is known to be linearly associated with the number of S1 that are strongly bound to actin [52]. The results indicated that all the mutants used here make the S1-ADP binding to actin filament cooperative. It is worth noting that all the plots shown in Figure 3-4 indicates transitions from a lower asymptote to a higher asymptote as the S1-ADP concentration increases. In the case of *sTm1*-dC4, -dC5, and -dC6, the lower asymptote is superimposed with the binding isotherm obtained from actin alone, and the higher asymptote is also superimposed that for the curve obtained from *sTm1* wild type. Further more, as more residues are deleted from the C-terminus, the transition occurs at higher concentration of S1-ADP; that is to say, the curvature shifts to the right hand side in Figure 3-4. This may suggest a transition to a new state of actin-tropomyosin complex induced by binding of two or more S1 per cooperative unit. The cooperative S1-ADP binding curves for *sTm1*-dC4, -dC5 and -dC6 can also be interpreted differently as follows. At lower concentration of S1-ADP, these variants did not bind to actin because of reduced actin affinity (Figure 3-2), and the binding of S1-ADP to bare actin could be measured. At higher concentration of S1-ADP, if we assume that the strongly bound S1 induces high affinity binding (ON-state binding) of tropomyosin to actin, then the binding of S1-ADP to actin-tropomyosin could be measured. Because the affinity of S1-ADP to actin-tropomyosin (in ON-state) is higher than the affinity of S1-ADP to bare actin, transition is observed from the lower asymptote to the higher asymptote.

If this interpretation is correct, then the plots in Figure 3-4 implies that binding of S1-ADP to actin induces high affinity binding (ON-state binding) of *sTm1* to actin, like in the case of rabbit skeletal α-tropomyosin. Now experiments are in progress to confirm the interpretation.

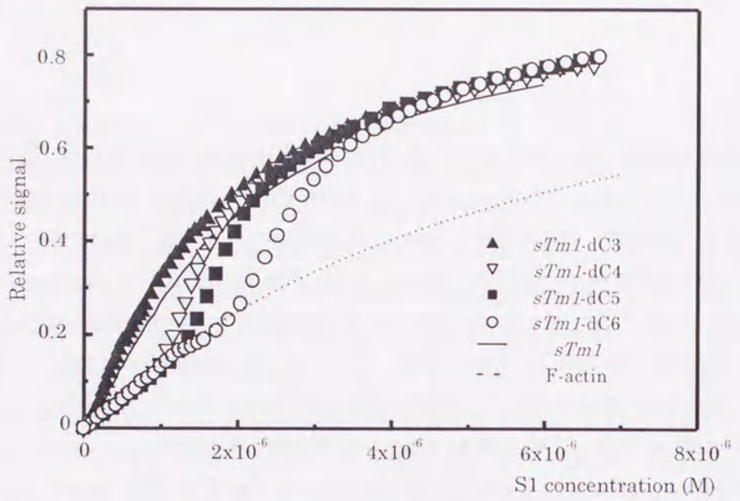

Figure 3-4 Fluorescence titration of pyrene-actin-tropomyosin complex with S1-ADP. S1-ADP was added to 0.5 μM pyrene-actin with or without 0.2 μM the C-terminal deletion *sTm1* mutants. The solid line shows the data for *sTm1* obtained in Figure 2-14, the dotted line shows the curve expected from the Michaelis-Menten type binding of S1 to actin (without tropomyosin) with the dissociation constant 5.6×10^{-6} M, which was obtained by averaging 5 data sets. The other symbols are identical to those used in Figure 3-4.

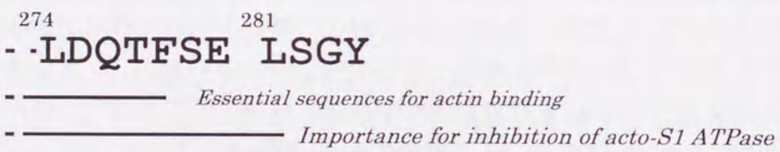

Figure 3-5 Summary of the present results indicated in Figure 3-2 and 3-3. The region of amino acid sequence of *sTm1* in relation to the requirement for each function.

	274	281
Lobster *fTm* & *sTm1*	LDQTFSE	LSGY
Human skeletal α	LDHALND	MTSI
Human skeletal β	LDNALND	ITSL
Chicken smooth γ	LDQTLLE	LNNM

Figure 3-6 Sequence comparison of C-terminal 11 residues of tropomyosins

Table 3-2 The properties of C-terminal deletion mutants of *sTm1*. The data of relative viscosity are from Figure 3-1. The data from the binding isotherms in Figure 3-2 are fitted to the Hill equation and data are described as K_{app} and Hill coefficient ± S. E. The relative ATPase rates are from Figure 3-3 A & B and each value is indicated as the average of three (without S.D.) or four data set ± S.D.

	Relative viscosity	*F-actin binding*		*Relative ATPase*
		K_{app}	*Hill coefficient*	
sTm1	4.05	$1.3 \pm 0.2 \times 10^{-7}$	1.2±0.3	0.23±0.05
sTm1-dC3	2.17	$2.0 \pm 0.2 \times 10^{-7}$	1.8±0.4	0.36±0.04
sTm1-dC4	1.29	$1.8 \pm 0.4 \times 10^{-6}$	1.9±0.4	0.47
sTm1-dC5	1.20	$1.6 \pm 0.2 \times 10^{-6}$	1.9±0.5	0.51
sTm1-dC6	1.15	$1.8 \pm 0.2 \times 10^{-6}$	2.6±0.6	0.69
sTm1-dC7	1.07	ND*	ND	NT**
sTm1-dC11	1.04	ND	ND	NT

*ND, not determined.

**NT, not tested.

Discussion

It is well established that the C-terminal region of skeletal muscle tropomyosin is important for its function. Previously, the effect of C-terminal deletions to the actin binding was studied by use of carboxypeptidase A digestion [14, 15]. In the present study, by employing recombinant proteins, I not only confirmed the importance of the C-terminal region, but also obtained the detailed functional map of this region (Figure 3-5).

The effect of deletion on the head-to-tail interaction

In the case of rabbit skeletal muscle α-tropomyosin, the deletion of three residues from the C-terminus did not substantially decrease its viscosity [15]. They interpreted that the hydrophobic interactions of head-to-tail interaction was still maintained, and the salt bridge could be formed between Lys-7 ε-NH_2 and the α-COOH group at the new C-terminus created after the deletion of three residues [68]. On the other hand, in the case of *sTm1*, the viscosity of *sTm1* is dramatically decreased by the deletion of three residues from the C-terminus. In this case, the bond between new α-COOH and Lys-7 ε-NH_2 appeared not to be formed. This would suggest that the conformation of the C-terminus of *sTm1* is different from that of vertebrate counterpart. The sequence of the N-terminal region of tropomyosin is highly conserved between invertebrate and vertebrate, suggesting that the conformation of the N-terminal region is also conserved. Therefore the difference between rabbit α-tropomyosin and lobster *sTm1* could only be explained in terms of conformational differences at the C-terminal region. The C-terminal conformation of *sTm1* must also be different from that of *fTm*. The relative viscosity of *sTm1* is much larger than *fTm* and the relative viscosity of *sTm*1-dC3 is almost the same as *fTm* (see Chapter 2), in spite that *fTm* and *sTm1* share both the N-terminal and C-terminal sequences. Since the N-terminal conformation is likely the same according to the proteolytic analysis using OmpT (see Chapter 2), the large difference in viscosity could originate from the different conformation at the C-terminus.

In summary, the conformation of the C-terminal three residues of *sTm1* might be different not only from vertebrate striated muscle α-tropomyosin but also from *fTm*. Therefore the drop of the viscosity by three residues deletion might be specific to *sTm1*.

The deletion of the forth residue from the C-terminus (Leu-281) further decrease the viscosity of *sTm1*. This could suggest that this hydrophobic residue plays a central space filling role in the head-to-tail interaction as originally proposed for Met-281 of mammalian skeletal muscle α-tropomyosin. Among tropomyosin species from lobster to human, the residue 281 is conserved to be a hydrophobic residue with a bulk side chain (Figure 3-6).

The effect of deletion on the actin binding property

The previous study by use of carboxypeptidase A showed that the affinity for actin of rabbit skeletal muscle α-tropomyosin was hardly reduced by the deletion of 3 or 4 residues from the C-terminus [15]. In contrast, in the case of *sTm1*, our results indicate that deletion of four residues reduces the apparent binding constant (K_{app}) by one order of magnitude compared with *sTm1* or *sTm1*-dC3. This indicates that the forth residue from the C-terminus, Leu-281, is important not only for the head-to-tail interaction in solution (as described above) but also for the actin binding affinity. Further deletion, up to six from the C-terminus, showed no large drop of actin affinity. The actin affinity was almost abolished by the deletion of seven and eleven residues. This stepwise decrease of actin binding affinity might be explained that the residue Leu-281 is at the position *a* of the heptad repeat of α-helical coiled-coil, and the deletion of Leu-281 should make disordering at the C-terminal region. Although an NMR study was interpreted that rabbit striated muscle α-tropomyosin does not form the α-helical coiled-coil structure to the C-terminus [69], *sTm1*, that has a distinct C-terminal sequence, may form α-helical coiled-coil structure to the C-terminus. In fact, a higher score was obtained from *sTm1* than from the rabbit skeletal muscle counterpart in the propensity for coiled-coil formation of C-terminal region

[70].

Properties of actin-tropomyosin deletion mutant complex

The stepwise decrease was also observed in the inhibitory activity of acto-S1 ATPase (Figure 3-3A&B). There might be an apparent correlation between the actin affinity and the inhibitory activity.

The results in Figure 3-4 may be interpreted in terms of the S1-induced high affinity binding (ON-state binding) of *sTm1* variants to actin. As more residues are deleted from the C-terminus, the transition points shifts more to the right hand side, that is, more S1 are required for the transition. The number of S1 required for the transition were estimated by curve fitting; 8 S1 molecules per 25 actin monomers (S1/7×Ac = 2.2) for *sTm1*-dC4, 9 and 11 S1 per 25 actin monomers (S1/7×Ac = 2.5 and 3.1) for *sTm1*-dC5 and -dC6, respectively. The recent experimental evidence indicated that the binding of 2 to 3 S1 molecules per 7 actin monomers were required to immobilize cardiac tropomyosin on the surface of actin filament [61]. This may be consistent with the present results.

In the framework of the two state model for the activation of actomyosin ATPase by actin-tropomyosin (see Chapter 1) [42], two states, ON and OFF states, are assumed and transition to ON-state must occur upon binding of one S1 in R-state (strong binding) per the cooperative unit (assumed to span seven or more actin). On the other hand, the present results indicate that the transition to the high affinity binding of tropomyosin to actin is induced by binding of 2 to 3 S1 in the strong binding state. It remains to be answered if the latter type of transition can be accounted for by the two state model.

Chapter 4

The effect of the substitution of serine-283 on the strength of the head-to-tail interaction and actin binding properties of rabbit skeletal muscle α-tropomyosin

Introduction

At low ionic strength, tropomyosin polymerizes [13] through head-to-tail interaction to form liner aggregates, presumably through the overlap of 7-9 residues between the N- and the C-termini of two adjacent tropomyosin molecules [11]. It is believed that this head-to-tail interaction also exists on the muscle thin filament where tropomyosin strands lie along the grooves of polymerized actin, and the cooperative actin binding of tropomyosin may be directly associated with by the head-to-tail interaction.

The penultimate Ser-283 of rabbit α-tropomyosin is known to be the unique phosphorylation site, and phosphorylated tropomyosin shows increased low salt viscosity. The increased viscosity may be partly due to the extra negative charge introduced by the phosphorylation, strengthening the head-to-tail interaction. In this study, we prepared tropomyosin variants in which this serine residue is replaced by other amino acids to alter the charge of this residue. By using these variants, the relationship was studied between the low salt viscosity (the strength of head-to-tail interaction in solution) on one hand, and the cooperativity in the binding of tropomyosin to actin on the other.

Measurement of the strength of the head-to-tail interaction in solution was carried out not only by viscometry but also by sedimentation equilibrium. This is the first direct measurement of the strength of the head-to-tail interaction of tropomyosin.

```
        10         20         30         40         50         60
ATGGACGCCATCAAGAAGAAGATGCAGATGCTGAAGCTCGACAAGGAGAATGCCTTGGAT
M  D  A  I  K  K  K  M  Q  M  L  K  L  D  K  E  N  A  L  D

        70         80         90        100        110        120
CGAGCGGAGCAGGCCGAGGCCGATAAGAAGGCGGCGGAAGACAGGAGCAAGCAGCTGGAA
R  A  E  Q  A  E  A  D  K  K  A  A  E  D  R  S  K  Q  L  E

       130        140        150        160        170        180
GATGAGCTGGTGTCGCTACAAAAGAAACTCAAGGGCACTGAAGATGAACTGGACAAATAC
D  E  L  V  S  L  Q  K  K  L  K  G  T  E  D  E  L  D  K  Y

       190        200        210        220        230        240
TCTGAGGCTCTCAAAGATGCCCAGGAGAAGCTGGAGCTGGCAGAGAAAAAGGCCACCGAC
S  E  A  L  K  D  A  Q  E  K  L  E  L  A  E  K  K  A  T  D

       250        260        270        280        290        300
GCTGAAGCCGATGTAGCGTCTCTGAACAGACGCATCCAGCTGGTTGAGGAGGAGCTGGAT
A  E  A  D  V  A  S  L  N  R  R  I  Q  L  V  E  E  E  L  D

       310        320        330        340        350        360
CGTGCCCAGGAGCGTCTCGCAACAGCCTTGCAGAAGCTGGAGGAGGCCGAGAAGGCAGCA
R  A  Q  E  R  L  A  T  A  L  Q  K  L  E  E  A  E  K  A  A

       370        380        390        400        410        420
GACGAGAGTGAGAGAGGCATGAAAGTCATTGAAAGCCGAGCCCAAAAGGATGAGGAAAAA
D  E  S  E  R  G  M  K  V  I  E  S  R  A  Q  K  D  E  E  K

       430        440        450        460        470        480
ATGGAAATTCAGGAGATCCAACTGAAAGAGGCCAAGCACATTGCTGAAGATGCCGACCGC
M  E  I  Q  E  I  Q  L  K  E  A  K  H  I  A  E  D  A  D  R

       490        500        510        520        530        540
AAGTATGAAGAGGTGGCCCGCAAGCTGGTCATCATTGAGAGCGACCTGGAGCGTGCAGAG
K  Y  E  E  V  A  R  K  L  V  I  I  E  S  D  L  E  R  A  E

       550        560        570        580        590        600
GAGCGGGCCGAGCTCTCAGAAGGCAAATGTGCCGAGCTTGAAGAAGAATTGAAAACTGTG
E  R  A  E  L  S  E  G  K  C  A  E  L  E  E  E  L  K  T  V

       610        620        630        640        650        660
ACGAACAACTTGAAGTCACTGGAGGCTCAGGCTGAGAAGTACTCACAGAAGGAAGACAAG
T  N  N  L  K  S  L  E  A  Q  A  E  K  Y  S  Q  K  E  D  K

       670        680        690        700        710        720
TATGAAGAAGAGATCAAGGTGCTTTCTGACAAGCTGAAGGAGGCTGAGACTCGGGCTGAG
Y  E  E  E  I  K  V  L  S  D  K  L  K  E  A  E  T  R  A  E

       730        740        750        760        770        780
TTTGCAGAGAGGTCGGTAACTAAGTTGGAGAAGAGCATTGATGACTTAGAAGACGAGCTG
F  A  E  R  S  V  T  K  L  E  K  S  I  D  D  L  E  D  E  L

       790        800        810        820        830        840
TACGCTCAGAAACTGAAGTACAAAGCCATCAGCGAGGAGCTGGACCACGCTCTCAACGAT
Y  A  Q  K  L  K  Y  K  A  I  S  E  E  L  D  H  A  L  N  D
*
       850        860        870        880        890        900
ATGACTTCCATATAAGTTTCTTTGCTTCACTTCTCCCGAGACTCCTGCGGCAAGCTGGGT
M  T  S  I  *
```

Figure 4-1 Nucleotide and amino acid sequences of rabbit skeletal muscle α-tropomyosin. Serine-283 was shown in red circle.

Construction of the tropomyosin transfer vectors and tropomyosin expression vectors

Oligonucleotides used in this study (Table 4-1) were designed on the basis of the reported sequence of rabbit skeletal muscle α-tropomyosin (Figure 4-1) [19].

Expression vectors for TmΔ1-140 and TmΔ1-140S283E were constructed by PCR. The sequence of the PCR primers were designed so that each PCR product had a *Nco*I site at the initiation codon and a *Bam*HI site after the termination codon. The PCR products were digested with *Nco*I and *Bam*HI. The fragments were ligated with expression vector pET3d [71] which had been digested by *Nco*I and *Bam*HI.

Construction of the transfer vector for TmΔ274-284 was performed by single stranded site directed mutagenesis. The mutagenesis was carried out using the tropomyosin gene subcloned into M13mp18 as a template DNA as described previously [19] according to the protocol provided by the supplier (Sculptor *in vitro* mutagenesis system, Amersham). The prepared double stranded DNA fragments were ligated into transfer vector pAcC4 [72] which had been digested with *Nco*I and *Bam*HI.

Transfer vectors for TmS283A, TmS283E, and TmS283K were constructed as follows. An *Mlu*I site was introduced at the C-terminal region of the Tm sequence by single stranded site-directed mutagenesis as described above. The isolated *Nco*I-*Mlu*I fragments of tropomyosin variants were ligated to the annealed oligonucleotides containing an altered C-terminal sequence and *Mlu*I or *Bam*HI cohesive sequences at each end, as well as to pAcC4 digested by *Nco*I and *Bam*HI.

The sequences of the tropomyosin variants in Table 4-1 were confirmed by DNA sequencing. Other procedures for DNA manipulation were performed according to Sambrook et al. [45]. Oligonucleotides used in this study were shown in Table 4-1, which were designed on the basis of reported sequence of rabbit skeletal muscle α-tropomyosin (Figure 4-1).

Table 4-1 List of mutants and primers used for mutagenesis

name	*mutation site*	*mutation primers*	*vector*	*host cell*	*yield*
bvTm			pAcC4	Sf9	6-10mg/l
Tm S283A	Ser283→Ala	5'-cgcgctcaacgatatgactgccatatag-3' 3'-gagttgctatactgacggtatatcctag-5'	pAcC4	Sf9	6-10mg/l
Tm S283E	Ser283→Glu	5'-cgcgctcaacgatatgactgagatatag-3' 3'-gagttgctatactgactctatatcctag-5'	pAcC4	Sf9	6-10mg/l
Tm S283K	Ser283→Lys	5'-cgcgctcaacgatatgactaagatatag-3' 3'-gagttgctatactgattctatatcctag-5'	pAcC4	Sf9	6-10mg/l
Tm△274-284	Leu274→amber	5'-agagcgtggtcctactcctcgctgat-3'	pAcC4	Sf9	25-50mg/l
Tm△1-140	Met141→initiate	5'-gatgaggaaaccatggaaattcag-3' 5'-ctcgggatccgtgaagcaaagaaac-3'	pET3d	*E. coli* BL21(DE3)	20-30mg/l
Tm△1-140 S283E	Met141→initiate Ser283→Glu	5'-gatgaggaaaccatggaaattcag-3' 5'-ctagaggatcctatatctcagtc-3'	pET3d	*E. coli* BL21(DE3)	20-30mg/l

Expression of rabbit skeletal α-tropomyosins

Expression of rabbit skeletal muscle α-tropomyosin variants in Sf9 cells were undertaken in the same way as the expression of lobster tropomyosin variants as already described in Chapter 2, "Experimental Procedures".

For expression in *E. coli*, the procedures already reported [19] were employed with some modifications. The expression vectors were transformed into *E. coli* BL21 (DE3) strain, and bacterial cells were cultured in LB or Standard 1 (Merck) medium with 50 μg/ml ampicillin at 37°C. Induction was carried out at OD600 0.8-0.9 by adding IPTG at a final concentration of 0.3 mM. The cells were harvested 3 hours after induction by centrifugation at 3,600×g for 10 min, washed with 50 mM Tris-HCl pH 8.0 and 1 mM EDTA, and stored frozen at -80 ℃.

Purification of expressed tropomyosin variants

All the tropomyosin variants used in the present study were purified in the same procedures as described in "Experimental Procedures" of Chapter 2&3.

Purification of rabbit muscle proteins and dephosphorylation of tropomyosin

Preparation of actin from rabbit muscle was already described in Chapter 2, "Experimental Procedures". Tropomyosin was purified from white skeletal muscle of rabbits according to Smillie et al. [73] as a mixture of αα- and αβ-tropomyosin. Purified tropomyosin was dialyzed against 100 mM Tris-HCl, pH 8.0, 1 mM $MgSO_4$, and 1 mM DTT. One hundred units of bacterial alkaline phosphatase C75 (Nippon Gene) was added to the dialyzed tropomyosin solution and the mixture was incubated for 4 h at 37 ℃. After the reaction, the solution was applied to the Mono-Q column described above to remove the bacterial alkaline phosphatase. The degree of dephosphorylation was checked by mass spectrometry as previously described by Taniguchi et al. [50] and by Takeda et al. [74].

Viscosity measurements

Viscosity measurements of tropomyosin mutants were carried out as described in Chapter 2, "Experimental Procedures".

Circular dichroism measurements

Circular dichroism spectra were measured with a JASCO model J-720 spectropolarimeter using a cell with a 2 mm path length. Ellipticity at 222 nm versus temperature were obtained automatically in 1 ℃ steps after an equilibration time of 1 min and a data averaging time of 1 sec. For each specimen, the temperature dependence was followed during both heating up and cooling down. The two curves were superimposed within experimental error. The solution conditions were either 5 μM (for TmΔ274-284) or 10 μM (for TmΔ1-140 and TmΔ1-140S283E) in 5 or 20 mM potassium phosphate buffer, pH 7.0, and 0.5 mM DTT.

Electron microscopy

For electron microscopic observation of tropomyosin was carried out using platinum-carbon rotary shadowing method. One-to-one mixtures of TmΔ1-140 and TmΔ274-284 at a total concentration of 5×10^{-8} M in 20 mM

potassium phosphate buffer, pH 7.0 were on a peeled-mica plate, and then rotary shadowing was carried out at 15 degree for 45 sec. After the shadowing, carbon was overlaid and observed under a JEM 1010 (JEOL) electron microscope.

Sedimentation equilibrium

Mixtures of 10-25 μM N-terminal truncated tropomyosin (TmΔ1-140 or TmΔ1-140S283E) and 5-20 μM C-terminal truncated tropomyosin (TmΔ274-284) in a solution containing 20 mM potassium phosphate buffer, pH 7.0, and 0.5 mM DTT were loaded into Epon charcoal-filled standard sector cells, and placed in an An-60 Ti rotor. Centrifugation was performed in a Beckman Optima XL-A analytical ultracentrifuge at 8,000, 10,000, and 12,000 rpm at 20 ℃. The concentration gradient of the protein in the cell was determined by UV absorption at 275 nm. Four scans were averaged.

The sedimentation data were analyzed using an ideal heterogeneously associating model of the form A +B ⇔ AB [75]. The absorbance A_r at radius r was fitted to the following equation.

$$A_r = \sum_{i=1}^{3} A_{i,ro} \exp\{\frac{M_i(1-\rho v_i)\omega^2}{2RT}(r^2 - r_0^2)\} \qquad (1)$$

where suffix *i* represents a kind of species; 1 denotes an N-terminal truncated tropomyosin; 2, a C-terminal truncated tropomyosin; 3, a complex of an N-terminal truncated and a C-terminal truncated tropomyosin. $A_{i,\ r0}$ is the absorbance of the species *i* at a radial reference distance r_0 (=6.9 cm); ϖ the angular velocity; *R*, the gas constant; *T*, the Kelvin temperature; v_i, the partial specific volumes of species *i*; r, the solution density (=1.00 g/ml); M_i, the molecular weight of species *i*, which is 33,476 for TmΔ1-140, 33,560 for TmΔ1-140S283E, or 63,038 for TmΔ274-284. The v_i, for each species was assumed to be 0.74 (ml/g), the value obtained from full-length tropomyosin [76]. The data were fitted to Eq. (1) by employing the Levenberg-Marquart Method using the routine in Origin version 4.0 (Microcal) with the constraint that the total optical density after integration over the cell depth should not exceed that of the protein loaded into the cell. The association constant is

represented as

$$Ka = \frac{\varepsilon_1 M_1 \varepsilon_2 M_2}{\varepsilon_3 M_3} \frac{A_{3,ro}}{A_{1,ro} A_{2,ro}} \qquad (2)$$

where ε_i is the weight absorption coefficient of species *i* in the centrifuge cell (absorbance values determined by centrifugation were checked using KNO3 standard solution): 0.306 $(mg/ml)^{-1}$ for TmΔ274-284, 0.419 $(mg/ml)^{-1}$ for TmΔ1-140, and TmΔ1-140S283E. The data sets were rejected in which the observed values systematically deviated from the fitted curve.

Actin binding assay

Actin binding assay was undertaken as described in Chapter 2, "Experimental Procedures".

Results

Viscosity measurements of tropomyosin variants

In rabbit muscle, the penultimate Ser-283 residue is partially phosphorylated (Figure 4-1) [77]. *In vitro*, the phosphorylation of Ser-283 increases the viscosity of tropomyosin solutions at low ionic strengths, indicative of stronger head-to-tail interactions between molecules [78]. This effect of phosphorylation is likely due to the extra negative charge associated with the phosphate group. Therefore, in order to alter the strength of the head-to-tail interaction, Ser-283 of α-tropomyosin was replaced by other residues to alter the charge. To evaluate the strength of the head-to-tail interaction, the relative viscosities of these α-tropomyosin variants were measured [13]. Figure 4-2A shows the effect of ionic strength on viscosity at a fixed protein concentration. KCl concentration was altered from 10 to 100 mM. Figure 4-2B shows the effect of protein concentration from 25 μg/ml to 1 mg/ml on the viscosity at a fixed ionic strength. At all ionic strengths and protein concentrations tested, species with an uncharged amino acid residue at position 283, the wild type α-tropomyosin (bvTm), dephosphorylated authentic Tm (a mixture of αα-tropomyosin and αβ-tropomyosin) and TmS283A, showed almost identical viscosities. With an extra negative charge at 283, TmS283E showed a higher viscosity, while with an extra positive charge, TmS283K showed a lower viscosity compared to the control (bvTm). These results confirm the suggestion that an extra charge at residue 283 is influential in the strength of the head-to-tail interaction, and that the strengthened head-to-tail interaction of phosphorylated tropomyosin may be largely, if not solely, due to the negative charge associated to the phosphate group at residue 283.

Measurements of the circular dichroism spectrum of truncated tropomyosin

For sedimentation equilibrium, the analysis is straight-forward if the interaction between molecules is restricted to the dimeric type. Two types of tropomyosin variants were therefore designed (Table 4-1), one with a

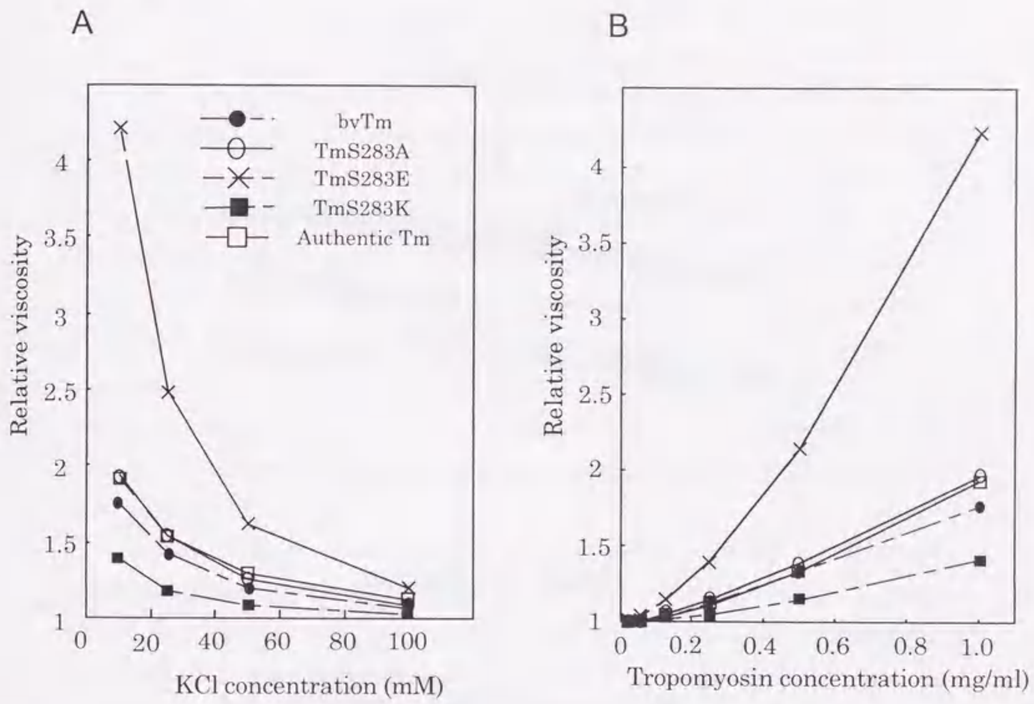

Figure 4-2 Relative viscosity of various Ser-283 mutants of tropomyosin. Filled circles, bvTm; open circles, TmS283A; crosses, TmS283E; filled squares, TmS283K; open square, dephosphorylated authentic Tm. The solution contained appropriate concentrations of KCl and serine mutants of tropomyosin, 10 mM TrisHCl pH 8.0, and 0.5 mM DTT. (A) The effect of ionic strength on viscosity, with a fixed concentration of tropomyosin at 1 mg/ml. (B) The effect of protein concentration on viscosity with the KCl concentration fixed at 10 mM. Viscosity measurements were carried out using an Ostowald type capillary viscometer at 25 ℃.

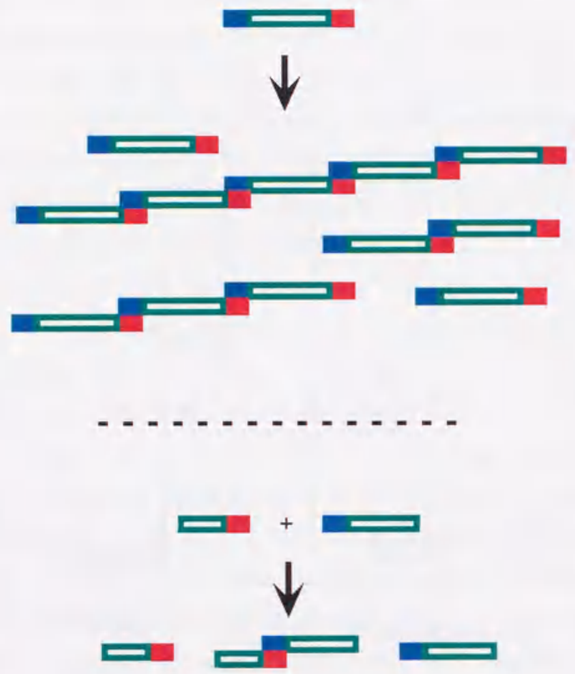

Figure 4-3 Schematic representations of the head-to-tail interaction and species of complex formed under different sets of experimental conditions employed in the present study. The upper panel, the conditions employed for the viscosity measurements, co-existing various species of different lengths; the lower panel, the conditions used for the sedimentation equilibrium experiments, being specially designed so that the number of co-existing species is restricted to be three; a monomer with a defective N- and an intact C-terminus (green with red box), a monomer with an intact N- and defective C-terminus (green with blue box) and one-to-one complex.

defective N-terminus and intact C-terminus and the other with an intact N-terminus and a defective C-terminus. By mixing these two species, only dimers are formed, multiple head-to-tail interactions being avoided (Figure 4-3).

It was then necessary to find suitable solution conditions for sedimentation equilibrium experiments. The criteria were (i) maintaining the α-helical structure of tropomyosin, as well as (ii) the head-to-tail interaction, and (iii) reducing non-specific interactions between molecules. If the ionic strength is too high, the strength of the head-to-tail interaction is reduced. On the other hand, if the ionic strength is too low, folding of the α-helical structure is lost, especially at the C-terminal part [79]. The α-helical contents of the species were measured by circular dichroism and the head-to-tail interaction as well as non-specific interactions were identified in the protein density profiles resulting from the sedimentation equilibrium itself (see below).

The effect of ionic strength on the overall stability of truncated tropomyosin variants was evaluated by measuring the ellipticity at 222 nm. Figure 4-4A shows melting transition profiles of truncated tropomyosin variants in 5 mM potassium phosphate buffer. The profiles indicated that the species including the C-terminal half, TmΔ1-140 and TmΔ1-140 S283E, were half unfolded at 26 ℃, whereas the specimen including most part, TmΔ274-284, was half unfolded at 34 ℃ (Figure 4-4B). At this ionic condition, N-terminal truncated variants started to melt at 20 ℃, indicating that the condition is not suitable for sedimentation equilibrium experiments .

To find out more suitable conditions for sedimentation equilibrium analysis, the ellipticity was then measured in 20 mM potassium phosphate buffer (Figure 4-5A). Thermal unfolding profiles indicated that the species including the C-terminal half, TmΔ1-140 and TmΔ1-140S283E, were half unfolded at 33 ℃ (Figure 4-5B). At 20 ℃, neither of the variants was substantially melted. At this ionic condition, the profile from TmΔ274-284 showed that the melting occurred in 2 steps. The first step is at relatively lower temperature with the midpoint at 39 ℃, being followed by the second

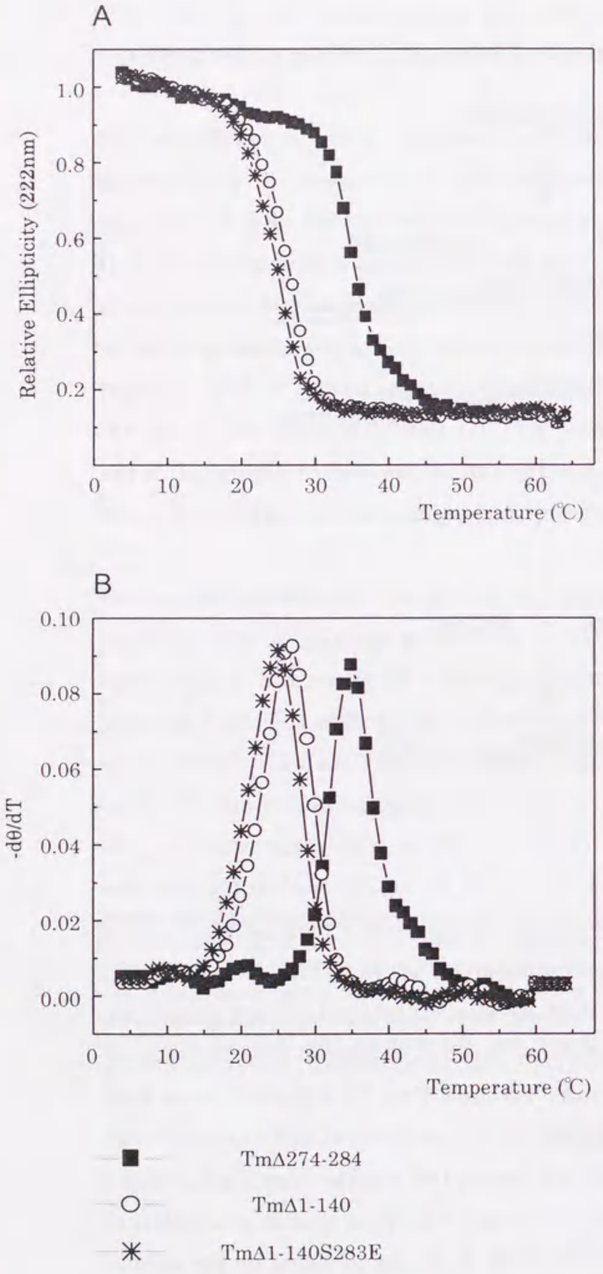

Figure 4-4 The thermal unfolding profiles of truncated tropomyosin variants. (A) The temperature dependence of α-helix content measured as the ellipticity at 222 nm. Solution conditions: 5 μM (TmΔ274-284) or 10 μM (TmΔ1-140 and TmΔ1-140S283E) truncated tropomyosins in 5 mM potassium phosphate buffer, pH7.0 and 0.5 mM DTT. Relative ellipticity at temperature T is given by $[\theta]^T/[\theta]^{10}$, where $[\theta]^{10}$ is the ellipticity at 10℃. (B) First derivative of the data in (A). Symbols: filled squares for TmΔ274-284; open circles for TmΔ1-140; and asterisks for TmΔ1-140S283E.

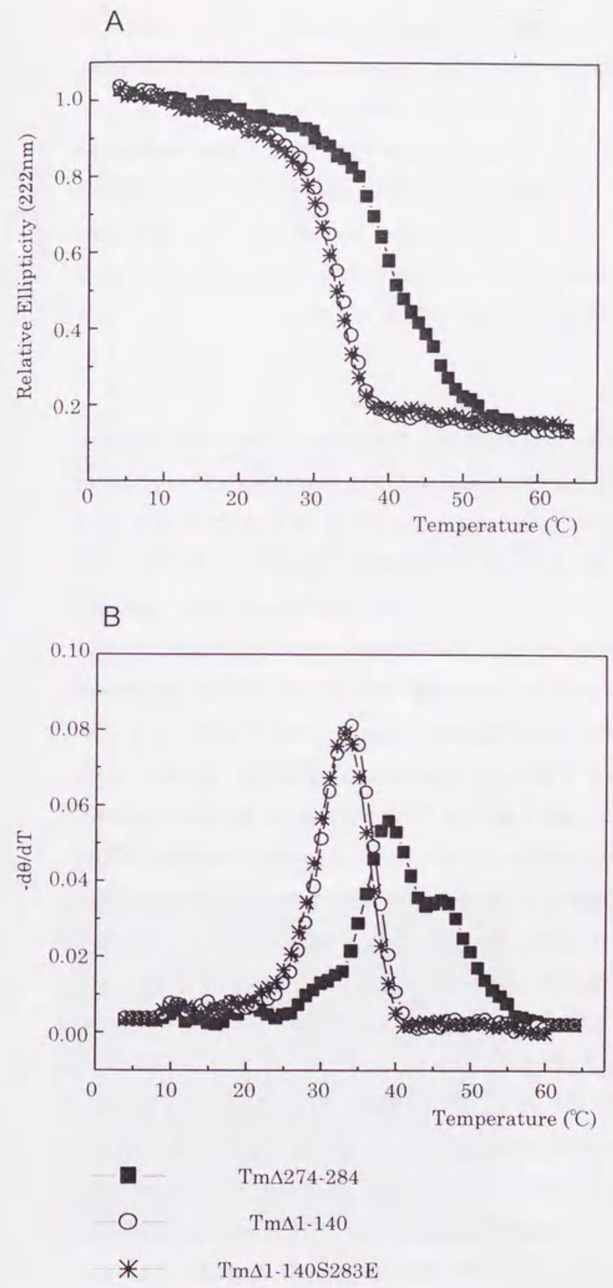

Figure 4-5 The thermal unfolding profiles of truncated tropomyosin variants. (A) The temperature dependence of α-helix content measured as the ellipticity at 222 nm. Solution conditions: 5 μM (TmΔ274-284) or 10 μM (TmΔ1-140 and TmΔ1-140S283E) truncated tropomyosins in 20 mM potassium phosphate buffer, pH7.0 and 0.5 mM DTT. Relative ellipticity at temperature T is given by $[\theta]^T/[\theta]^{10}$, where $[\theta]^{10}$ is the ellipticity at 10℃. (B) First derivative of the data in (A). Symbols: filled squares for TmΔ274-284; open circles for TmΔ1-140; and asterisks for TmΔ1-140S283E.

step with the midpoint at 47 ℃. Such a melting pattern with 2 steps is characteristic to skeletal muscle α-tropomyosin under medium to high ionic strength condition.

Figure 4-6 shows the circular dichroism spectra of the truncated tropomyosin variants at 10 ℃ in 20 mM potassium phosphate buffer. These patterns show that all three tropomyosin species tested take the α-helical conformation. Therefore, sedimentation equilibrium experiments were undertaken in 20 mM potassium phosphate buffer at 20 ℃.

Sedimentation equilibrium

The association constant of the tropomyosin head-to-tail interaction was measured directly using the sedimentation equilibrium method. Two pairs of tropomyosin variants were used, each consisting of an N-terminal defective variant (either TmΔ1-140 or TmΔ1-140S283E) and a C-terminal defective variant (TmΔ274-284) (Figure 4-3). At first, we confirmed that neither variant exhibited self-association or non-ideal behavior when a single species was centrifuged. Moreover, electron micrograph of a rotary-shadowed mixture of the two species showed no multimer aggregates (Figure 4-7). For these reasons, it was assumed that only three tropomyosin species were present in the centrifuge cell: monomeric N-terminus defective variant, monomeric C-terminal defective variant, and the one-to-one complex of the two through head-to-tail interaction (Figure 4-3). Based on this assumption, the sedimentation equilibrium data were analyzed according to an ideal heterogeneously associating model: A + B ⇔ AB [75]. In general, the sedimentation equilibrium method has potential for obtaining association constants in the range of 10^3-10^8 M^{-1} [75].

For the mixture of TmΔ274-284 and TmΔ1-140, when sedimentation equilibrium was attained, concentration gradient was formed in the cell as indicated in Figure 4-8. The analysis of the gradients from five independent data sets yielded association constants between 0.8×10^4 and 3.5×10^4 M^{-1}, with an average 2.6×10^4 M^{-1} (SD =1.0×10^4). It is assumed that the obtained value corresponds to the association constant of the head-to-tail interaction

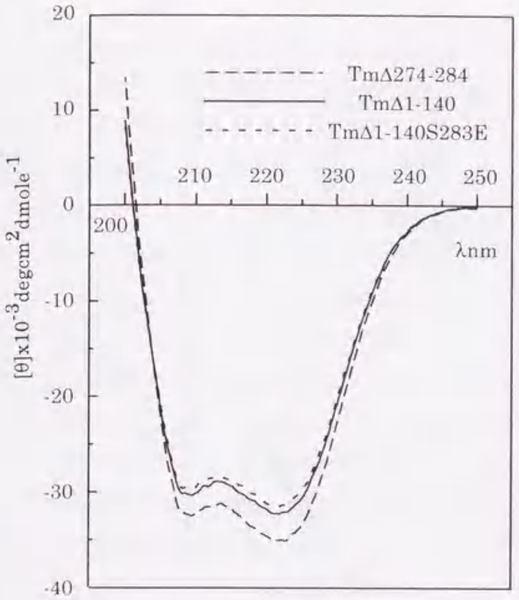

Figure 4-6 Circular dichroism spectra of truncated tropomyosin variants. The broken line is TmΔ274-284; the continuous line is TmΔ1-140; the dotted line is TmΔ1-140S283E. 5 μM (TmΔ274-284) or 10 μM (TmΔ1-140 and TmΔ1-140S283E) truncated tropomyosins in 20 mM potassium phosphate buffer, pH7.0 and 0.5 mM DTT.

Figure 4-7 Electron micrograph of tropomyosins. Mixture of TmΔ1-140 and TmΔ274-284 each at concentration of 5×10^{-8} M in 20 mM potassium phosphate buffer, pH 7.0 were on the peeled mica plate, and then rotary shadowing was done at 15 degree for 45 sec.

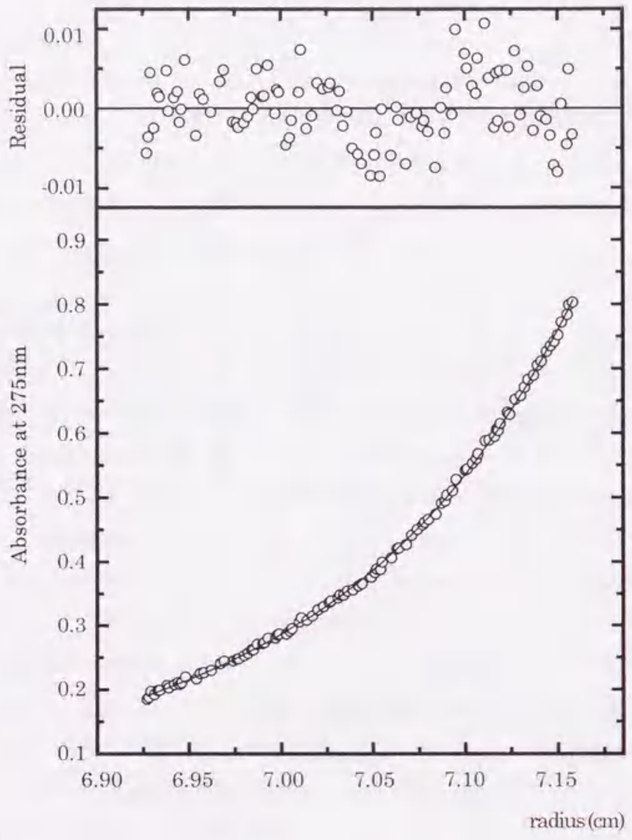

Figure 4-8 Distribution of protein concentration as a function of the radius of a sector cell after sedimentation equilibrium is reached with a mixture of truncated tropomyosin variants. In the lower panel, open circles are observed absorbance at 275 nm averaged over five independent runs, while the continuous line is the fitted curve derived from the equation (1). The upper panel indicates the residuals, the difference between the observed and the calculated at each radial position. The protein solution contained 40 μM N-terminal truncated Tm (TmΔ1-140) and 20 μM C-terminal truncated Tm (TmΔ274-284) in 20 mM potassium phosphate buffer, pH7.0, with 0.5 mM DTT. Centrifugation has been performed in an An-60Ti rotor on a Beckman Optima XL-A analytical ultracentrifuge at 12,000 rpm at 20 ℃.

of the non-phosphorylated authentic rabbit skeletal tropomyosin. This value is consistent with the previous estimation obtained by the light scattering measurements, 1.2 x 10^4 M^{-1} at 100 mM KCl [80]. On the other hand, the association constants for TmΔ274-284 and TmΔ1-140S283E were between 1.8×10^4 and 7.2×10^4 M^{-1} from seven data sets, with an average 3.9×10^4 M^{-1} (SD =1.6×10^4). This likely represents the association constant of the head-to-tail interaction of tropomyosin phosphorylated at Ser-283. The results indicate that, regardless of the amino acid at residue 283, the affinity of the head-to-tail interaction between adjacent tropomyosin molecules is weak. Moreover, the sedimentation equilibrium experiments apparently support the results of viscometry that an extra negative charge at residue 283 slightly strengthens the head-to-tail interaction, although the difference between the two variants is less significant as determined by sedimentation equilibrium ($p < 0.18$, Student's two-tailed t-test) than by viscometry.

Actin binding of tropomyosin variants

The actin affinities of the tropomyosin variants were measured by co-sedimentation (Figure 4-9 and Table 4-2). The binding isotherms shown in Figure 4-9 indicate the pooled data points obtained from two or three independent experiments for each tropomyosin variant. The data points were fitted by the Hill's equation to obtain an apparent binding constant (K_{app}) and Hill coefficient (n), which are summarized in Table 4-2. Since bvTm is known to be identical to the authentic tropomyosin in actin affinity [18, 19], bvTm is used in the present study as the control. Since the phosphorylation of Ser-283 did not alter the actin affinity [78], we had anticipated that the actin affinity of TmS283E might not differ from that of bvTm. However, TmS283E showed substantially lower actin affinity than bvTm.also the parameter of cooperativity, n, differ clearly between species. As indicated in Table 4-2, n for TmS283E is significantly smaller than those for TmS283A and TmS283K. Due to the strong affinity of bvTm, the data points at the lowest TmS283A and TmS283K bind actin even more weakly than TmS283E. Interestingly, not only the apparent binding constant but

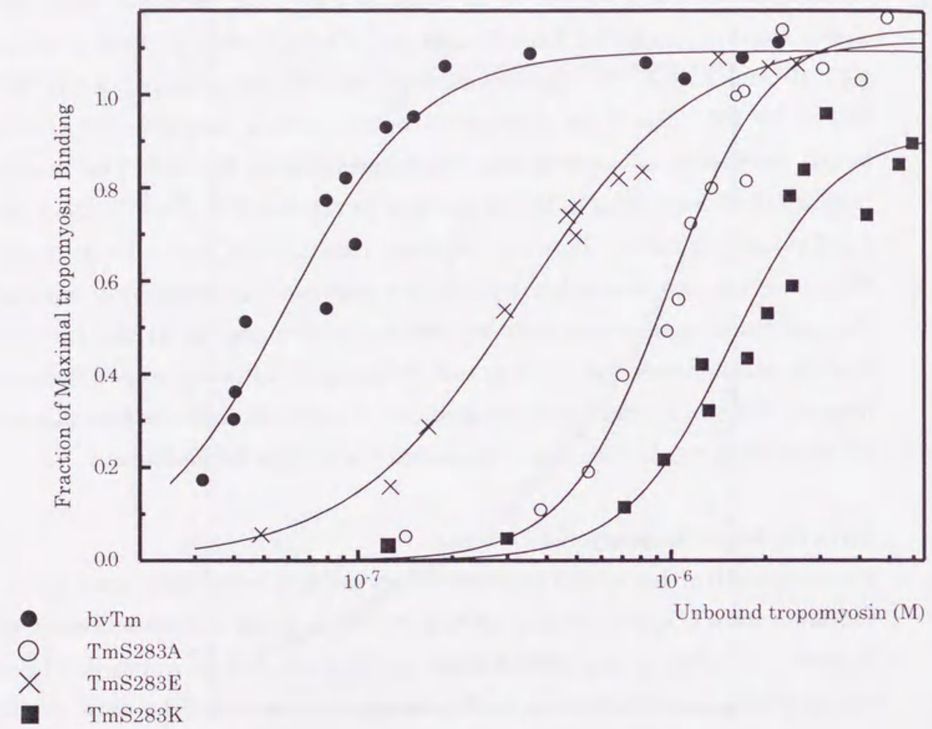

Figure 4-9 Actin binding of various Ser-283 variants of tropomyosin. Fitted curves were drawn using the Hill equation (see Experimental Procedures). For each tropomyosin variant, two to three independent sedimentation assays with F-actin were performed and the pooled data points are shown. Tropomyosin variants at 0.2-8 μM were cosedimented with 21 μM actin at room temperature in buffer containing 13 mM HEPES-NaOH, pH 7.0, 60 mM NaCl, 3 mM $MgCl_2$, 0.5 mM DTT, and 1 mM NaN_3. The symbols are; filled circles, bvTm; open circles, TmS283A; crosses, TmS283E; filled squares, TmS283K.

concentrations of free bvTm are missing, making *n* for this species somewhat unreliable. The data points in the region of higher concentrations of free TmS283K are also scattered. The level of saturation for this species might be different from that of other species.

Table 4-2 Apparent actin binding constants and Hill's coefficients of tropomyosin variants. The data in the binding isotherms in Figure 4-9 was analyzed by fitting to the Hill's equation.

Tropomyosins	K_{app} (M^{-1})	Hill coefficient
bvTm	$1.7 \pm 0.1 \times 10^7$	2.0 ± 0.3
TmS283A	$1.0 \pm 0.1 \times 10^6$	2.7 ± 0.4
TmS283E	$3.0 \pm 0.2 \times 10^6$	1.6 ± 0.2
TmS283K	$6.5 \pm 0.7 \times 10^5$	2.6 ± 0.6

Discussion

When tropomyosin is arranged on the actin filament, 7-9 residues overlap between N- and C-terminus of the tropomyosin. The head-to-tail interaction of tropomyosin in solution at low ionic strength might be reflected in the strength of the interaction of this overlap on the actin filament. Before starting the present work, therefore, we anticipated that the strength of head-to-tail interaction in solution and the cooperativity in actin binding are directly associated to each other.

The results presented here indicate that the strength of the head-to-tail interaction of tropomyosin molecules is substantially influenced by an extra charge at residue 283; an extra negative charge strengthens, as in TmS283E and phosphorylated tropomyosin, whereas an extra positive charge (as in TmS283K) weakens the head-to-tail interaction. On the other hand, the affinity of tropomyosin to actin, as well as the cooperativity of actin binding, depends on amino acid residues in a more complicated manner. TmS283E shows a lower affinity than phosphorylated tropomyosin, although both species have an extra negative charge at 283. TmS283E binds to actin in a less cooperative manner than TmS283K or TmS283A. To confirm cooperativity of actin binding, the binding data points on Figure 4-9 were also analyzed using a linear lattice model [81] giving rise to the same conclusion. These results suggest that the interaction with actin, the affinity and the cooperativity in actin binding, of skeletal muscle α-tropomyosin is dependent on many factors including the stereoscopic occupancies of side chains at residue 283, and therefore these parameters are not simply correlated with the strength of the head-to-tail interaction between tropomyosin molecules in solution.

After the experiments in this study were completed, a positive correlation between the strength of the head-to-tail interaction and the cooperative activation of acto-S1 ATPase was reported [67]. By undertaking comparative studies using rabbit skeletal muscle tropomyosin (RSTm), chicken gizzard muscle tropomyosin (GTm), and non-muscle tropomyosin

from rat fibroblast cells (5aTm), the authors interpreted the results to indicate that the higher cooperativity in the activation of ATPase is related to the GTm type of the C-terminal sequence shared by GTm and 5aTm but not by RSTm. They suggested that the sequence, therefore the structure, of the C-terminus should be a determining factor in the strength of the communication between adjacent tropomyosin molecules on the actin filament, whereas the head-to-tail interaction of tropomyosin alone, free from actin, should depend on both the N-terminus and C-terminus sequences. Their suggestion is consistent with our observations; there is no clear correlation between the strength of the head-to-tail interaction of tropomyosin alone and the actin binding properties.

The present results indicate that the head-to-tail affinity between two tropomyosin molecules in solution is weak. It may be too weak and the difference in affinity may be too small to be a significant factor in cooperative actin binding. The cooperativity in the actin binding must be governed by other factors, such as the manner of interaction between the C-terminus and actin molecules. It is worth noting that the difference in the head-to-tail affinity as determined by sedimentation equilibrium measurement is much smaller than what would be expected from the large difference in viscosity, as is shown between two species of tropomyosin with and without a negative charge at 283 (S283E versus the wild type with Ser-283). This may be due to the fact that the viscosity is roughly in proportion to the square of the particle length, making the viscosity highly sensitive to the length of tropomyosin polymers. It may be that viscosity measurements did not pick up the elasticity of the tropomyosin solution. Within the conditions employed in the present study, no effect of shear stress on the viscosity measurements was observed; the value of relative viscosity was independent on the number of experiments using the same viscometer.

In the present study, the association constant between two tropomyosin molecules through the head-to-tail interaction has been measured directly for the first time. For this purpose, sedimentation equilibrium measurements were employed with two pairs of truncated

tropomyosin variants, one between TmΔ274-284 and TmΔ1-140, and the other between TmΔ274-284 and TmΔ1-140S283E. Truncated variants had to be used in order to prevent the formation of contiguous polymers that makes the analysis extremely complicated and ambiguous (Figure 4-3). Because these were variants, the possibility can not be excluded that the association constants obtained differ from those of the authentic molecule. It is suggested that, however, that these values are likely to be correct. First, as indicated in Figure 4-4, 5 & 6, the measurements were undertaken with the molecules in the coiled-coil configuration as the authentic molecules. Second, care was taken to reject any molecular species that showed non-specific (either attractive or repulsive) interactions. In the present study, a repulsive interaction between molecules of the full length tropomyosin with an unacetylated N-terminus expressed in *E. coli* was observed; the sedimentation equilibrium of this single species gave rise to an apparent molecular weight that decreased with increasing protein concentration. This is indicative of a repulsive force between the molecules, which may also be responsible for the loss of polymerizability and actin affinity.

It is worth noting that the tropomyosin species used in the present study were carefully designed based on the following considerations. First, Sf9 cells with baculovirus based expression systems were used for expressing any variant that extended to the original N-terminus, because N-terminal acetylation is required for actin binding and the head-to-tail interaction of tropomyosin [17]. As an alternative to molecules with an acetylated N-terminus, molecules with extra residues at the N-terminus have been proposed, which facilitate both actin binding and the head-to-tail interaction [18, 82]. In the present study, however, species with an extended N-terminus were not used because the extra residues likely alter the association constant of the head-to-tail interaction. Moreover, there are no serious technical problem in the expression and purification of large quantities of these tropomyosin species at high purity using the baculovirus-based expression system. Second, in order to study the effect of substituting one amino acid residue on the physicochemical and physiological properties of tropomyosin,

two or more species were used that differ from each other only by one residue. Comparative studies of the physico-chemical properties using naturally occurring tropomyosin species that differ from each other in the number of residues, may give rise to results that are difficult to interpret. In tropomyosin the α-helical coiled-coil spans over almost the entire length of the polypeptide chain, so that almost all the residues may be involved in either intra- or inter-molecular interactions. Therefore replacement of any single residue may have a substantial effect on the manner of interaction with each other as well as with other protein molecules. The present study actually demonstrates such multiple effects of single residue replacements of α-tropomyosin molecules.

Chapter 5

Expression of muscle proteins in baculovirus based expression system; Increased amount of protein expression due to the leader sequence from lobster tropomyosin.

Introduction

Because N-terminal acetylation is essential for the function of tropomyosin and the N-acetylated tropomyosin is expressed by the baculovirus based expression system, not by an *E. coli* expression system, the baculovirus based expression in Sf9 cells was employed throughout the present studies. In the course of present studies, I found that, among different species of tropomyosin expressed in Sf9 cells, lobster tropomyosin was yielded at much higher level than rabbit tropomyosin. I thought that the high level of expression of lobster tropomyosin should be due to the extra 21 bp 5' leader sequence (L21) which was present in the transfer vectors for lobster tropomyosin, but not those for rabbit tropomyosin. To test if this is true, the sequence for rabbit α-tropomyosin was inserted downstream of L21, and let it expressed. As anticipated, the expression level of rabbit α-tropomyosin increased by a factor of 10-20. I have tested L21 for Sf9 expression of other proteins, like actin and CapZ. The results of our tests so far undertaken, through the tests are on a small number of proteins and only semi-quantitative, have indicated that L21 does increase the expression level not only of tropomyosin but also of other proteins.

Experimental Procedures

Construction of transfer vectors and expression of various tropomyosin variants

Constructions of transfer vectors, pVL1392-*sTm1* and pAcC4-RαTm were described in "Experimental Procedures" in Chapter 2 and Chapter 4, respectively (Figure 5-1A&B). Transfer vector pVL-L21-RαTm was constructed as follows. The *Nco*I-*Bam*HI fragment of rabbit α-tropomyosin coding sequence was isolated from pVL1392-*sTm1*, an *Nco*I-*Bam*HI fragment was isolated which is 9.5 kb long and consists of pVL1392 and 21 bp lobster tropomyosin leader sequence (pVL-L21). Then the two *Nco*I-*Bam*HI fragments were ligated (Figure 5-2).

The procedures for expression of proteins were already described in "Experimental Procedures" in Chapter 2.

Estimation of expression level

For quick and semi-quantitative estimate of the expression level of tropomyosin variants, densitometry of SDS-PAGE gels was employed. From 3 liter culture of tropomyosin expression, 10 ml of Sf9 cell suspension was taken and the cells were collected by centrifugation. The cells were then lysed by suspending in 500 μl of the hypotonic lysis buffer (see "Experimental Procedures" in Chapter 2), and the supernatant was collected by centrifugation. The supernatant containing tropomyosin was heated at 90 ℃ for 10 min. After cooling down to room temperature, denatured proteins were removed by centrifugation, and 10 μl of the supernatant was applied on a 15 % SDS-PAGE gel. After electrophoresis, gel was stained by Coomassie Brilliant Blue and analyzed by Gel-Doc 2000 (BioRad) image analyzer.

To estimate the expression level quantitatively with higher precision, tropomyosin was partially purified from a larger volume of culture and subjected to colorimetry of SDS-PAGE gel. Tropomyosin from 3 liter of Sf9 cell culture was purified as described in "Experimental Procedures" of

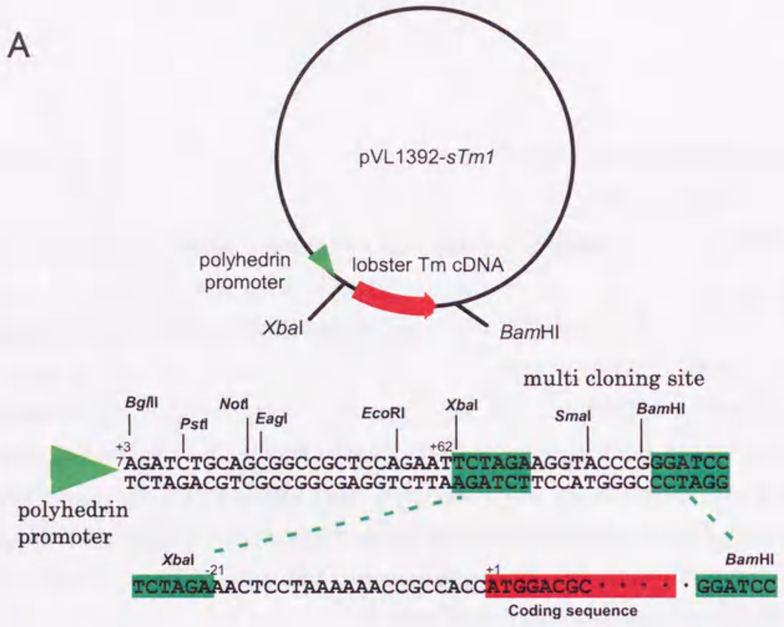

Figure 5-1 Construction of transfer vectors for expression of tropomyosin variants. The triangles in light green indicate the polyhedrin promoter, the boxes in green indicate restriction sites used and the boxes in red indicate the coding sequences of tropomyosin. A; construction of pVL1392-*sTm1*. The *Xba*I-*Bam*HI fragment of *sTm1* cDNA was subcloned into pVL1392. B; construction of pAcC4-RαTm. The *Nco*I-*Bam*HI fragment of rabbit α-tropomyosin cDNA was subcloned into pAcC4. The details of procedures for each construction are described in "Experimental Procedures" in Chapter 2 and 4, respectively.

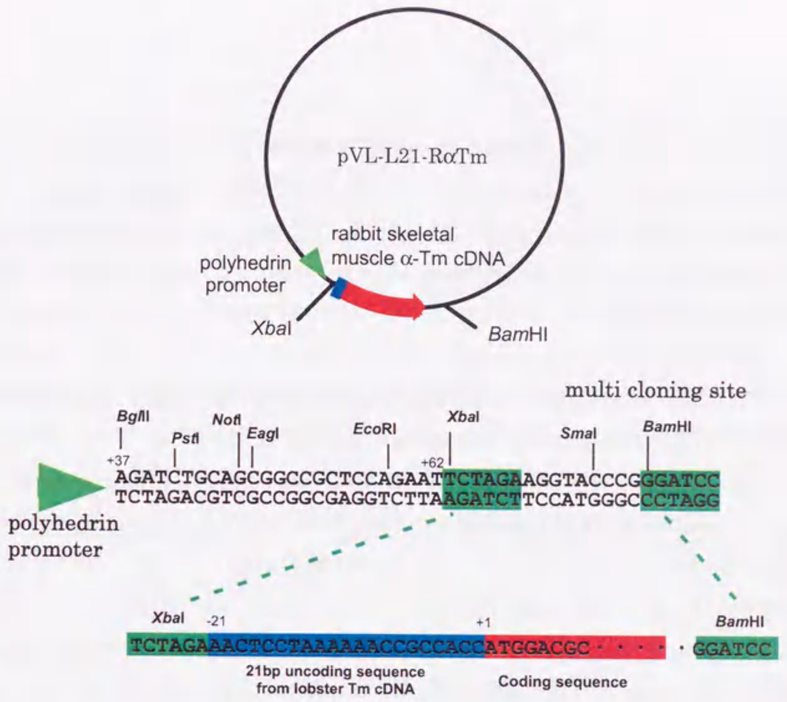

Figure 5-2 Construction of transfer vector pVL-L21-RαTm. The triangles in light green indicate the polyhedrin promoter, the boxes in green indicate restriction sites used and the boxes in red indicate the coding sequences of tropomyosin. The *Nco*I-*Bam*HI fragment of rabbit α-tropomyosin cDNA was subcloned into pVL-L21. (For details, see "Experimental Procedures")

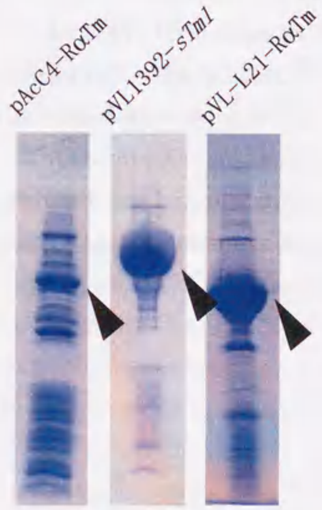

Figure 5-3 Quick analysis of expression level by densitometry of SDS-PAGE gels. The arrowheads indicate tropomyosin.

Chapter 2 up to the column chromatography. The total protein amount of this preparation was quantified by the micro-bullet method. And the relative content of tropomyosin was evaluated by colorimetry of 15 % SDS-PAGE gel stained with Coomassie Brilliant Blue by using an image analysis system of Gel-Doc 2000.

Construction of transfer vectors for and protein expression of actin and CapZ

Subcloning of human α-actin was carried out by PCR. The primers were designed so that the product has an *Xba*I site and 21 bp lobster tropomyosin leader sequence (L21) upstream of α-actin coding sequence, as well as a *Bam*HI site downstream of the stop codon (Table 5-1). The cDNA of human α-actin in pBR322 (a gift from Dr. J. L. Mandel of CNRS, Strasbourg) was used as the template [83], and the PCR product was subcloned into pGEM-T vector (Promega). The *Xba*I-*Bam*HI fragment which contains L21 and the whole α-actin coding sequence was isolated and, after confirming the sequence, was ligated into the *Xba*I-*Bam*HI sites of pVL1392.

CapZ is a hetero-dimer consisting of one α- and one β- subunit. From the cDNA bank of chicken muscle (STRATAGENE), the cDNA of each subunit of CapZ was cloned using the primers (summarized in Table 5-1) which were designed on the basis of previously reported sequence [84, 85]. An *Nco*I and a *Bam*HI site were attached at either end of cDNA, which was then inserted into the same sites of pTV118N for confirming the cDNA sequence. From pTV118N, the *Nco*I-*Bam*HI fragments of *capZα* and β were isolated and separately ligated into pVL-L21 as described above.

For each construct, construction, purification, and amplification of recombinant baculovirus was conducted as described in "Experimental Procedures" in Chapter 2.

Table 5-1 Oligonucleotide sequences of primers used in the study described in this chapter.

	sequence
primers for cloning human α-actin	5'-TCTAGAAACTCCTAAAAAACCGCCACCATGTGCGACGAAGACGAGACC-3'
	5'-AAAGGATCCGCTGGAGGTGGAGTGTGTTAGAAG-3'
primers for cloning chicken capZα	5'-CCCACCATGGCCGACTTTGAGGACCGGG-3'
	5'-CCTTGGATCCATACTAAGCATTCTGCATTTCTTTGCC-3'
primers for cloning chicken capZβ	5'-CCGCCATGGGTGACCAGCAGCTGG-3'
	5'-GACCTGGATCCGTTTAGTTATCAGGCTGG-3'

Expression of actin and CapZ

Expression was checked as follows. On a 9 cm plate, in 10 ml of 10 % fetal calf serum containing TNM-FH medium, 7.5×10^6 of Sf9 cells were infected with recombinant virus. After 48-52 hours post-infection, cells were collected and lysed by 500 μl of the hypotonic lysis buffer. The supernatant of cell lysate was collected by centrifugation and 10 μl of the supernatant was applied on a SDS-PAGE gel, which was either stained by Coomasie Brilliant Blue or transferred onto a nitrocellulose membrane for Western blotting. Blotting was undertaken using a mini transblot system (BioRad) at a constant current of 150 mA for 2 hours at 4 ℃ in 25 mM Tris, 250 mM glycine, and 20 % methanol. For blocking, 2.5 % skim milk in PBS was used. To detect only the exogeneous α-actin, excluding actin species which are endogeneous to the Sf9 cell, the monoclonal anti α-sarcomeric actin IgM (Sigma) was used as the primary antibody. As the secondary antibody, the alkaline phosphatase-conjugated goat IgG to mouse IgM was used. The labeled gel was developed with BCIP/NBT TABLETS (SIGMA).

Expression of exogenic proteins with 21 bp lobster tropomyosin leader sequence in Sf9 cells

When lobster tropomyosin variants were expressed in Sf9 cells, large amount of proteins were obtained, whereas in the case of rabbit skeletal tropomyosin, the amount of recovered protein was about 1/20-30 of the lobster counterpart (Figure 5-3, Table 5-2). The reason for this large difference in expression level can be different codon usage between lobster and rabbit tropomyosin genes, and lobster codon can be much more suitable for expression in Sf9 cells. In general, to express exogenic genes, the codons of about first 10 amino acid residues are believed to be influential to the expression level. Therefore it is a common practice to alter the DNA sequence in this region to match the usage of the host cell. Figure 5-4 shows comparison of cDNA sequences between lobster and rabbit tropomyosins. While first 9 amino acids are identical to each other, one codon is different; alanine 3rd is coded as GCA in the lobster, while as GCC in the rabbit tropomyosin cDNA. However the codon usage of the host cell, *Spodoptera frugiperda*, favors the codon in the rabbit cDNA; alanine is more frequently coded as GCC (35.3) than as GCA (12.8). Therefore the codon usage of first 9 amino acids does not account for the difference in the expression level.

Table 5-2 Comparison of expression levels between transfer vectors

transfer vector	*expression level* (ODU) *(quick colorimetric estimation)*	*Yield* (mg / liter culture)
pAcC4-RαTm	12 ODU	6-10 mg / L
pVL1392-*sTm1*	123 ODU	200-400 mg / L
pVL 1392-L21-RαTm	107 ODU	120-200 mg / L

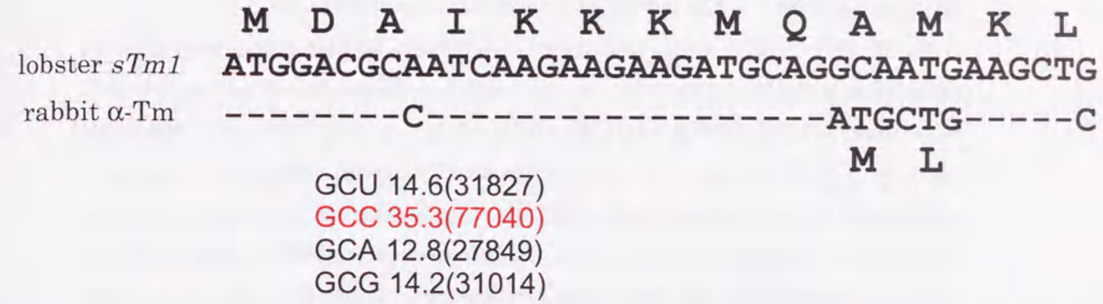

Figure 5-4 Comparison of codon usage for the N-terminal region between *sTm1* and rabbit α-tropomyosin cDNA.

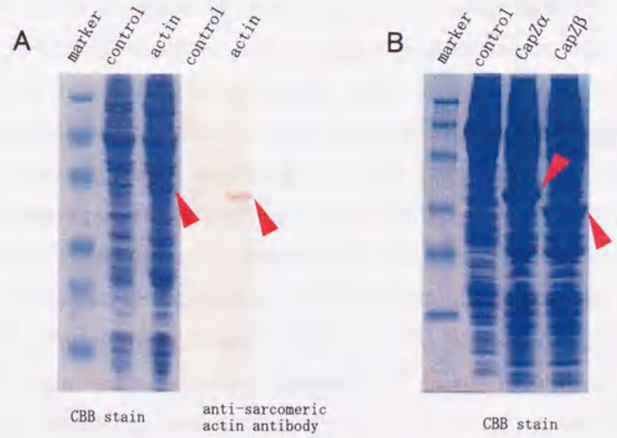

Figure 5-5 Expression of actin and CapZ in Sf9 cells in the presence of the leader sequence. 48-52 hours post-infection, cells were collected and the soluble fraction of the cell lysate was analyzed with SDS-PAGE. A; actin expression. 3 lanes on the left were stained with CBB, and 2 lanes on the right were Western blot pattern detected with an anti-α-sarcomeric actin antibody. B; CapZ expression detected by CBB staining. Arrows show target proteins.

In search for another possible explanation, transfer vectors were compared and at least two differences were found (Figure 5-1A & B). Firstly, in the transfer vector (pVL1392-*sTm1*) for lobster tropomyosin, the original polyhedrin initiation codon is broken, while in the transfer vector (pAcC4-RαTm) for rabbit tropomyosin, the original polyhedrin initiation codon is intact and used for protein expression. Secondly, the lobster tropomyosin transfer vector, but not the vector for rabbit tropomyosin, contains the leader sequence 21 bp long which was carried over from the lobster cDNA. Altogether, the putative mRNA for translating lobster tropomyosin in Sf9 cells has a leader sequence which is longer than that for rabbit mRNA; for the lobster mRNA 89 bases (68 bases originating from the transfer vector plus 21 bases carried over from the cDNA).

To test if the leader sequence increases the expression level of a foreign gene, rabbit α-tropomyosin was inserted downstream of this leader sequence (Figure 5-2), and the expression level was measured (Figure 5-3, Table 5-2). The results were clear; the leader sequence did work as *cis* element for large amount of exogenic gene expression in Sf9 cells. At present, however, the mechanism how the leader sequence increases the expression level remains unknown. The leader sequence may work either as a stabilizing factor for mRNA or as a translational activator. The former possibility may be tested by a Northern analysis, whereas the latter possibility may be proved by an *in vitro* translation experiment.

Moreover, another question arises; which part of the leader sequence is essential for the enhanced expression, either only L21 or whole segment 89 bases long? To answer this question, tropomyosin is not a suitable target protein for expression. This is because tropomyosin has no enzymatic activity, which makes a quantitative assay of expressed protein extremely difficult without purifying the protein. Moreover, because the purification procedures include the heat denaturation step, the yield is not reproducible. For quantitative measurements of expressed protein, we are now constructing transfer vectors for enzymes like lacZ which encodes β-galactosidase.

Expression of other muscle proteins with leader sequence

Positive effect of the leader sequence was also concluded from our trials of preparing muscle proteins other than tropomyosin.

α-Actin from human skeletal muscle was expressed using this leader sequence. The soluble fraction (Figure 5-5A) of the cell lysate shows one extra band, as indicated by the arrowhead, which showed the same mobility as actin and was reacted with the anti-α-sarcomeric actin monoclonal antibody. This extra band was not observed when actin expression was tried in Sf9 without this leader sequence (Maeda, K. personal communication). This may indicate that the leader sequence increased the level of expression of actin, in the same way as for the expression of tropomyosin.

CapZ is an actin barbed-end (the fast-growing end) capping protein, and is a hetero-dimer consisting of one α- and one β-subunit. When expressed in *E. coli*, each subunit predominantly goes into inclusion bodies, and hardly recovered as a soluble fraction. To overcome this problem, cDNA of each subunit of CapZ from chicken skeletal muscle was separately inserted into the transfer vector with the leader sequence, and the protein was expressed. From the cell lysate the soluble fraction was collected and was applied on SDS-PAGE gels (Figure 5-5B). As indicated in this figure, the expressed subunits were soluble and the expression level was high. When Sf9 cells were co-infected by recombinant virus of α and β subunits, the CapZ complex was recovered, and the final yield after purification was 11 mg/liter Sf9 culture (Yamashita, A. personal communication). In the case of expression of CapZ, since no control experiment has been conducted, we can not evaluate the effect of the leader sequence on the expression level. Nevertheless it is clear that the expression level is fairly high and high enough for many purposes.

Further applications of the enhanced Sf9 based expression system

In this chapter, I have discussed the leader sequence which causes dramatic increase in the yield of exogenic gene expression in Sf9 cells. In near future, this system may be applied in industries, like pharmaceutical industries.

The advantages of Sf9-baculovirus expression system against bacterial expression system are as follows; (i) the expressed proteins would be more often correctly folded, (ii) post-translational modifications would more often properly occur, and (iii) expression would less suffer from proteolytic digestions. Especially in industrial applications, the former two points are of crucial importance, because proper folding and modifications are essential for the physiological activity of a protein. Sf9-baculovirus system is also more advantageous than mammalian expression systems, because the Sf9 system is less expensive, easier to manipulate, easier to scale up, and yields more.

Acknowledgements

The present work is based on the studies carried out at the International Institute for Advanced Research Laboratory in Panasonic (IIAR) from 1994 to 1999 and RIKEN Harima Institute at SPring-8 Laboratory for Structural Biochemistry (RIKEN SBC) from 1999 to 2000.

I would like to thank Dr. Yuichiro Maéda of IIAR and RIKEN SBC for his continuous guidance and encouragement throughout this study and also his critical reading of the manuscript.

I also wish to express sincere thanks to Dr. Kayo Maeda of IIAR and RIKEN SBC for her invaluable advice and discussions throughout this study and also her critical reading of the manuscript.

I am deeply grateful Dr. Tomoyoshi Kobayashi, IIAR and University of Maryland Biotechnology Institute, for his instruction of manipulation of proteins. I wish to thank Ms. Yumiko Saijo, IIAR and ERATO Protonic NanoMachine Project, for her helpful advice and sample preparation.

I am deeply grateful to Professor Yoshinori Fujiyoshi of IIAR and Kyoto University, and Dr. Kenji Iwasaki of IIAR and National Institutes of Health for their help in instruction and EM photography. I am also deeply grateful to Professor Michael A. Geeves in University of Kent at Canterbury for his suggestion and encouragement about cooperative study.

I also thank to Dr. Makoto Miyata, Osaka City University for his valuable and careful guidance on a base of scientific research work.

I express my thanks to all the members of IIAR and RIKEN SBC for their kind assistance and encouragement.

I wish to express sincere thanks to Professor Hirokazu Hotani of Nagoya University for investigation of this thesis.

Finally, I thank my parents and my friends for their incessant understanding and encouragement.

References

1. Huxley, H.E., and Hanson, J. (1954) Changes in the cross-striations of muscle during contraction and stretch and their structural interpretation. *Nature* **173**, 973-976.
2. Huxley, A.F., and Niedergerke, R. (1954) Structural changes in muscle during contraction. *Nature* **173**, 971-973.
3. Ebashi, S. (1972) Calcium ions and muscle contraction. *Nature* **240**, 217-218.
4. Potter, J.D. (1974) The content of troponin, tropomyosin, actin, and myosin in rabbit skeletal muscle myofibrils. *Arch Biochem and Biophys* **162**, 436-441.
5. Greaser, M.L., and Gergely, J. (1971) Reconstitution of troponin activity from three protein components. *J Biol Chem* **246**, 4226-4233.
6. Greaser, M.L., and Gergely, J. (1973) Purification and properties of the components from troponin. *J Biol Chem* **248**, 2125-2133.
7. Leavis, P.C., and Gergely, J. (1984) Thin filament proteins and thin filament-linked regulation of vertebrate muscle contraction. *CRC Crit Rev Biochem* **16**, 235-305.
8. Ebashi, S., and Endo, M. (1968) Calcium ion and muscle contraction. *Prog in Biophys Mol Biol* **18**, 125-183.
9. Bailey, K. (1948) Tropomyosin: A new asymmetric protein component of the muscle fibril. *Biochem J* **43**, 271-279.
10. Crick, F.H.C. (1953) The Fourier transform of a coiled-coil. *Acta Crystallog* **6**, 685-697.
11. McLachlan, A.D., and Stewart, M. (1975) Tropomyosin coiled-coil interactions: evidence for an unstaggered structure. *J Mol Biol* **98**, 293-304.
12. Stone, D., and Smillie, L.B. (1978) The amino acid sequence of rabbit skeletal α-tropomyosin. The NH2-terminal half and complete sequence. *J Biol Chem* **253**, 1137-1148.
13. Kay, C., and Bailey, K. (1960) Light scattering in solutions of native and guanidinated rabbit tropomyosin. *Biochem Biophys Acta* **40**, 149-156.
14. Ueno, H., Tawada, Y., and Ooi, T. (1976) Properties of non-polymerizable tropomyosin obtained by carboxypeptidase A digestion. *J Biochem Tokyo* **80**, 283-290.
15. Johnson, P., and Smillie, L.B. (1977) Polymerizability of rabbit skeletal tropomyosin: effects of enzymic and chemical modifications. *Biochemistry* **16**, 2264-2269.

16. Cho, Y.J., Liu, J., and Hitchcock-DeGregori, S.E. (1990) The amino terminus of muscle tropomyosin is a major determinant for function. *J Biol Chem* **265**, 538-545.
17. Hitchcock-DeGregori, S.E., and Heald, R.W. (1987) Altered actin and troponin binding of amino-terminal variants of chicken striated muscle α-tropomyosin expressed in Escherichia coli. *J Biol Chem* **262**, 9730-9735.
18. Urbancikova, M., and Hitchcock-DeGregori, S.E. (1994) Requirement of amino-terminal modification for striated muscle α-tropomyosin function. *J Biol Chem* **269**, 24310-24315.
19. Kluwe, L., Maeda, K., Miegel, A., Fujita-Becker, S., Maéda, Y., Talbo, G., Houthaeve, T., and Kellner, R. (1995) Rabbit skeletal muscle α α-tropomyosin expressed in baculovirus- infected insect cells possesses the authentic N-terminus structure and functions. *J Muscle Res Cell Motil* **16**, 103-110.
20. Bazari, W.L., Matsudaira, P., Wallek, M., Smeal, T., Jakes, R., and Ahmed, Y. (1988) Villin sequence and peptide map identify six homologus domains. *Proc Natl Acad Sci U S A* **85**, 4986-4990.
21. Matsuzaki, F., and Matsumoto, S., Yahara, I., Yonezawa, N., Nishida, E., and Sakai, H. (1988) Cloning and characterization of porcine brain cofilin cDNA. *J Biol Chem* **263**, 11564-11568.
22. Yonezawa, N., Nishida, E., Iida, K., Kumagai, H., Yahara, I., and Sakai, H. (1991) Inhibition of actin polymerization by a synthetic dodecapeptide patterned on the sequence around the actin-binding site of coffilin. *J Biol Chem* **266**, 10485-10489.
23. Mak, A.S., Smillie, L.B., and Stewart, G.R. (1980) A comparison of the amino acid sequences of rabbit skeletal muscle α- and β-tropomyosins. *J Biol Chem.* **255**, 3647-3655.
24. Ruiz-Opazo, N., and Nadal-Ginard, B. (1987) α-tropomyosin gene organization. *J Biol Chem* **262**, 4755-4765.
25. Lees-Miller, J.P., Goodwin, L.O., and Helfman, D.M. (1990) Three novel brain tropomyosin isoforms are expressed from the rat α-tropomyosin gene through the use of alternative promoters and alternative RNA processing. *Mol Cell Biol* **10**, 1729-1742.
26. Lees-Miller, J.P., and Helfman, D.M. (1991) The molecular basis for tropomyosin isoform diversity. *Bioessays* **13**, 429-437.
27. Pittenger, M.F., Kazzaz, J.A., and Helfman, D.M. (1994) Functional properties of non-muscle tropomyosin isoforms. *Curr Opin Cell Biol* **6**, 96-104.
28. Matsumura, F., and Yamashiro, M.S. (1985) Purification and characterization of multiple isoforms of tropomyosin from rat cultured cells. *J Biol Chem* **260**, 13851-

13859.

29. Cho, Y.J., and Hitchcock-DeGregori, S.E. (1991) Relationship between alternatively spliced exons and functional domains in tropomyosin. *Proc Natl Acad Sci U S A* **88**, 10153-10157.

30. Landis, C.A., Bobkova, A., Homsher, E., and Tobacman, L.S. (1997) The active state of the thin filament is destabilized by an internal deletion in tropomyosin. *J Biol Chem* **272**, 14051-14056.

31. Hitchcock-DeGregori, S.E. (1994) Structural requirements of tropomyosin for binding to filamentous actin. *Adv Exp Med Biol* **358**, 85-96.

32. Hammell, R.L., and Hitchcock-DeGregori, S.E. (1996) Mapping the functional domains within the carboxyl terminus of α-tropomyosin encoded by the alternatively spliced ninth exon. *J Biol Chem* **271**, 4236-4242.

33. Greenfield, N.J., and Hitchcock-DeGregori, S.E. (1995) The stability of tropomyosin, a two-stranded coiled-coil protein, is primarily a function of the hydrophobicity of residues at the helix-helix interface. *Biochemistry* **34**, 16797-16805.

34. Pittenger, M.F., Kistler, A., and Helfman, D.M. (1995) Alternatively spliced exons of the β tropomyosin gene exhibit different affinities for F-actin and effects with nonmuscle caldesmon. *J Cell Sci* **108**, 3253-3265.

35. Watson, M.H., Kuhn, A.E., Novy, R.E., Lin, J.J., and Mak, A.S. (1990) Caldesmon-binding site on tropomyosin. *J Biol Chem* **265**, 18860-18866.

36. Mak, A.S., and Smillie, L.B. (1981) Structural interpretation of the two-site binding of troponin on the muscle thin filament. *J Mol Biol* **149**, 541-550.

37. Hammell, R.L., and Hitchcock-DeGregori, S.E. (1997) The sequence of the alternatively spliced sixth exon of α-tropomyosin is critical for cooperative actin binding but not for interaction with troponin. *J Biol Chem* **272**, 22409-22416.

38. Bremel, R.D., and Weber, A. (1972) Cooperation within actin filament in vertebrate skeletal muscle. *Nat New Biol* **238**, 97-101.

39. Greene, L.E., and Eisenberg, E. (1980) Cooperative binding of myosin subfragment-1 to the actin-troponin-tropomyosin complex. *Proc Natl Acad Sci U S A* **77**, 2616-2620.

40. Lehrer, S.S., and Morris, E.P. (1982) Dual effects of tropomyosin and troponin-tropomyosin on actomyosin subfragment 1 ATPase. *J Biol Chem* **257**, 8073-8080.

41. Lehrer, S.S., and Geeves, M.A. (1998) The muscle thin filament as a classical cooperative/allosteric regulatory system [published erratum appears in J Mol Biol 1998 Jun 19;279(4):1024]. *J Mol Biol* **277**, 1081-1089.

42. Geeves, M.A., Halsall, D.J. (1987) Two-step ligand binding and cooperativity. A model to describe the cooperative binding of myosin subfragment 1 to regulated actin [published erratum appears in Biophys J 1988 **53**(5):845]. *Biophys J* **52**,215-220.

43. Monod, J., Wyman, J., and Changeux, J.-P. (1965) On the nature of allosteric transitions. *J Mol Biol* **12**, 88-118.

44. Bernstein, S.I., O'Donnell, P.T., and Cripps, R.M. (1993) Molecular genetic analysis of muscle development, structure, and function in Drosophila. *Int Rev Cytol* **143**, 63-152.

45. Sambrook, J., Fritsch, E.F., and Maniatis, T. (1989) *Molecular cloning: A laboratory manual, 2nd Ed.* Cold Spring Harbor Laboratory, Cold Spring Harbor, NY.

46. Summers, M.D., and Smith, G.E. (1987) *A manual of methods for Baculovirus Vectors and Insect cell culture procedures.* Texas Agricultural Experiment Station.

47. Suzuki, N., and Mihashi, K. (1991) Binding mode of cytochalasin B to F-actin is altered by lateral binding of regulatory proteins. *J Biochem Tokyo* **109**, 19-23.

48. Pato, M.D., Mak, A.S., and Smillie, L.B. (1981) Fragments of rabbit striated muscle α-tropomyosin. II. Binding to troponin-T. *J Biol Chem* **256**, 602-607.

49. Ueno, H. (1984) Local structural changes in tropomyosin detected by a trypsin-probe method/. *Biochemistry* **23**, 4791-4798.

50. Taniguchi, H., Suzuki, M., Manenti, S. and Titani, K. (1994) A mass spectrometric study on the in vivo posttranslational modification of GAP-43. *J Biol Chem* **269**, 22481-22484.

51. Nagashima, H., and Asakura, S. (1982) Studies on co-operative properties of tropomyosin-actin and tropomyosin-troponin-actin complexes by the use of N-ethylmaleimide-treated and untreated species of myosin subfragment 1. *J Mol Biol* **155**, 409-428.

52. Criddle, A.H., Geeves, M.A., and Jeffries, T. (1985) The use of actin labeled with N-(1-pyrenyl)iodoacetamide to study the interaction of actin with myosin subfragments and troponin/tropomyosin. *Biochem J* **232**, 343-9.

53. Kouyama, T., and Mihashi, K. (1981) Fluorimetry study of N-(1-pyrenyl)iodoacetamide-labelled F-actin. Local structural change of actin protomer both on polymerization and on binding of heavy meromyosin. *Eur J Biochem* **114**, 33-38.

54. McKillop, D.F., and Geeves, M.A. (1993) Regulation of the interaction between actin and myosin subfragment 1: evidence for three states of the thin filament. *Biophys J* **65**, 693-701.

55. Yang, Y.Z., Korn, E. D. and Eisenberg, E. (1979) Cooperative binding of tropomyosin to muscle and Acanthamoeba actin. *J Biol Chem* **254**, 7137-7140.

56. Grodberg, J. and Dunn, J.J. (1988) ompT encodes the Escherichia coli outer membrane protease that cleaves T7 RNA polymerase during purification. *J Bacteriol* **170**, 1245-1253.

57. Hvidt, S., Ferry, J. D., Roelke, D.L. and Greaser, M.L. (1983) Flexibility of light meromyosin and other coiled-coil α-helical proteins. *Macromolecules* **16**, 740-745.

58. Swenson, C.A. and Stellwagen, N.C. (1989) Flexibility of smooth and skeletal tropomyosins. *Biopolymers* **28**, 955-963.

59. Phillips, G.N. Jr and Chacko, S. (1996) Mechanical properties of tropomyosin and implications for muscle regulation. *Biopolymers* **38**, 89-95.

60. Szczesna, D. and Fajer, P.G. (1995) The tropomyosin domain is flexible and disordered in reconstituted thin filaments. *Biochemistry* **34**, 3614-3620.

61. Chandy, I.K., Lo, J.C. and Ludesher, R.D. (1999) Differential mobility of skeletal and cardiac tropomyosin on the surface of F-actin. *Biochemistry* **38**, 9286-9294.

62. Harbury, P.B., Zhang, T., Kim, P.S. and Alber, T. (1993) A switch between two-, three-, four-stranded coiled coils in GCN4 leucine zipper mutants. *Science* **262**, 1401-1407.

63. Wagschal, K., Tripet, B., Lavigne, P., Mant, C. and Hodges, R.S. (1999) The role of position a in determining the stability and oligomerization state of α-helical coiled coils: 20 amino acid stability coefficients in the hydrophobic core of proteins. *Protein Sci* **8**, 2312-2329.

64. O'Shea, E.K., Klemm, J.D., Kim, P.S., and Alber, T. (1991) X-ray structure of the GCN4 leucine zipper, a two-stranded, parallel coiled coil. *Science* **254**, 539-544.

65. Monera, O.D., Kay, C.M., and Hodges, R.S. (1994) Electrostatic interactions control the parallel and antiparallel orientation of α-helical chains in two-stranded α-helical coiled-coils. *Biochemistry* **33**, 3862-3871.

66. McKillop, D.F., and Geeves, M.A. (1991) Regulation of the acto-myosin subfragment 1 interaction by troponin/tropomyosin. Evidence for control of a specific isomerization between two acto.myosin subfragment 1 states. *Biochem J* **279**, 711-718.

67. Lehrer, S.S., Golitsina, N.L., and Geeves, M.A. (1997) Actin-tropomyosin activation of myosin subfragment 1 ATPase and thin filament cooperativity. The role of tropomyosin flexibility and end-to-end interactions. *Biochemistry* **36**, 13449-13454.

68. Smillie, L.B. (1979) Structure and functions of tropomyosins from muscle and non-muscle sources. *Trends Biochem Sci* **4**, 151-155.

69. Stewart, M., and Roberts, G.C. (1983) Nuclear magnetic resonance evidence for a flexible region at the C-terminus of α-tropomyosin. *J Mol Biol* **166**, 219-225.

70. Berger, B., Wilson, D.B., Wolf, E., Tonchev, T., Milla, M., and Kim, P.S. (1995) Predicting coiled coils by use of pairwise residue correlations. *Proc Natl Acad Sci U S A* **92**, 8259-8263.

71. Studier, F.W., Rosenberg, A.H., Dunn, J.J., and Duberndorf, J.W. (1990) *Use of T7RNA polymerase to direct expression of cloned genes.* Academic Press, San Diego.

72. O'Reilly, D.R., MIller, L.K., and Luckow, V.A. (1992) *Baculovirus Expression Vectors: A Laboratory Manual.* W. H. Freeman, New York.

73. Smillie, L.B., Pato, M.D., Pearlstone, J.R., and Mak, A.S. (1980) Periodicity of α-helical potential in tropomyosin sequence correlates with alternating actin binding sites. *J Mol Biol* **136**, 199-202.

74. Takeda, S., Kobayashi, T., Taniguchi, H., Hayashi, H., and Maeda, Y. (1997) Structural and functional domains of the troponin complex revealed by limited digestion. *Eur J Biochem* **246**, 611-617.

75. Hensley, P. (1996) Defining the structure and stability of macromolecular assemblies in solution: re-rmergence of analytical ultracentrifugation as a practical tool. *Structure* **4**, 367-373.

76. Tanford, C. (1961) *Physical Chemistry of Macromolecules.* John Wiley & Sons, New York.

77. Ribulow, H. and Barany, M. (1977) Phosphorylation of tropomyosin in live frog muscle. *Arch Biochem Biophys* **179**, 718-720.

78. Heeley, D.H., Watson, M.H., Mak, A.S., Dubord, P., and Smillie, L.B. (1989) Effect of phosphorylation on the interaction and functional properties of rabbit striated muscle α α-tropomyosin. *J Biol Chem* **264**, 2424-2430.

79. Pato, M.D., Mak, A.S., and Smillie, L.B. (1981) Fragments of rabbit striated muscle α-tropomyosin. I. Preparation and characterization. *J Biol Chem* **256**, 593-601.

80. Ooi, T., Mihashi, K., and Kobayashi, H. (1962) On the polymerization of tropomyosin. *Arch Biochem Biophys* **98**, 1-11.

81. McGhee, J. D. and Hippel, P. H. von (1974) Theoretical aspects of DNA-protein interactions: co-operative and non-co-operative binding of large ligands to a one-dimensional homogeneous lattice. *J Mol Biol* **86**, 469-489.

82. Monteiro, P.B., Lataro, R.C., Ferro, J.A., and Reinach, F.d.C. (1994) Functional α-tropomyosin produced in Escherichia coli. A dipeptide extension can substitute the amino-terminal acetyl group. *J Biol Chem* **269**, 10461-10466.

83. Hanauer, A., Levin, M., Heilig, R., Daegelen, D., Kahn, A., and Mandel, J.L. (1983) Isolation and characterization of cDNA clones for human skeletal muscle α actin. *Nucleic Acids Res* **11**, 3503-3516.

84. Casella, J.F., Casella, S.J., Hollands, J.A., Caldwell, J.E., and Cooper, J. (1989) Isolation and characterization of cDNA encoding the α subunit of CapZ(36/32), and actin-capping protein from Z-line of skeletal muscle. *Proc Natl Acad Sci U S A* **86**, 5800-5804.

85. Caldwell, J.E., Waddle, J.A., Cooper, J.A., Hollands, J.A., Casella, S.J., and Casella, J.F. (1989) cDNAs encoding the β subunit of cap Z, the actin-capping protein of the Z line of muscle. *J Biol Chem* **264**, 12648-12652.

List of publications

In Chapter 2

Ken-Ichi Sano, Kayo Maeda, Hisaaki Taniguchi, and Yuichiro Maéda.
"Amino-acid replacements in an internal region of tropomyosin alter the properties of the entire molecule."
Eur J Biochem. (2000) **267**:4870-4877.

Andrea Miegel, Ken-Ichi Sano, Kazuhiro Yamamoto, Kayo Maeda, Yuichiro Maéda, Hisaaki Taniguchi, Min Yao, and Soichi Wakatsuki
"Production and crystallization of lobster muscle tropomyosin expressed in Sf9 cells."
FEBS Lett. (1996) **394**:201-205.

Donald L. Mykles, Julie L. S. Cotton, Hisaaki Taniguchi, Ken-Ichi Sano, and Yuichiro Maéda
"Cloning of tropomyosins from lobster (*Homarus americanus*) striated muscles: fast and slow isoforms may be generated from the same transcript."
J Muscle Res Cell Motil. (1998) **19**:105-115

In Chapter 3

Ken-Ichi Sano, Kayo Maeda, and Yuichiro Maéda
"The cooperative activation of myosin subfragment 1 ATPase by actin-tropomyosin. The role of head-to-tail interaction of tropomyosin", *submitted*

In Chapter 4

Ken-Ichi Sano, Kayo Maeda, Toshiro Oda, and Yuichiro Maéda
"The effect of single residue substitutions of serine-283 on the strength of head-to-tail interaction and actin binding properties of rabbit skeletal muscle α-tropomyosin."
J Biochem (*Tokyo*). (2000) **127**:1095-102.

Others

Masao Miki, Tomoo Miura, Ken-Ichi Sano, Hiroyuki Kimura, Hiroyuki Kondo, Hiroshi Ishida and Yuichiro Maéda

"Fluorescence resonance energy transfer between points on tropomyosin and actin in skeletal muscle thin filaments: Does tropomyosin move?"

J Biochem (*Tokyo*). (1998) **123**: 1104-1111.

Miyata Makoto, Ken-Ichi Sano, Ryosuke Okada and Takashi Fukumura

"Mapping of replication initiation site in *Mycoplasma capricolum* genome by two-dimensional gel-electrophoretic analysis"

Nucleic Acids Res. (1993) **21**: 4816-4823.

Ken-Ichi Sano and Makoto Miyata

"The gyrB gene lies opposite from the replication origin on the circular chromosome of *Mycoplasma caplicolum*"

Gene, (1994) **151**, 181-183.